Influence of Formulation Parameters of Doxorubicin - Poly(butyl Cyanoacrylate) Nanoparticles on the Treatment of Glioblastomas and Evaluation of the Body Distribution of Labelled Nanoparticles in Healthy and Glioblastoma - Bearing Rats

A Thesis

Submitted to the Faculty

of

The Department of

Pharmaceutical Technology

at

The Johann Wolfgang Goethe University

Frankfurt am Main, Germany

by

Alessandra Ambruosi

(Bari, Italy)

In Partiall Fulfillment of the

Requirements for the Degree

of

Doctor of Philosophy

(Pharmaceutics)

Frankfurt am Main, 2005

Ai miei genitori

Abbreviations

Apo – E	Apolipoprotein E
ABC	ATP-binding cassette
AUC	Area under the curve
BBB	Blood-brain barrier
BCA	Butyl cyanoacrylate
CNS	Central nervous system
CSF	Cerebrospinal fluid
DMF	Dimethylformamide
DOX	Doxorubicin
EPR	Enhanced permeability and retention effect
GBM	Glioblastoma multiforme
GC	Gas chromatography
JAM	Junctional adhesion molecule
LDL	Low-density lipoprotein
MWCO	Molecular weight cut off
MRP	Multidrug resistance associated protein
NP	Nanoparticles
PBCA	Poly(butyl cyanoacrylate)
PCS	Photo-correlation spectroscopy
PHCA	Poly(hexyl cyanoacrylate)
PHICA	Poly(iso-hexyl cyanoacrylate)
PIBCA	Poly(iso-butyl cyanoacrylate)
PMMA	Poly(metyl methacrylate)
P-gp	P-glycoprotein efflux system
PS 80	Polysorbate 80
RES	Reticulo endothelial system
WBA	Whole-body autoradiography
WHO	World Health Organization
ZO	Zonula occludens

1 Zusammenfassung

Systematisch verabreichte Chemotherapeutika sind oft uneffektiv bei der Behandlung von Krankheiten des zentralen Nervensystems (ZNS). Eine der Ursachen hierfür ist der unzureichende Arzneistoff-Transport ins Gehirn aufgrund der Blut-Hirn-Schranke, die den Austausch von Substanzen zwischen Blutkreislauf und der extrazellularen Flüssigkeit des Gehirns einschränkt. Die Blut-Hirn-Schranke wird aus Endothelzellen der Hirngefäße gebildet, die im Gegensatz zu peripheren Endothelien durch die sogenannten „tight junctions" verbunden sind. Während diese strukturelle Barriere die Diffusion hydrophiler Substanzen in die parazelluläre Flüssigkeit des Gehirns verhindert, wird eine Anreicherung lipophiler Moleküle im Gehirn durch die sehr leistungsfähigen ABC-Efflux-Transporter wie zum Beispiel P-Glykoprotein (P-gp) oder „Multidrug Resistance"-Proteine konterkariert.

Eine der Strategien für den nicht-invasiven Wirkstoff-Transport ins Gehirn ist die Verwendung von Nanopartikeln. Wie groß angelegte pharmakologische Studien gezeigt haben, können Polybutylcyanoacrylat-Nanopartikel, die mit Polysorbat 80 (Tween® 80) überzogen wurden, die Blut-Hirn-Schranke passieren und somit Wirkstoffe ins Gehirn transportieren. Es konnte gezeigt werden, dass die Wirkung der Polysorbat 80-Beschichtung nicht mit anderen Tensiden wie Poloxamer 188, 338 und 407 und Poloxamin 908 erreicht werden konnte. Einzig die mit Polysorbat 80 beschichteten Polybutylcyanoacrylat-Nanopartikel konnten den Transport des Wirkstoffes ins Gehirn gesunder Versuchtiere ermöglichen. Dieses Phänomen wurde durch die selektive Adsorption bestimmter Plasmaproteine (insbesondere der Apolipoproteine E und B) an die Oberfläche der Polysorbat 80-beschichteten Nanopartikel erklärt. Auf diese Art ahmten die überzogenen Nanopartikel Lipoproteinteilchen nach und wurden durch Rezeptor-vermittelte Endozytose über die Blut-Hirn-Schranke transportiert.

Wird die Blut-Hirn-Schranke durch einen Hirntumor partiell beschädigt und hierdurch ihre Permeabilität am Ort des Tumors erhöht, können Nanopartikel den Tumor zusätzlich durch den sogenannten EPR-Effekt („Enhanced Permeability and Retention") erreichen. Es ist bekannt, dass dieser Effekt besonders ausgeprägt bei lang-zirkulierenden Nanopartikeln ist, die nicht schnell durch das retikulo-endotheliale System (RES) aus der Blutzirkulation entfernt werden, was letztlich ihre Extravasation in den Nicht-RES-Geweben erhöht.

Im ersten Teil der vorliegenden Arbeit wurde die Beladung der Nanopartikel durch Variation der Formulierungparameter mit dem Ziel optimiert, eine Formulierung mit höherer Wirksamkeit für die Therapie von Glioblastom-tragenden Ratten zu entwickeln. Außerdem wurde das Potential von Doxorubicin, das an mit „Stealth Agents" überzogenen Polybutylcyanoacrylat-Nanopartikel gebunden war, für die Chemotherapie von Hirntumoren untersucht.

Im zweiten Teil dieser Studie wurden die Gehirn- und Körperverteilung in gesunden und in Glioblastom-101/8-tragenden Ratten nach i.v.-Gabe von Poly(butyl-2-cyano[3- ^{14}C] acrylat)-Nanopartikeln, die mit Polysorbat 80 beschichtet wurden, und solchen, die noch zusätzlich mit Doxorubicin geladen waren (DOX-^{14}C-PBCA + PS), untersucht.

Anti-tumoraler Effekt von Doxorubicin-beladenen Polybutylcyanoacrylat-Nanopartikeln im Ratten-Gliom-Modell

Die Standardformulierung von Doxubicin-Polybutylcyanoacrylat-Nanopartikeln (DOX-NP) wurde durch anionische Polymerisierung von Butylcyanoacrylat in Anwesenheit von DOX hergestellt. Zusätzlich wurden unterschiedliche DOX-NP Formulierungen durch Veränderung der Herstellung produziert. Diese veränderten Parameter waren: pH, Konzentration und Art der Monomere, Konzentration und Art des Stabilisators, sowie Polymerisationszeit und Zugabe des Arzneistoffs am Anfang des Polymerisations prozesses. Die Bestimmung der Beladung wurde mit Hilfe von HPLC und Spektrophotometrie durchgeführt. Außerdem wurde die Verwendung von iso-BCA anstelle von n-BCA untersucht, und dabei wurden Nanopartikeln mit verbesserter Beladung erhalten. Die Veränderung der Herstellungparameter führten durch Verkleinerung der n-BCA-Konzentration (0.75 % w/v), Erhöhung der Dextran-Konzentration (2 % w/v), Verlängerung der Polymerisationszeit auf 4 h und Zugabe von DOX schon vor dem Start des Polymerisationsprozesses ebenfalls zu einer neuer Formulierung mit verbesserter Beladung. Das therapeutische Potential der beschriebenen Formulierungen wurde in Ratten mit ins Gehirn transplantieren Glioblastom 101/8 untersucht und mit der Standardformulierung verglichen. Die Applikation allen Präparationen erfolgte durch intavenöse Injektion in die Schwanzvene. Neben Polysorbat 80 wurden Poloxamer 188 und Poloxamin 908 als Überzugsmaterial verwendet. Die Resultate ergaben, dass die mit

Polysorbat 80 überzogene Standardformulierung am effektivsten war: 35 % der Tiere überlebten 180 Tage lang nach Tumorimplantation. In den Tiergruppen, die mit iso-PBCA-Nanopartikeln oder der neuen Formulierung behandelt wurden, lag der Prozentsatz der Langzeit-Überlebenden bei 15 % (3/20) beziehungsweise 10 % (2/20). Der Prozentsatz der Langzeit-Überlebenden, die mit Poloxamer 188 oder mit Poloxamin 908 beschichteten DOX-Nanopartikeln behandelt wurden, lag bei 20 % (4/20).

Die höhere Wirksamkeit von DOX-NP+PS 80 könnte durch die Fähigkeit dieser Träger erklärt werden, den Wirkstoff während eines frühen Stadiums der Tumorentwicklung durch einen Rezeptor-vermittelten Mechanismus, der durch den PS 80-Überzug aktiviert wurde über die intakte Blut-Hirn-Schranke, zu transportieren. Auf diesem Weg könnte DOX auch jene Teile des Gehirns erreichen, die trotz des Tumors noch immer durch eine intakte Blut-Hirn-Schranke geschützt wurden. Unsere Ergebnisse zeigen auch, dass Poloxamer 188 und Poloxamin 908 den antitumoralen Effekt von DOX-PBCA beträchtlich verbessern, obgleich der an die Partikel gebundene Wirkstoff durch das Beschichten mit diesen Tensiden gemäß früherer Ergebnisse nicht ins gesunde Gehirn transportiert werden konnte. Der anti-tumorale Effekt dieser Formulierungen könnte möglicherweise dem EPR-Effekt zugeschrieben werden. Es ist bekannt, dass die tumorale Arzneistoff-Aufnahme durch den EPR-Effektes für lang-zirkulierende Wirkstoffträger ausgeprägter ist und so mehr Wirkstoff durch die Tumor-geschädigte Blut-Hirn-Schranke gelangt. Die Strategie hierzu, die Blut-Halbwertszeit der Partikel zu erhöhen, ist die Abschirmung ihrer Oberfläche. Infolgedessen erfolgt durch das Beschichten mit Tensiden wie Poloxamer 188 und Poloxamin 908 eine Reduktion der Opsonisierung.

Der Prozentsatz der überlebenden Tiere nach Behandlung mit der neuen Formulierung mit der erhöhten Beladung war in den vorliegenden Untersuchung nicht besser als die Standardformulierung. Eine mögliche Erklärung hierfür könnte der erhöhte Dextran-Gehalt (2 % w/v) sein. Die Dextran-Moleküle stehen von der Nanopartikel-Oberfläche wie hydrophile Schleifen oder Ketten ab, so dass sie mit der Polysorbat 80-Schicht interagieren und so die Partikel-Interaktion mit den Gehirn-Endothelzellen behindern könnten. Infolgedessen wird der Prozess der Endozytose von den Endothelzellen der Blut-Hirn-Schranke vermindert, und dementsprechend der Transport von DOX ins Gehirn. Im Falle von iso-Butyl-NP könnte es möglich sein, dass beide Polymere unterschiedliches Verhalten *in vivo* zeigen. Dies genau zu ermitteln würde jedoch weitere Untersuchungen erfordern.

Korpenverteilung von DOX-^{14}C PBCA-Nanopartikeln in gesunden und Glioblastom

101/8-tragenden Ratten

Unbeschichtete Nanopartikel, Polysorbat 80-beschichtete Nanopartikel oder mit Doxorubicin beladene und mit Polysorbat 80 beschichtete Nanopartikel wurden in die Schwanzvene von gesunden Ratten injiziert. Nach unterschiedlichen Zeitintervallen (10 Minuten, 1 h, 6 h, 24 h, 1 Woche, 4 Wochen), wurden die Tiere getötet. Blut sowie Leber, Milz, Lungen, Nieren, Gonaden wurden gesammelt und das Gehirn entfernt. Nach der Solubilisierung der Gewebe wurde die Radioaktivität mittels eines Scintillation gemessen. Das gleiche Verfahren wurde für Tumor-tragende Ratten verwendet. Die Verabreichung der Nanopartikel wurde an den Tagen 5, 8 und 10 nach Tumorimpfung durchgeführt und die Tiere 10 Minuten, 1 h, 6 h, 24 h nach Verabreichung getötet. Das Blut und die Organe wurden gesammelt und deren Radioaktivität bestimmt. Drei verschiedene Nanopartikel-Präparationen wurden verwendet: 1. [^{14}C]-PBCA NP, 2. [^{14}C]-PBCA NP beschichtet mit PS 80 und 3. mit DOX-beladene [^{14}C]-PBCA NP beschichtet mit PS 80. Diese zeigten einer unterschiedliche Korpenverteilung in den Ratten. Wie erwartet, sammelten sich unbeschichtete Nanopartikel in den RES-Organen wie Lunge, Leber und Milz an. Mit PS 80 beschichtete NP reduzierten die Aufnahme der NP in Leber und Milz, während sich die Konzentration der NP in der Lunge erhöhte. Diese Beobachtungen deuten darauf hin, dass die Änderung der Oberflächeneigenschaften der NP durch das Tensid analog zu den Arbeiten der Arbeitsgruppe Müller, Berlin, zu einer Interaktion mit unterschiedlichen Opsoninen führt, welches die Aufnahme der NP von verschiedenen phagozitierenden Zellen erleichtert.

Hingegen war die Aufnahme der mit DOX beladenen, PS 80-beschichteten Nanopartikel den unbeschichteten Partikel ähnlich. Das Vorhandensein von DOX führte sogar zu einer geringfügigen Zunahme der RES-Aufnahme und wirkte dem beschichtenden Polysorbat entgegen. Die unterschiedlichen Muster der Nanopartikelverteilung können durch ihre unterschiedlichen physikalisch/chemischen Parameter erklärt werden. Die Messung des Zeta-Potentials der in Wasser resuspendierten NP und der in Rattenplasma inkubierten NP zeigte, dass unbeladene NP negativ geladen waren, während nach DOX-Bindung die Ladung positiv wurde. Nach der Inkubation im Serum wurde die Ladung der DOX - NP wieder negativ, was durch eine starke Interaktion mit Serumbestandteilen bewirkt wurde. Hieraus kann geschlossen werden, dass die Oberflächenladung, die auf den Nanopartikeln

vorhanden ist, eine wichtige Rolle in der Proteininteraktion spielt, welche wiederum die Verteilung im Körper beeinflusst.

Das Verteilungsmuster von [^{14}C]-Nanopartikeln in den Körpern von gesunden- und Tumor tragenden Ratten außerhalb des Gehirns war ähnlich. Dieses Resultat zeigt, dass der Gehirntumor nicht die Physiologie des vollständigen Körpers beeinflusst.

Im Vergleich mit gesunden Ratten und mit Ratten, welche 5 bzw. 8 Tage vorher mit dem Tumor infiziert wurden, hingegen war die Konzentration der NP im Gehirn von Tumor tragenden Ratten 10 Tage nach der Tumor-implantation signifikant höher. In Anwesenheit des Glioblastoms ist der Transport von NP in das Gehirn das Resultat verschiedener Faktoren: zusätzlich zur Fähigkeit von PS 80-Nanopartikeln, die Blut-Hirn-Schranke zu passieren, welche in einem frühen Stadium der Tumorentwicklung noch intakt ist, extravasieren diese Träger wegen des EPR Effekts über das durch den Tumor undichte Endothelium. In einigen Teilen des Tumors sind die Kapillaren nämlich hyper-permeabel, wogegen in anderen Teilen des Tumors ihre Sperrfunktion beibehalten wird. Dadurch wird die Fähigkeit von PS 80-coated Nanopartikeln Arzneistoffe über die intakten Blut-Hirn-Schranke zu transportieren aufgrund des „EPR-Effekts", erhöht. Die Konzentration von PS 80 [^{14}C]-PBCA NP war im Glioblastom signifikant höher als mit DOX [^{14}C]-PBCA NP. Dieses Phänomen kann durch die unterschiedliche Mikroumgebung von zerebralem intra-tumoralen und intaktem Gehirngewebe erklärt werde. Die tumorale Regionen sind hypoxisch, ein physiologisches Anzeichen dafür ist die erhöhte Azidose in den betroffenen Regionen. Diese erhöhte Azidose kann sich in die nähere Umgebung der tumoralen Regionen ausdehnen. Hierdurch wiederum kann die Anreicherung der Nanopartikeln beeinflusst werden. Insbesondere können sich die positive Ladung der tumoralen Regionen und die positive Ladung der DOX [^{14}C]-PBCA NP negativ beeinflussen. Dennoch waren die Doxorubicin-Konzentration in Glioblastom ausreichend, einen therapeutischen Effekt zu ermöglichen.

2 Introduction

2. 1 Glioblastoma multiforme

2.1.1 Background

Brain tumours represent a heterogeneous group of central nervous system (CNS) neoplasms. The World Health Organization (WHO) recognizes approximately 100 different types of brain tumours classified according to pathological diagnosis. In general, however, these tumours can be classified into either primary or secondary tumours, depending on whether they originate in the brain or simply spread to the central nervous system from elsewhere. Approximately half of all primary brain tumours are glial-cell neoplasms, and more than three quarters of all glial tumours are astrocytomas. Astrocytomas differ in their pathological and clinical behaviour: some astrocytomas are classified as low-grade tumours, meaning they are slow growing, whereas others, such as glioblastoma multiforme (GBM), represent the most aggressive type of tumour known to occur within the CNS (Fig 2.1).
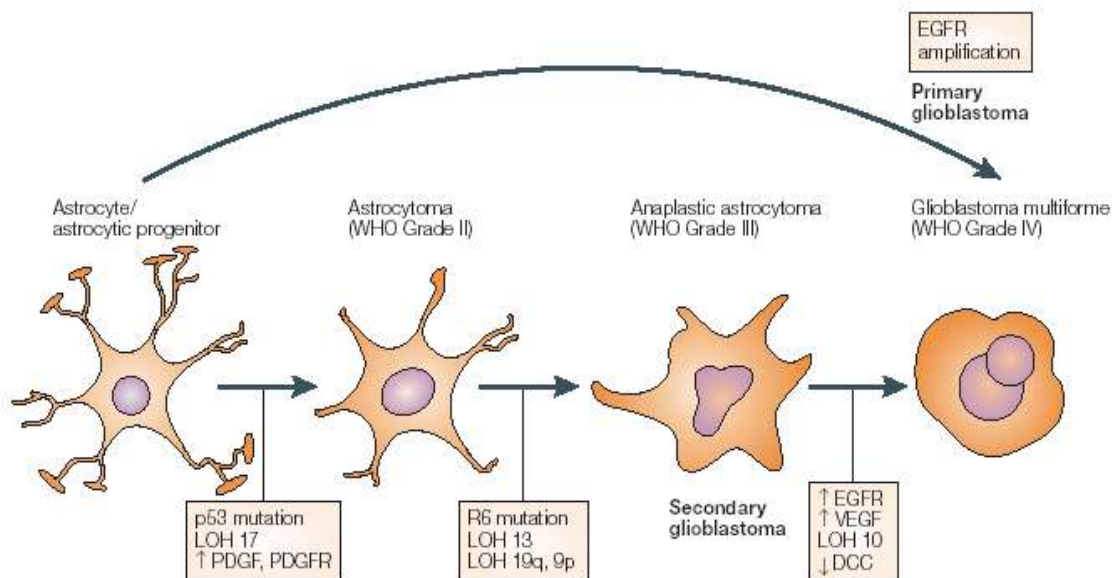
Figure 2.1. Development and progression of astrocytic brain tumours. Malignant brain tumours can arise in one of two ways. On the one hand, astrocytes undergo genetic changes accompanied by upregulation of certain receptors, such as the platelet-derived growth factor (PDGF), endothelial growth factor receptor (EGFR) or vascular endothelial growth factor (VEGF). These progressive changes culminate in the formation of a glioblastoma. On the other hand, most primary glioblastomas arise de novo, without the need for gradual progression from an astrocytoma to a high-grade astrocytoma to a glioblastoma multiforme.

2.1.2 Pathophysiology

Over the past 5 years, the concept of different genetic pathways leading to the common phenotypic endpoint (i.e., GBM) has gained general acceptance. Genetically, primary and secondary glioblastomas show little overlap and constitute different disease entities. Some of the more common genetic abnormalities are described as follows (Fig 2.1):

p53: Mutations in *p53,* a tumour suppressor gene, were among the first genetic alterations identified in astrocytic brain tumours. While present in less than 10 % of primary glioblastomas, more than 65 % of secondary glioblastomas have *p53* mutations.

Epidermal growth factor receptor (*EGFR*) gene: The *EGFR* gene is involved in the control of cell proliferation and is either amplified or overexpressed in more than one third of glioblastomas, sometimes in a truncated and rearranged form. *EGFR* amplification is much more common in primary glioblastomas. These tumours typically show a simultaneous loss of chromosome 10 but rarely a concurrent *p53* mutation.

MDM2: Amplification or overexpression of *MDM2* constitutes an alternative mechanism to escape from *p53*-regulated control of cell growth by binding to *p53* and abolishing its activity. Overexpression of *MDM2* is observed in more than 50 % of primary GBMs but rarely in secondary glioblastomas.

Platelet-derived growth factor (*PDGF*) gene: The *PDGF* gene acts as a major mitogen for glial cells by binding to the *PDGF* receptor (PDGFR). Amplification or overexpression of PDGFR is typical (60%) in the pathway leading to secondary glioblastomas.

PTEN: *PTEN* (also known as *MMAC* and *TEP1*) encodes a tyrosine phosphatase located at 10q23.3. The function of *PTEN* as a cellular phosphatase is consistent with possible tumour suppressor function. Phosphatases act by turning off signaling pathways dependent upon phosphorylation. When phosphatase activity is lost because of genetic mutation, signaling pathways can become activated constitutively, resulting in aberrant proliferation. *PTEN* mutations have been found in as many as 30 % of glioblastomas.

2.1.3 Treatment strategies for brain gliomas

Current treatments for malignant or high-grade gliomas rarely achieve long-term tumour control. Even when treated with aggressive combined surgery, chemotherapy, and radiotherapy, in patients with high-grade malignant brain gliomas such as glioblastomas,

recurrence occurs between 6 and 12 months and for anaplastic astrocytomas, within 18–36 months.

Conventional therapy for glioblastomas consists primarily of surgical debulking followed by radiation therapy. However glioblastoma tumours can be difficult to resect due to the lack of a defined tumour edge; the tumour may extend onto normal-looking brain tissue, and/or can be localized near critical areas of the brain. The median survival after surgical intervention is six months (Shand et al. 1999).

Following surgery to remove as much tumour mass as possible or if the tumour is in a non-operable region of the brain, radiation treatment can be performed to kill residual tumour cells and to relieve symptoms associated with the disease. Exposure of radiation is confined to the tumour mass and 2 cm of surrounding tissue. As with all radiation treatments, the side effects include swelling of the brain and the accumulation of dead cells, making it difficult to assess tumour reduction during routine scans.

The use of chemotherapy is now well established in the treatment of brain tumours. As is also the case with many systemic cancers, chemotherapy of brain tumours is not curative, and the goals of the treatment are mainly to control the growth of the tumour and to maintain good performance and quality of life for the patient for as long as possible (Burton and Prados 2000, Beauchesne 2002; Kleinberg et al. 2002; Tentori and Graziani 2002, Trent et al. 2002, Watling and Cairncross 2002). Chemotherapy can be used as a primary therapy or an additional therapy following surgery and/or radiation therapy. The most common agents are the nitrosoureas (BCNU, CCNU), platinum-based drugs (cisplatin, cisplatinum, carboplatin), temozolomide, procarbazine, and natural-occurring compounds (taxol). The failure of aggressive chemotherapy to eradicate brain tumour is due in part to the presence of the blood-brain barrier (BBB) which restricts the influx of molecules from the bloodstream into the brain and prevent the effective therapy of brain tumour (Hofer and Merlo 2002). Compounds which temporary disrupt the BBB can increase the penetration of drug into the brain parenchyma. Certain hyperosmolar agents, such mannitol, draw water out of endothelial cells, thereby shrinking them and opening the gaps between cerebral endothelial cells. Other compound, such as the bradykinin agonist RMP-7, directly distrupt the BBB (Bonstelle et al. 1983, Nomura et al. 1994). However, the enhanced toxicity associated with the disruption of the BBB limits the applicability of these methods.

2.2 Blood-brain barrier

2.2.1 Structure of the Blood-Brain Barrier

The brain functions within a well-controlled environment separate from the milieu of the periphery. The mechanisms that control the unique environment of the brain are collectively referred to as the blood-brain barrier.

 Paul Ehrlich (1885, 1906) and Edwin Goldman (1909, 1913) observed that water soluble dyes injected into the peripheral circulation did not stain the brain or color the cerebrospinal fluid (CSF). Lewandowsky, while studying potassium ferrocyannide penetration into the brain (1900), was the first to coin the term blood-brain barrier and called it "Blut-Hirn-Schranke". The observations drawn from the dye studies brought about the concept of a barrier between blood and brain, as well as between blood and CSF. Electron microscopic cytochemical studies performed in the late 1960s by Reese and Karnovsky (1967), and later by Brightman and colleagues (1969) visualized the BBB.

 The BBB is the specialized system of capillary endothelial cells that protects the brain from harmful substances in the blood stream, while supplying the brain with the required nutrients for proper function. Unlike peripheral capillaries that allow relatively free exchange of substance across / between cells, the BBB strictly limits transport into the brain through both physical (tight junctions) and metabolic (enzymes) barriers. Thus the BBB is often the rate-limiting factor in determining permeation of therapeutic drugs into the brain.

The structure of the BBB is schematised in Fig 2.2. The cerebral endothelial cells form tight junctions at their margins where they meet, which completely seal the aqueous paracellular pathways between the cells. Pericytes are distributed discontinuously along the length of the cerebral capillaries and partially surround the endothelium. Both, the cerebral endothelial cells and the pericytes are surrounded by, and contribute to, the same extracellular matrix. Foot processes from astrocytes form a network fully surrounding the capillaries. Axons from neurons also abut closely against the endothelial cells and contain vasoactive neurotransmitters and peptides. Microglia (perivascular macrophages) are the

resident immunocompetent cells of the brain and are derived from systemic circulating monocytes and macrophages.
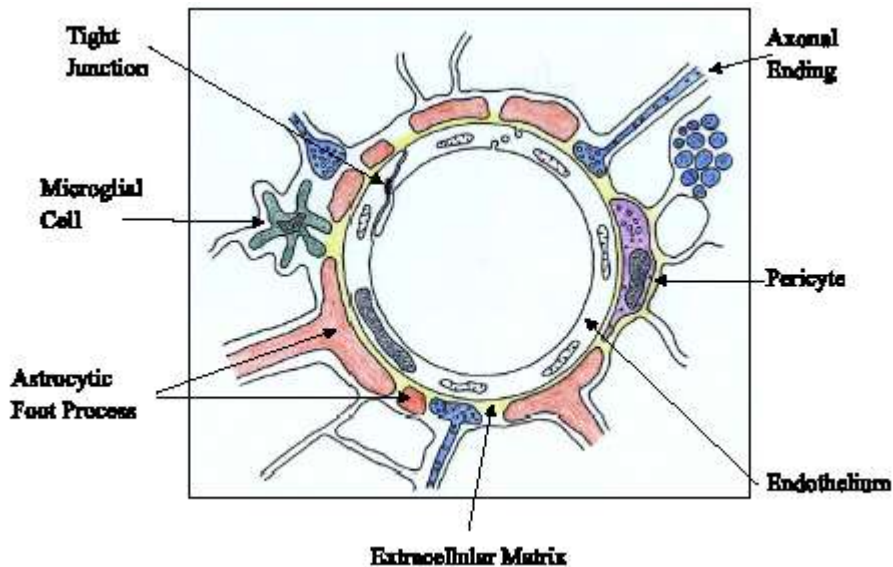
Figure 2.2. Schematic diagram of the neurovascular unit/cell association forming the BBB.

2.2.2 Anatomy and physiology of the cerebral capillary endothelia

The surface area of the brain microvasculature is ~ 100 cm$^2 \cdot$g^{-1} tissue, with the capillary volume and endothelial cell volume constituting approximately 1 % and 0.1 % of the tissue volume, respectively (Pardridge et al. 1990). The mean intercapillary distance in the human brain is ~ 40 μm (Duvernoy et al. 1983). This short distance allows for near instantaneous solute equilibration throughout the brain interstitial space for small molecules, once the BBB has been overcome. The microvasculature of the central nervous system (CNS) can be differentiated from the peripheral tissue endothelia in that it possess uniquely distinguishing characteristics:

a) Cerebral capillary endothelial cells contain *tight junctions*, which seal cell-to-cell contacts between adjacent endothelial cells forming a continuous blood vessel. The tight junctions between BBB endothelial cells lead to a high endothelial electrical resistance, in the range of 1500-2000 $\Omega \cdot$ cm^2 (pial vessels), as compared to 3-33 $\Omega \cdot$ cm^2 in other tissues (Crone and Christensen 1981; Butt et al. 1990). The electrical resistance across *in vivo* cerebral microvessel endothelial cells, of non-pial origin, has been estimated to be as high as 8000 cm^2 (Smith and Rapoport 1986). The net result of this elevated resistance is low

paracellular permeability.

The endothelial and epithelial tight junction consists of three integral membrane proteins: claudins, occludin, and a junctional adhesion molecule (JAM) which, together with several peripheral proteins, constitute the junctional complex (Fig 2.3). A number of peripheral proteins, regarded as scaffolding or linkers for the integral molecules of the tight junction in endothelia and epithelia, form a cytoplasmic plaque adjacent to the junctional cell membrane. The plaque proteins are part of the tight junction complex and include the guanylate kinases: ZO-1 (220 kDa), ZO-2 (160 kDa) and ZO-3 (130 kDa). Another plaque protein is cingulin (140 kDa), which is myosin-like and binds to the ZO complex and to F-actin of the cytoskeleton (Cordonesi et al. 1999).
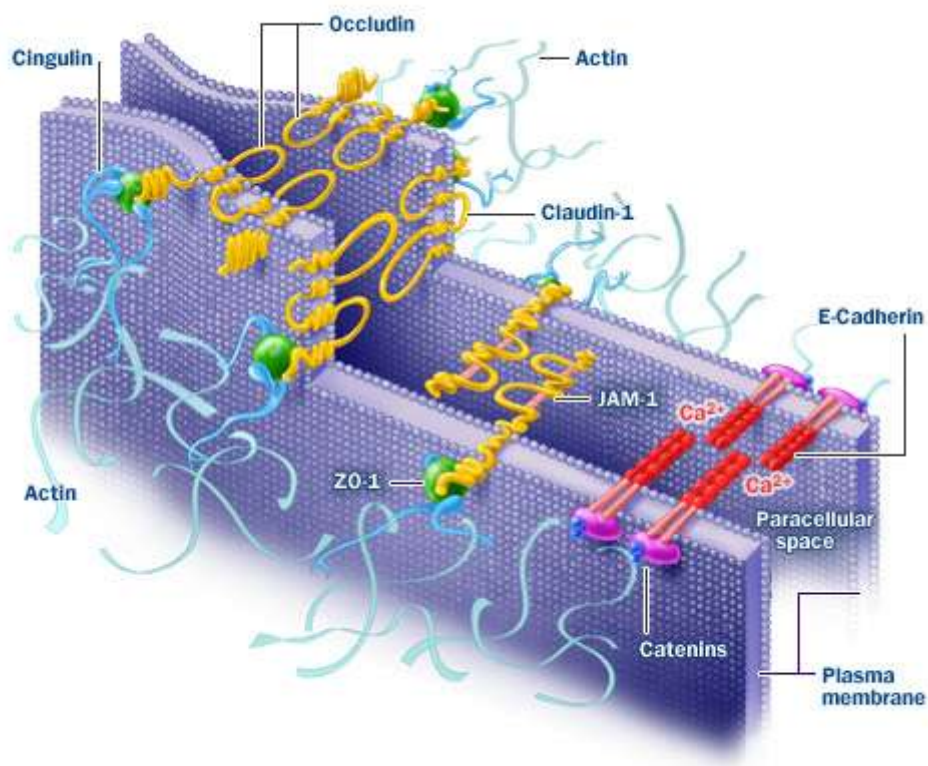
Figure 2.3. Schematic representation of *tight junctions*

 b) The cytoplasm of the *endothelial cell* is of uniform thickness, with very few pinocytotic vesicles (hollowed out portion of cell membrane filled with fluid, forming a vacuole which

allows for nutrient transport), and lack fenestrations (i.e. openings). Therefore, transit across the BBB involves translocation through the capillary endothelium, the internal cytoplasmic domain, and then through the ablumenal membrane and pericyte and / or basal lamina. Three principle types of transendothelial transport have been postulated.

c) There is a *greater number and volume of mitochondria* in BBB endothelial cells compared to peripheral endothelia in rat (Odendorf et al. 1977). This increase in mitochondria, and increased energy potential is thought to be required for active transport of nutrients to the brain from the blood. Oldendorf and Brown (1975) estimated that 5 - 6 times more mitochondria per capillary cross-section exist in rat cerebral capillaries than in rat skeletal muscle capillaries. These finding suggest that the enhanced cerebral capillary work capacity may be related to energy-dependent transcapillary transport.

d) There is also an *enzymatic barrier* at the cerebral endothelia, capable of metabolizing drug and nutrients (Brownlees et al. 1993; Brownson et al. 1994). These enzymes are principally directed at metabolizing neuroactive blood-borne solutes. Enzymes such as γ-glutamyl transpeptidase (γ-GTP), alkaline phosphatase, and aromatic acid decarboxylase are in elevated concentrations in cerebral microvessels, yet often in low concentrations or absent in non-neuronal capillaries.

e) A *polarity exists between the lumenal and ablumenal membrane surfaces* of the endothelial cells. The concept of the functional polarity of the BBB emerged from quantitative biochemical studies (Betz and Goldstein 1978). The enzymes γ-GTP and alkaline phosphatase are shown to be present at the lumenal endothelium, whereas Na^+-K^+-ATPase and the sodium dependent (A-system) neutral amino acid transporter are associated with the ablumenal portion of the endothelium (Betz et al. 1980). The glucose receptor GLUT-1 was shown, through use of immunogold labeling and electron microscopy, to have a 3 : 1 ratio of distribution, ablumenal to lumenal at the BBB (Farrell and Pardridge, 1991). Na^+-K^+-ATPase is enriched at the ablumenal surface (Betz et al. 1980). Additionally, the P-glycoprotein (P-gp) drug efflux transporter is presently thought to exist at the lumenal membrane surface, although arguments that P-gp is actually associated with the astrocytes which enfold the endothelial cells (Pardridge 1997) is presently being debated. Structural, pharmacological, and biochemical evidence for lumenal and ablumenal polarization of receptors, enzymes, and channels at the cerebral endothelia (Vorbrodt 1993) establishes the BBB to be a working non-stagnant membrane unequivocally evolved to maintain brain homeostasis.

2.2.3 Transport at the blood-brain barrier

2.2.3.1 Cell migration

The barrier endothelium that restricts polar solutes from entering normal brain also restrains circulating immunocytes. Activated cells, nevertheless, can penetrate the brain. T-lymphocytes, stimulated non-specifically, *in vitro*, with the mitogenic lectin, concanavalin-A and re-injected into blood, enter CNS randomly then leave. T cells not only enter the CNS but are retained within it only after they are presented with and recognize brain-specific antigens (Hickey 1999) (Fig 2.4 a). Passage across endothelium must be preceded by temporary adhesion of the lymphocytes to the endothelium by way of cell adhesion molecules expressed on both immunocytes and endothelium. Immunocytes migrate across CNS endothelium both paracellularly and transcellularly.

2.2.3.2 Passive diffusion

The passive diffusion proceeds from low to high concentrations. Simple diffusion is a spontaneous process depending on random movement of solutes. The free-energy change of a solute diffusing across a membrane is directly dependent on the magnitude of the concentration gradient (Fig 2.4 b).

2.2.3.3 Carrier-mediated efflux

The carrier-mediated efflux is involved in extruding drugs from the brain and is a major obstacle for many pharmacological agents, with the ABC (ATP binding cassette) transporter P-glycoprotein being the principle efflux mechanism of these agents (Cordon-Cardo et al. 1989) (Fig 2.4 c). There also exists efflux transporters for organic anions, via multidrug resistance associated protein (MRP) (Kusuhara et al. 1998), and anionic and cationic cyclic peptide (Tsuji 2000).

2.2.3.4 Facilitated diffusion

Facilitated diffusion is a form of carrier-mediated endocytosis, in which solute molecules

bind to specific membrane protein carriers, also from low to high concentration. The binding of a solute to a transporter on one side of the membrane triggers a conformational change in the protein; this results in a carrying through of the substance to the other side of the membrane, from high to low concentration. Facilitated diffusion is passive (i.e. energy independent) and contributes to transport at the BBB of substances such as monocarboxyates, hexoses amines, amino acids, nucleoside, glutathione, small peptide, etc. (Tamai and Tsuji 2000) (Fig 2.4 d).

2.2.3.5 Vesicular transport

Although certain ions and solutes are selectively transferred across CNS endothelium by special carriers, some solutes and viruses are transported across cells by vesicular transcytosis. Transcytosis begins as a microinvagination of the cell membrane to form a pit or caveola. The pit pinches off as a free vesicle that migrates across the cell to the opposite cell membrane to which it fuses and releases its contents into the periendothelial basal lamina. What little solute is incorporated by fluid-phase endocytosis in brain endothelium is usually destined for enzymatic degradation in cytoplasmic organelles such as lysosomes.

2.2.3.5.1 Receptor-mediated transcytosis (RMT)

This process provides a means for selective uptake of macromolecules. Cells have receptors for the uptake of many different types of ligands, including hormones, growth factors, enzymes, and plasma proteins. RMT occurs at the brain for substances, such as transferrin (Morgan and Moos 2002), insulin (Duffy and Pardridge 1987), leptin (Banks et al. 1996), and IGF-I & IGF-II (Duffy et al. 1988), and is a highly specific type of energy dependent transport (Fig 2.4 f).

2.2.3.5.2 Absorptive-mediated trancytosis (AMT)

AMT is triggered by an electrostatic interaction between a positively charged substance, usually a charge moiety of a peptide, the negatively charge plasma membrane surface (i.e. glycocalyx) (Gonatas et al. 1984). AMT has a lower affinity and higher capacity than receptor-mediated endocytosis. The development of many new drug delivery technologies focuses on AMT (Pardridge 1999).

2.2.3.6 Tight junction modulation

The phosporylation of the proteins constituting tight junctions enhances their permeability, as assesed *in vitro*, by the passive flux or extracellular probes such albumin or inulin. Moreover extracellular signals can influence the permeability of the tight junction by the cytoskeleton (Begley and Brightman 2003) (Fig 2.4 g).
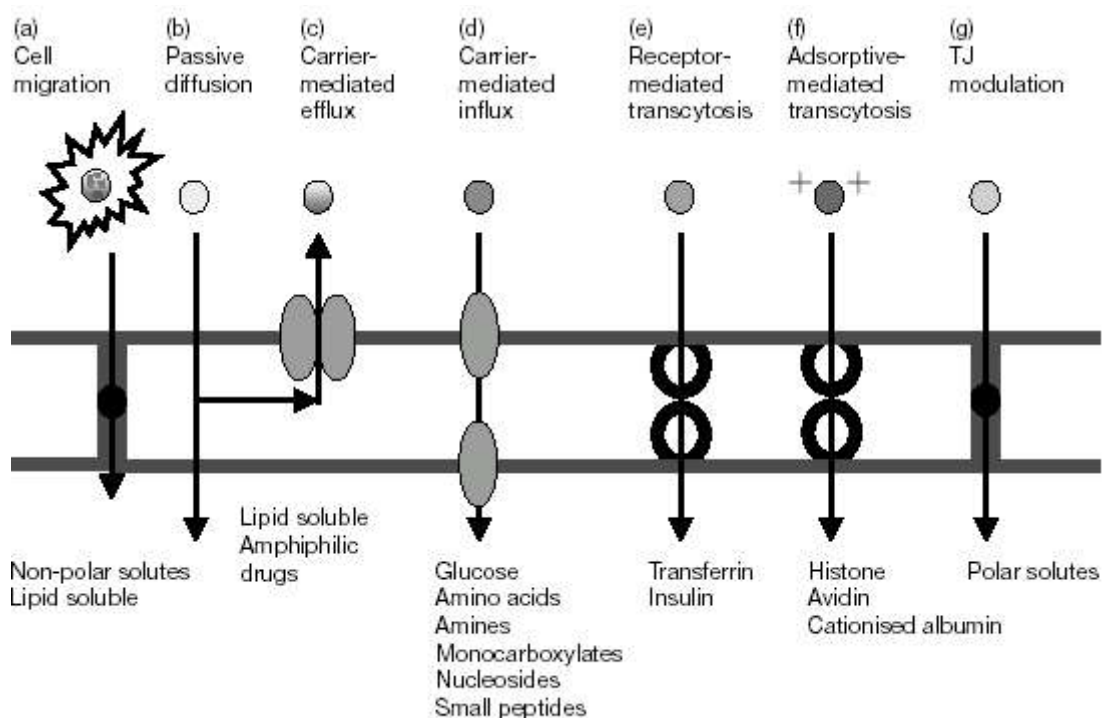
Figure 2.4. Potential routes for transport across the BBB. (a) Leukocytes may cross the BBB adjacent to, or by modifying, the tight junctions. (b) Solutes may passively diffuse through the cell membrane and cross the endothelium. Greater lipid solubility favors this process. (c) Active efflux carriers may intercept some of these passively penetrating solutes and pump them out of the endothelial cell. (d) Carrier-mediated influx, which may be passive or secondarily active, can transport many essential polar molecules such as glucose, amino acids, and nucleosides into the CNS. (e) RMT can transport macromolecules such as peptides and proteins across the cerebral endothelium. (f) AMT appears to be induced nonspecifically by negatively charged macromolecules and can also result in transport across the BBB. (g) Tight junctions may be modulated to allow an increased movement of polar solutes through the aqueus paracellular pathway.

2.3 Drug targeting

2.3.1 Background

The efficacy of many drugs is often limited by the difficulty to reach the site of action. In most cases, only a small amount of the administered dose of the drug reaches the site, while the rest of the drug is distributed to the rest of the body depending on its chemical-physical properties. A site-specific delivery would not only increase the amount of the drug reaching the site but also decrease the amount being distributed to other parts of the body, thus reducing unwanted site effect. Site-specific or targeted delivery, therefore, would also enable a reduction in the dose to be administrated. By decreasing side effects, it would also increase the therapeutic index of the drug.

A more specific accumulation at the target site may be achieved by altering the chemical structure yielding more suitable physicochemical and biochemical properties of the drug. This strategy involves the synthesis of either a totally new compound or a so-called prodrug from which the active drug is produced by the body's own metabolism. Although these approaches may be very successful in some cases, in others the synthesis of a more site-specific drug is not possible. For this reason, delivery of the original drug by specially designed drug delivery systems is the better solution.

A large number of drug delivery systems have been conceived and developed. Among these systems, colloidal drug delivery systems hold great promise for reaching the goal of drug targeting.

2.3.2 Strategies for drug targeting

The first idea of drug targeting was originally formulated by Paul Ehrlich in the nineteenth century. After visiting the opera *Der Freischütz* by Carl Maria von Weber, in which so called *Freikugeln* played a major role, Ehrlich came upon the idea of *Zauberkugel* - magic bullets (Kreuter 1992). The *Freikugeln* in the opera could be fired in any direction yet still reach their goal. Ehrlich imagined that similar targeted tiny drug-loaded magic bullet would significantly improve therapy.

In this model, the magic bullet is composed of two parts: drug and carrier (Fig 2.5). The targeting of the drug is achieved by a carrier that has a specific affinity to certain organs,

tissue, or cell.

Gregoriadis worked on the association between effective and tissue - unspecific drugs, and inactive and tissue - specific carrier systems (Gregoriadis 1977).

Afterwards Poste (Poste et al. 1984) and Davis (Davis and Illum 1986) differenced the concept of *Drug Targeting* into passive and active targeting.

Passive targeting is defined as a method whereby the physical and chemical properties of carrier systems increase the target/nontarget ratio of the quantity of drug delivered by adjusting these properties to the physiological and the histological characteristics of the target and non - target tissues, organs, and cells. Influential characteristics of passive targeting are chemical factors such as hydrophilicity/hydrophobicity and positive/negative charge and physical factors such as size and mass.
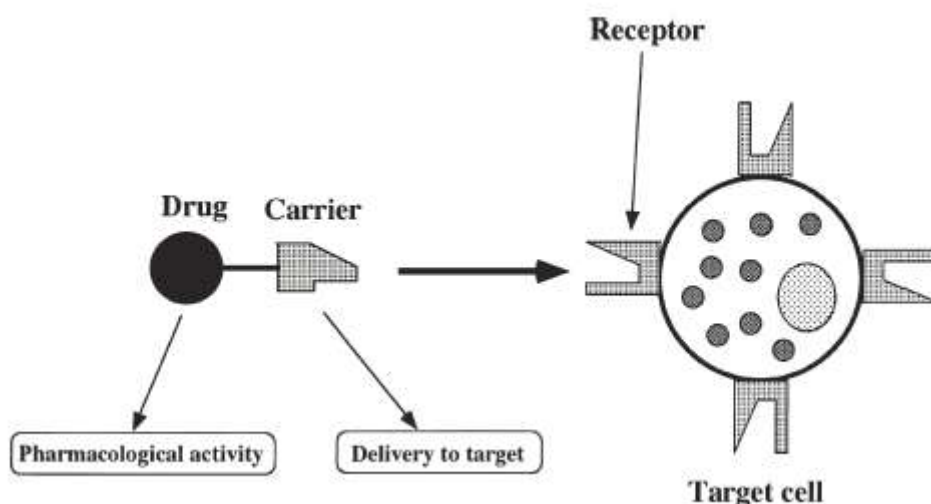
Figure 2.5. Concept of the magic bullet

The active targeting refers to efforts to increase the delivery of drugs to a target through the use of specific interactions at target sites where a drug's pharmacological activities are required.

The active targeting was classified from Widder (Widder et al. 1979) and Kreuter (Kreuter 1985) in:

Targeting 1. order -   Achievement of the capillary - bed of target organs

Targeting 2. order -   Accumulation in the cells of target organs

Targeting 3. order -   Accumulation in determined cellular - systems of target organs

2.3.3 Drug targeting applies to tumour

The ideal therapeutic system should attack only the tumour and should be not toxic for the healthy tissues. Colloidal systems possess the tendency to reach some type of tumour after intravenous injection (Matsumura and Maeda 1986).

This behaviour makes the colloidal systems a suitable carrier for cytostatic drugs. The reason of this behaviour is not fully explained so far, but it is indisputable that the increase of the tissue permeability and the adherence of particles to the tissues play a relevant role (Luo and Prestwich 2002; McDonald and Baluk 2002).

Furthermore, the growth of the tumour is associated to a inflammatory reactions, and this phenomenon leads to the enhanced endocytosis by endothelial cells, to the fenestration of endothelium, and to the migration of T-lymphocytes to the enflamed tissues (Mahaley 1968; Giometto et al. 1996; Tran et al. 1998).

The first colloidal systems applied for drug targeting were liposomes. A branch concerning the application of nanoparticles was developed from the liposome studies.

Sugibayashi employed nanoparticles for the cure of tumour in animals (Sugibayashi et al. 1979). He used 5-fluorouracil loaded albumin-nanoparticles for the treatment of Ehrlich-ascites-tumour. The nanoparticles loaded with 5-Fluorouracil showed a higher therapeutic effect in comparison to the free drug.

Kreuter used equally 5-fluorouracil bound to poly(butyl cyanoacrylate) nanoparticles as a carrier system (Kreuter and Hartmann 1983). The tumour investigated was a Crocker – Sarcoma - S 180. An increase of antitumoural activity of the drug but also toxic effects (leucopoenia, lose of weight, death of some animals) were observed.

Brasseur (Brasseur et al. 1980) employed PMMA, PHCA and PIBCA as nanoparticle material for the drug delivery. Again a higher therapeutic effect of the cytostatic drug used - dactinomycyn - was observed, whereas side effects were reduced overall.

Doxorubicin is one of the most important anthracyclines in oncology. However, this drug induces several dose limiting side effects as such cardiac miopathy, alopecia, etc. Couvreur (Couvreur et al. 1986) showed that the toxicity of doxorubicin bound to nanoparticles was

decreased, but this preparation was effective only for a form of leukaemia.

Further studies were carried out with the purpose to enlarge the therapeutic range of doxorubicin nanoparticles. Kattan (Kattan et al. 1992) investigated the effect of doxorubicin loaded PHICA particles on healthy men. He researched the tolerance of this preparation on healthy men, during the phase I of clinical trials. No cardiac toxicity was observed for 85 % of the volunteers. Fever was observed for some individuals and allergy reactions appeared only in one volunteer. The tolerated dose of doxorubicin nanoparticles preparations was established at 75 mg/m^2 at the conclusion of the study.

Further studies used PBCA nanoparticles coated with poloxamer as carrier system (Beck et al. 1993), and mitoxantrone was applied as the cytostatic drug.

2.3.4 Enhanced permeability and retention effect (EPR effect)

Differences in the structure and behavior of normal and tumour tissue could be used for designing drug delivery systems facilitating tumour-specific delivery of the drug or prodrug and specific drug activation. Generally, three locations in the tumour tissue are used as targets for delivery of anti-cancer drugs in drug delivery research: tumour vasculature, extracellular space in the tumour tissue, and tumour cells.

In principle, accumulation of polymer-based drugs in many tumours can be achieved by a nonspecific or by a specific targeting process. Tumour vasculature continuously undergoes angiogenesis to provide blood supply that feeds the growing tumour (Hanahan and Folkman 1996). High-molecular-weight (HMW) molecules and nano-sized particles accumulate in solid tumours at much higher concentrations than in normal tissues or organs due to the enhanced permeability and retention (EPR) effect (Maeda 2001; Seymour et al. 1995; Maeda et al. 2000, 2003). In this case, a leaky vasculature and limited lymphatic drainage, typical of tumour and missing in normal tissue, result in the accumulation of macromolecules, e.g. macromolecular drug carrier systems in the interstitial space of a large variety of tumours (Maeda 2001; Maeda et al 1992, 2001) (Fig 2.6). These systems can release cytotoxic drugs into the extracellular fluid of the tumour tissue (Christie and Grainger 2003; Takakura and Hashida 1995), or they can release a drug after entering the

umor cells via fluid-phase, adsorptive or receptor-mediated pinocytosis (Alberts et al 2002).
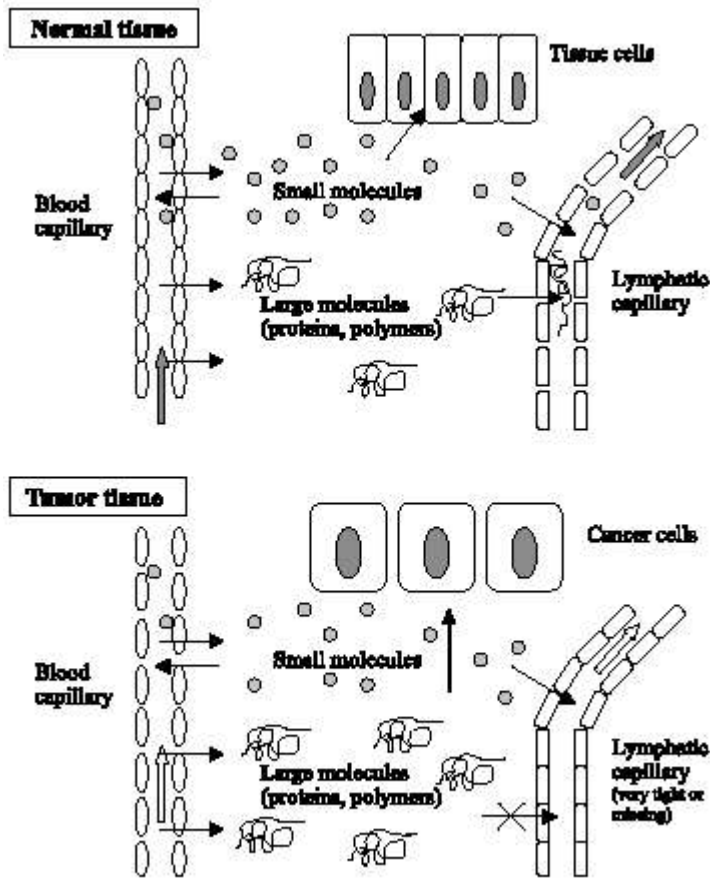
Figure 2.6. Schematic illustration of the EPR effect principle. Angiogenesis and enhanced vascular permeability of tumour capillaries and impaired or missing lymphatic clearance of macromolecules result in accumulation of macromolecules (polymers) in tumour tissue.

2.4 Nanoparticles

2.4.1 Background

Nanoparticles are solid colloidal particles ranging in size from 10 nm to 1000 nm (1 μm). They consist of macromolecular materials in which the active principle (drug or biologically active material) is dissolved, entrapped, or encapsulated, and/or to which the active principle is adsorbed or attached (Kreuter 1983). This definition includes not only particles with structures as described by Birrenbach and Speiser (1976) by the term "nanopellets" but also "nanocapsules" with a schell-like wall as well as "microspheres", if they are below 1μm in size (Kramer 1974; Widder et al. 1970; Kaufmann et al. 1979; Gallo et al. 1984). It also includes polymer lattices such the "molecular scale drug entrapment" products by Banker et al. (Goodman and Banker 1970; Larson and Banker 1976).

2.4.2 Nanoparticles as delivery system for CNS-targeting

The central nervous system (CNS) represents one of the most important human organ. Drugs penetrate hardly into this organ, and the chances to cure disease associated to the CNS are very limited. The cure of cerebral illness with nanoparticles was conceived relative early (Kabanov et al. 1989).

Tröster and Kreuter (1992) investigated the body distribution with labelled PMMA nanoparticles coated with different surfactants. They found out that the higher value of radioactivity in the CNS was associated with nanoparticles coated with polysorbate 80. Tröster explained this phenomenon by the adsorption on nanoparticles to the endothelial cells of cerebral capillaries.

Bochard demonstrated later, by in vitro studies, that bovine capillaries could take up nanoparticles coated with surfactants. He could assert that the velocity of nanoparticles uptake depends on the type of surfactant and on its quantity and the uptake occurred preferably for polysorbate 80-coated nanoparticles (Bochard and Kreuter 1993). Bochard attributed this phenomenon to a membrane permeabilization effect due to surfactants.
Kreuter and Alyautdin (Kreuter et al. 1995; Alyautdin et al. 1997) investigated the

transport of a drug into the CNS by PBCA particles *in vivo*. For this purpose, they used the opiate –receptor-agonist hexapeptide dalargin. This drug is not able to cross the BBB after intravenous injection. The high dose of 20 mg/Kg of dalargin has no effects (Kalenikova et al. 1988). After drug binding to nanoparticles coated with polysorbate 80 a antinociceptive effect was observed after intravenous injection. The effects appeared rapidly and reached the maximun after 45 minutes. The results were confirmed later by Schöder (Schröder and Sabel 1996).

Alyautdin repeated the experiments with nanoparticles bound to loperamide (Alyautdin et al. 1997). As dalargin, loperamide is not able to cross the BBB. The study showed that loperamide-nanoparticles coated with polysorbate 80 could reach the CNS. The maximal possible effect was observed at 15 min post injection. Tubocurarin was used in other studies (Alyautdin et al. 1998).

2.4.3 Mechanism of nanoparticles-mediated drug transport to the brain

A number of possibilities exist that could explain the mechanism of the delivery of substances across the BBB:

a) An increased retention of the nanoparticles in the brain blood capillaries combined with an adsorption to the capillary walls. This could create a higher concentration gradient that would enhance the transport across the endothelial cell layer and as a result the delivery to the brain.

b) A general surfactant effect characterized by a solubilization of the endothelial cell membrane lipids that would lead to membrane fluidization and an enhanced drug permeability through the BBB.

c) The nanoparticles could lead to an opening of the tight junctions between the endothelial cells. The drug could then permeate through the tight junctions in free form or together with the nanoparticles in bound form.

d) The nanoparticles may be endocytosed by the endothelial cells followed by the release of the drugs within these cells and delivery to the brain.

e) The nanoparticles with bound drugs could be transcytosed through the endothelial cell layer.

f) The polysorbate 80 used as the coating agent could inhibit the efflux system, especially P-glycoprotein (Pgp).

All these mechanisms also could work in combinations

At present the most likely mechanism of nanoparticle - mediated transport of drugs to the brain is the mechanism of endocytosis of the nanoparticles and release of the drug in these cells. Lück (1997) observed an adsorption of apolipoprotein E (apo E) on the surface of polysorbate 20, 40, 60 or 80-coated nanoparticles after incubation for 5 min in human citrate-stabilized plasma at 37° C. Only after polysorbate 20, 40, 60, or 80 overcoating an apo E adsorption was detected.

These results corroborate the in vivo findings where only polysorbate 20, 40, 60, or 80 induced an antinociceptive effect with dalargin nanoparticles whereas the other surfactants including those of the in vitro plasma incubation study were unable to induce a significant effect. The antinociceptive effect of the dalargin nanoparticles was significantly lower if the nanoparticles were incubated in apo E alone without polysorbate prior to injection, but it remained similar to coating with polysorbate 80 alone if the particles were coated with the polysorbate before the incubation with apo E (Alyautdin et al. 1997).

These results are a strong indication that apo E is involved in the nanoparticle-mediated drug transport to the brain.

Lipoproteins are of critical importance for the delivery of essential lipids to this organ. The presence of an LDL receptor in the BBB has been demonstrated by a number of authors (Dehouck et al. 1994, 1997; Méresse et al. 1989; De Vries et al. 1993; Lucarelli er al. 1997; Cecchelli et al. 1997), and apo E and apo A-I containing particles have been detected in human cerebrospinal fluid (Pitas et al. 1997). It is very possible that the polysorbate-coated nanoparticles mimic LDL-particles after apo E adsorption following injection into the blood. In this way they could act as Trojan horses by interacting with the LDL receptor leading to their uptake by endocytic processes. Hence, the role of polysorbates would be

that of an anchor for apo E.

2.4.4 Poly alkyl(butyl cyanoacrylate) nanoparticles

Poly alkyl(butyl cyanoacrylate) nanoparticles are generally prepared from butyl cyano acrylate monomers (Fig 2.6 a) by emulsion anionic polymerisation (Fig 2.6 b) in an acidic aqueous solution of a colloidal stabilizer such as dextran 70 000, polysorbates, and poloxamers. The polymerization is initiated by the hydroxyl ions of water, and elongation of the polymer chains occurs by an anionic polymerization mechanism. It should be pointed out that the anionic polymerization of such a reactive monomer can be controlled in an aqueous medium. The main parameters involved are the adjustment of the pH with a strong acid such as hydrochloric acid and the concentration of the anionic polymerization inhibitor (SO_2) in the monomer (Lescure et al. 1992). Inclusion of drug can be made during the polymerization process or by adsorption onto preformed nanoparticles. The length of the alkyl pendant governs degradation rates (Müller et al. 1990, 1992) and toxicity (Lherm et al. 1992; Kante et al. 1982) of poly(alkyl cyanoacrylate) nanoparticles, which decrease in the order methyl> ethyl> butyl/isobutyl> hexyl/isohexyl.
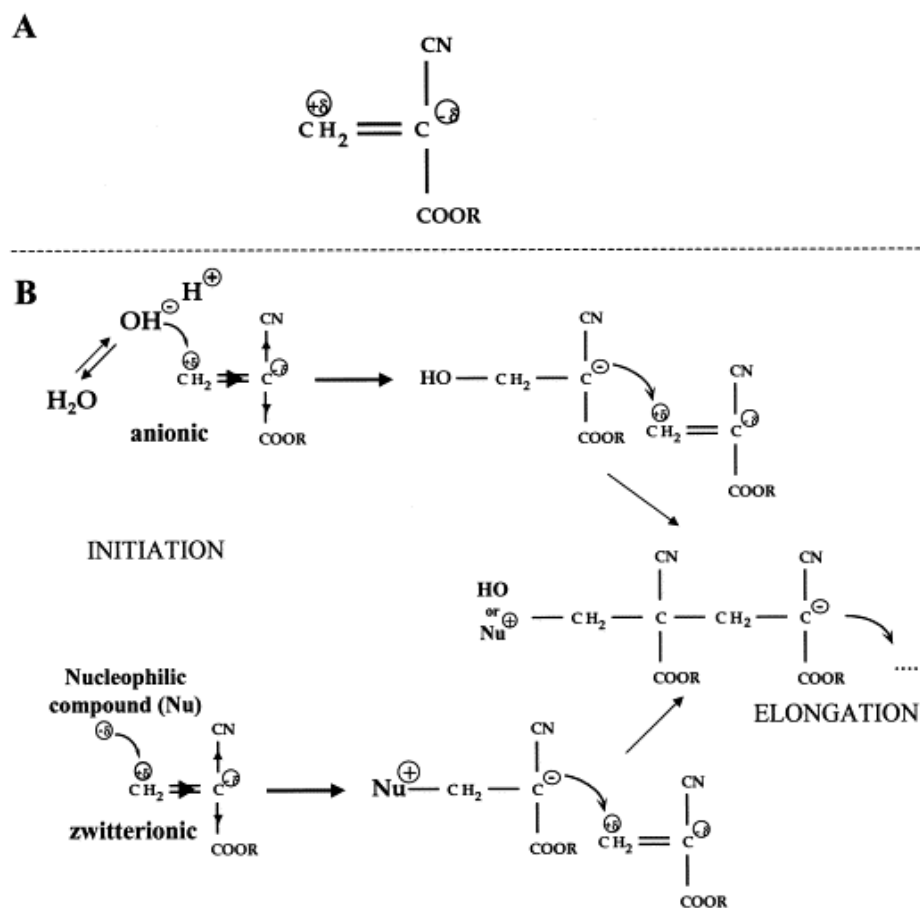
Figure 2.6. Chemical structure of alkylcyanoacrylates (A) and scheme of their anionic and zwitterionic polymerization (B).

2.5 Body distribution of nanoparticles after intravenous injection

2.5.1 Reticuloendothelial system uptake

After intravenous injection, nanoparticles, like other colloidal carriers, are taken up by the reticuloendothelial system (RES). The intravenously injected colloids mainly distribute into the RES organs liver (60-90 % of the injected dose), spleen (2-10 %), lungs (3-20 %) and a low amount (>1 %) into the bone marrow (Kreuter 1983b, 1985). It has been acknowledged for over a decade (Kreuter 1983c, Singer 1969) that coating of the injected colloid particulates with serum components - opsonins - precedes the uptake by the RES and that opsonization process strongly facilitates or even is necessary to induce phagocytosis of the particles (Van Oss et al. 1975, 1978, 1984; Borchard and Kreuter 1993).

The surface properties of the particles seems to influence strongly the spectrum of the adsorbed serum components (Blunk et al. 1991).

The adsorption of the serum components, mainly proteins, is competitive (Kim et al. 1974) and is found to be only partially reversible or even irreversible (Soderquist and Walton 1980). Soderquist and Walton supposed that the hydrophobic bounding was the predominant force in the adhesion of the protein to foreign surfaces. These hydrophobic interactions seem to occur due to the unfolding of the proteins that reveals the hydrophobic interior. This process optimizes hydrophobic interactions and increases the entropy of the adsorbed material.

The opsonins coat around the injected particulates then seems to trigger their uptake by cells of the RES (Van Oss et al. 1975, 1984; Van Oss 1978).

2.5.2 Modification of body distribution by coating with surfactants

Based on the above assumption that opsonin adsorption determines the body distribution of nanoparticles, it can be speculated that different surface properties of the particles will lead to a different spectrum as well as to different quantities of adsorbed serum component (Wilkins 1967a). It can further speculated that different types of adsorbed serum components will prevent or trigger the uptake of different cells of the RES. Following along these lines it was early suggested to design or artificially alter the surface properties

of the particles in order to alter and later to be able to monitor their body distribution (Kreuter 1983b; Wilkins 1967a, b).

Illum et al. (1983, 1984, 1986a, 1987), Leu et al. (1984), and Tröster et al. (1988, 1990, 1992a, b) used surfactants and polymers to coat nanoparticles in order to modify their body distribution. All authors could show that surfactants coated onto the surface of the particles reduce the nanoparticle liver uptake and simultaneously increase their blood serum concentration.

In their study, Tröster et al. (1990, 1992a, b) investigated 13 surfactants as coating materials for ^{14}C-labelled nanoparticles and examined the radioactivity in organs and tissue at different time points after intravenous injection to rats. Among these surfactants two lead substances were identified by the work of Tröster et al., poloxamine 1508 and polysorbate 80. Poloxamine 1508 reduces lever uptake and keeps the particles in the blood circulation. Since this material in not available any more, poloxamine 908 may be used. Polysorbate 80 was overall the optimal material for increasing nanoparticles concentration in non - RES organs (Tröster et al. 1990).

2.5.3 Mechanism of the reduction of the RES uptake

Studies were carried out to explain the mechanism of the reduction of the RES uptake and especially the liver uptake and the simultaneous increase in blood circulation time and increased distribution into other organs and tissues. Hydrophilicity of the particles definitively plays an important role. However, hydrophilicity does not explain all *in vitro* and all body distribution data. Tröster and Kreuter (1988) determined the contact angles of surfactant solutions on poly(methyl methacrylate) nanoparticles. They observed that low receding angles were combined with long blood circulation times and a low liver uptake of particles coated with these surfactants. They challenged their observations experimentally but they found out the polyoxyethylene(23)laurylether, which fulfils the contact angle requirement, had no influence on the body distribution on the nanoparticles in comparison to the uncoated nanoparticles (Tröster et al. 1990; Tröster and Kreuter 1992).

Other hypothesises to explain the efficacy of surfactants in preventing the liver and RES were made by Illum at al. (1986). They suggested that an increasing length of the hydrophilic polyoxyethylene chains protruding into the aqueous serum phase, and consequently the increasing thickness of the hydrophilic coat, would reduce the

opsonization and subsequently the RES uptake by steric stabilization.

Carstensen et al. (1991), Wesemeyer et al. (1993), and Tröster et al. (1992b) later observed that in the case of poloxamers an increased polyoxyethylene chain length and coating layer thickness indeed reduced the hydrophobicity as well as the RES uptake.

Presently the mechanism of the reduction of the RES uptake and the increase in blood circulation time is not totally explained.

2.6 Nanoparticles drug release

2.6.1 Background

Drug release from biodegradable polymeric nanoparticles depends on the Fickian diffusion through the polymer matrix and on the degradation rate of the polymer. The prediction of the release profile is complex because it results from a combined effect of various parameters: solid-state drug polymer solubility (Panyam et al. 2004) and drug-polymer interactions (Niwa et al. 1994, Perracchia et al. 1997, Lee et al. 2004, Ubrich et al. 2004), polymer degradation rate (Horisawa et al. 2002), block copolymer molecular weight and polydispersity (Matsumoto et al. 1999), water uptake by nanoparticles (Quellec et al. 1999) and drug solubility in the biological medium. In most studies, *in vitro* release profiles are characterized by an initial fast release (burst) of drug close to or at the surface followed by a sustained release (Perracchia et al. 1997, Matsumoto et al. 1999, Ubrich et al. 2004). Removing the low molecular weight fraction from the polymer was shown to reduce the initial burst of drug release (Matsumoto et al. 1999). Depending on formulations *in vitro*, drug releases last from a few hours (Allemann et al. 1993, Perracchia et al.1997, Ubrich et al. 2004) or a few days (Dong et al. 2004) to several weeks (Allemann et al. 1993, Fishbein et al. 2004, Horisawa et al. 2002, Feng et al. 2004).

2.6.2 Release Mechanisms

Nanoparticles exhibit their special drug effect in most cases by direct interaction with their biological environment (Diepold et al. 1989; Kreuter 1983d). Drug release may occur by different mechanisms.

2.6.2.1 Diffusion

Diffusion occurs when a drug or other active agent passes through the polymer that forms the controlled-release device. The diffusion can occur on a macroscopic scale — as through pores in the polymer matrix — or on a molecular level, by passing between polymer chains.

2.6.2.2 Nanoparticles matrix erosion

The release of the drug by nanoparticle erosion occurs in case of biodegradable polymers. These materials degrade within the body as a result of natural biological processes, eliminating the need to remove a drug delivery system after release of the active agent has been completed.

Most biodegradable polymers are designed to degrade as a result of hydrolysis of the polymer chains into biologically acceptable, and progressively smaller, compounds. Degradation may take place through bulk hydrolysis, in which the polymer degrades in a fairly uniform manner throughout the matrix. For some degradable polymers the degradation occurs only at the surface of the polymer, resulting in a release rate that is proportional to the surface area of the drug delivery system.

2.6.2.3 Desorption of surface-bound drug

The release of drugs adsorbed onto the particles surface is usually faster and the burst release higher compared to encapsulated drugs since only desorption and diffusion process have to take place but no degradation of the polymer (Brasseur et al. 1991). The release of the adsorbed drug depends on the affinity of the drug to the particle surface and to the release medium (Wood et al. 1985, Fresta et al. 1996).

2.6.3 Study of drug release *in vitro*

The release rate of drugs from nanoparticles is strongly influenced by the biological environment. For example the coating of particles by plasma proteins (Kreuter 1983c) can create an additional barrier and lead to a retardation of the release, or the interaction with

biological membranes can lead to an enhanced delivery of drugs though these membranes (Kreuter 1983d, Diepold et al. 1989). As a consequence, the *in vitro* drug release may have very little in common with the delivery and release situation *in vivo* as frequently observed (Harmia et al. 1986, Diepold et al. 1989).

The characterization of the *in vivo* drug release from a colloidal carrier is difficult to achieve. This can be attributed to the inability of effective and rapid separation of the particles from the dissolved or release drug in the surrounding solution.

The common methods for determining the in vitro release are the following:

- Side by side diffusion cells with artificial or biological membranes (Harmia et al. 1986, Diepold et al. 1989, Kreuter et al. 1983d, Cappel and Kreuter 1991).
- Dialisys bag diffusion techniques (Krause et al. 1986, El-Samaligy 1986, Watanabe et al. 1978, Malaiya and Vyas 1988).
- Reverse dialysis sac techniques (Cappel and Kreuter 1991).
- Ultracentrifugation (Krause et al. 1986).
- Centrifugal ultrafiltration techniques (Magenheim and Benita 1991).

2.7 Isotope and devices detecting radioactivity

2.7.1 Carbon-14

Carbon-14 is a radioactive isotope of carbon discovered on 27th February, 1940, by Martin Kamen and Sam Ruben (Kamen er al.1985).

Its nucleus contains 6 protons and 8 neutrons. Its presence in organic materials is used in radiocarbon dating. It occurs naturally and has a relative abundance of 0.001 %. The half-life of carbon-14 is 5730 years. It decays into nitrogen-14 through beta-decay.

$$^{14}_{6}C \rightarrow ^{14}_{7}N + ^{0}_{-1}\beta$$
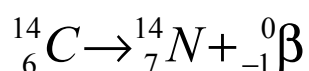
It is produced in the upper layers of the troposphere and the stratosphere by thermal (low energy) neutrons absorbed by nitrogen. It can also be produced in ice by high-energy neutrons causing spallation reactions in oxygen.

Carbon-13	Isotopes of Carbon	Carbon-15
Produced from: **Nitrogen-18** **Boron-14**	**Decay chain**	Decays to: **Nitrogen-14**

2.7.2 Liquid scintillation counting

Liquid scintillation counting is a standard laboratory method in the life-sciences for measuring radiation from beta-emitting nuclides. Scintillating materials are also used in differently constructed counters in many other fields.

Samples are dissolved or suspended in a "cocktail" containing an aromatic solvent (historically benzene or toluene, but more recently less hazardous solvents have come into favor) and small amounts of other additives known as fluors. Beta particles emitted from the sample transfer energy to the solvent molecules, which in turn transfer their energy to the fluors; the excited fluor molecules dissipate the energy by emitting light. In this way, each beta emission (ideally) results in a pulse of light. Scintillation cocktails often contain

additives that shift the wavelength of the emitted light to make it more easily detected.

The samples are placed in small transparent or translucent (often glass) vials that are loaded into an instrument known as a liquid scintillation counter. The counter has two photomultiplier tubes connected in a coincidence circuit. The coincidence circuit assures that genuine light pulses, which reach both photomultiplier tubes, are counted, while spurious pulses (due to line noise, for example), which would only affect one of the tubes, are ignored.

Counting efficiencies under ideal conditions range from about 30 % for Tritium (a low-energy beta emitter) to nearly 100 % for phosphorus-32, a high-energy beta emitter. Some chemical compounds (notably Chlorine compounds) and highly colored samples can interfere with the counting process. This interference, known as "quenching", can be overcome through data correction or through careful sample preparation.

3 Materials and Methods

3.1 Nanoparticles

3.1.1 Materials

3.1.1.1 Chemicals

Dextran 70 000……………………………………………………………*Sigma,Dreisenhofen*

Doxorubicin hydrochloride (Adriablastin®)…………..……………………. *Sicor, Rho-Milan*

D(-)Mannitol…………………………………………………………… *Merk, Darmstadt*

n-butyl-2-cyanoacrylate………..………………………………….....*Sichelwerte, Hannover*

iso-butyl-2-cyanoacrylate…………………………………………*Sichelwerte, Hannover*

1N sodium hydroxide.. *Merck, Darmstadt*

3.1.1.2 Instruments

Becker……………………………………………..…………………. *Schott, Mainz*

Freeze dryer….. *LYOVAC® GT 2, Koln*

Glasfilter……………………………………………………………......

Schott,Mainz   Pipettes...………………………………………………………

Eppendorf, Hamburg

Stirrer..*IKA®, Staufen*

3.2 Nanoparticles preparation

3.2.1 Poly(butyl cyanoacrylate) nanoparticles

Poly(butyl cyanoacrylate) nanoparticles were prepared by emulsion polymerisation. The cyanoacrylate monomers were added to the aqueous polymerisation medium in a concentration of 1 % (w/v) (Kreuter 1992). Because the solubility of the cyanoacrylate

monomers were exceeded at this concentrations, monomer droplets were formed and the system had to be stirred permanently. These droplets acted as monomer reserves and single molecules of monomer were progressively released to form the polymeric chain. The polymerisation mechanism is an anionic process initiated by OH^- ions resulting from the dissociation of water. This OH^--induced polymerisation is very rapid. For this reason the reaction was carried out at pH 2 using an aqueous solution of 0.01 HCl (pH 2). To avoid the agglomeration of growing particles, it was necessary the addition of Dextran 70 000 in the concentration of 1 % (w/v) as sterical stabilizer (Douglas et al. 1984, 1985). Particles adsorb dextran from the solution and the sterical interaction between the particles prevents their agglomeration. The polymerization was stopped after 4 h neutralizing with 0.1N NaOH in the amount necessary to obtain a suspension of pH 7. The nanoparticle suspension was filtered through a sintered glass filter G2 (pore size of 90-150 μm) to remove polymer residuals. The final suspension of nanoparticles was lyophilised in vials of 1-2 ml with the addition of 3 % mannitol as cryoprotector.

3.2.2 Doxorubicin poly(butyl cyanoacrylate) nanoparticles

Doxorubicin poly(butyl cyanoacrylate) nanoparticles (DOX-PBCA NP) were prepared by anionic polymerisation as previously described (paragraph 3.2.1). Doxorubicin hydrochloride was added as a solution to the mixture to obtain a final concentration 0.25 %. The polymerisation process was carried out for 2.5 h instead of 4 h in order to prevent the degradation of doxorubicin in the acid medium.

3.2.3 Different formulations of doxorubicin poly(butyl cyanoacrylate) nanoparticles

Different formulations of doxorubicin nanoparticles were prepared and characterized changing the parameters of normal procedure (paragraph 3.2.2) in order to obtain nanoparticles with a higher content of bound doxorubicin.

The changed parameters were the following:

pH: Nanoparticles were prepared at different pH (pH 2, pH 3, pH 4) to compare the loading of the DOX-PBCA NP obtained.

Concentration of n-butylcyanoacrylate : Concentration of 0.75 % w/v , 0.5 % w/v, 0.25 % w/v of n-butylcyanoacrylate were used instead of 1 % w/v of n-BCA.

Type of monomer: DOX-PBCA NP were prepared using iso-butylcyanoacrylate instead of n-butylcyanoacrylate. The concentration of iso-BCA used was 1 % w/v.

Concentration of dextran: 2 % w/v, 1 % w/v, 0.5 % w/v solutions of dextran were used to prepare DOX nanoparticles.

Type of steric stabilizer: 1 % w/v solution of Pluronic F 68 was used as steric stabilizer instead of 1 % w/v solution of dextran 70 000.

Polymerization time: the process of polymerization war prolonged to 4 h in presence of DOX. Moreover DOX was added into the medium before the monomer.

3.3 Nanoparticles characterization

3.3.1. Size

3.3.1.1 Principle

Size is one of the most important feature of nanoparticles. Other parameters, such as molecular weight and density, influence nanoparticles release and degradation properties, whereas charge, surface, hydrophilicity, and hydrophobicity influence the interaction with the biological environment.

The size was determined by photon-correlation spectroscopy (PCS) or dynamic light scattering. Photon-correlation spectroscopy determines the hydrodynamic diameter of the nanoparticles via Brownian motion, which requires knowledge of the exact viscosity of the medium.

3.3.1.2 Equipment

PCS.. Malvern Zetasizer 3000HS$_A$, Worcs, U.K.

3.3.1.3 Working parameters

Scattering angle…………..……………………………………………………………90°

Temperature…………..……………………………………………………………….25°

Viscosity………………..…………………………………….…………………………..0.01 poise

Refractive index…………………………………………………………..……………1.333

3.3.1.4 Size determination

Particle size and polydispersity of the size distribution was measured after dilution of the NP suspension approx. 1 : 40 with Milli-Q water using a Malvern Zetasizer.

3.3.2 Doxorubicin assay

3.3.2.1 Principle

Assay of doxorubicin in the freeze-dried formulation was performed by spectrophotometry after dissolution of poly(butyl cyanoacrylate) and doxorubicin.

3.3.2.2 Equipment

Spectrophotometer…………………………..UV-DU 800, Beckmann Coulter, Hannover

3.3.2.3 Procedure

3.3.2.3.1 Calibration curve

Accurately weighed quantities of doxorubicin hydrochloride were dissolved in a mixture of water - DMF (2 : 7) to obtain solutions with known concentrations in the range of 10 - 60 µg/ml. The spectra of these solutions were registered against the same mixture, and absorption was measured in the maximum at 480 nm by spectrophotometer. The calibration graph was plotted.

3.3.2.3.2 Sample preparation

2 ml of DMF was transferred into a vial with the freeze-dried formulation. The vial was placed in the ultrasonic bath for 15 min, then 3 ml of mixture water - DMF (2 : 7) was added, and the vial was stored at room temperature for 1 h to ensure polymer dissolution. Then the content of the vial was quantitatively transferred into 50 ml volumetric vessel and

diluted to the volume with the mixture water - DMF (2 : 7). 5 ml of this mixture were transferred into a 50 ml volumetric vessel and diluted to the volume with the same mixture (= sample solution). The absorbance of the sample solution was measured and the concentration of doxorubicin in the sample was calculated using the calibration graph.

The amount of doxorubicin in the vial (Ct) is calculated as follows:

$$Amount\ of\ doxorubicin\ in\ the\ vial\ (mg) = Ct = \frac{Cs \times 5 \times 10 \times 10}{1000} = \frac{Cs}{2},$$

where

$Cs =$ concentration of doxorubicin in the sample (μg/ml)

3.3.3 Drug loading

3.3.3.1 Principle

Drug loading is a relative amount of drug bound to the nanoparticles. Drugs are bound to the nanoparticles mainly by absorption, that is an equilibrium process and usually some amount of the free drug remains in the medium. Hence this parameter reflects the efficacy of drug sorption into the polymer matrix. The method of choice for the determination of drug loading is the separation of the particles by ultracentrifugation and following quantitative analysis of the free drug in supernatant.

Drug loading was assessed in the lyophilized formulation after reconstruction. The assay of free doxorubicin was performed by spectrophotometry and by HPLC and the results of the two methods were compared.

3.3.3.2 Determination by spectrophotometer

3.3.3.2.1 Equipment

Spectrophotometer……………………………..UV-DU 800, Beckmann Coulter, Hannover
Centrifuge……………………………..………………………..…5415 D, Eppendorf, Hamburg
Microcentrifuge Filters…..MWL 100,000 Da, Polysulfone membrane, Sigma, Deisenhofen

3.3.3.2.2. Calibration Curve

Accurately weighed quantities of doxorubicin hydrochloride were dissolved in water to

obtain solutions with known concentrations in the range of 1 - 25 µg/ml. The spectra of these solutions were measured against water, and the adsorption was determined at the maximum of 480 nm using a spectrophotometer.

3.3.3.2.3 Sample preparation

The contents of the vials with the lyophilised DOX NP were reconstituted in 2 ml of water. 200 µl of resuspended nanoparticles were transferred to a microcentifuge filter, and centrifuged for 40 min at 13 200 rpm. 100 µl of clear supernatant was carefully evacuated with a pipette and diluted 100 - fold with water. The spectra of the samples were recorded against water, and the adsorption was measured in the maximum at 480 nm.

Relative drug loading (% of total amount) was calculated by subtraction of the free drug amount in the supernatant from the total amount in the vials.
Relative drug loading is calculated as follows:

% drug loading = Ct-(Cf /10) /Ct x 100%,
where
Ct= concentration of total doxorubicin used to prepare nanoparticles (mg/ml)
Cf= concentration of doxorubicin in the sample solution (µg/ml).

3.3.4.2 Determination by HPLC

3.3.4.2.1 Equipment

Liquid chromatograph…………………..…………….D-7000, Merck-Hitachi, Darmstadt

Packing………………………………LiChrospher® 100 RP-18 (5µm), Merck, Darmstadt

Column…………..……………LiChroCART® 250-4 HPLC-Cartridge, Merck, Darmstadt

Guard column…….………………………….…………LiChroCART® 4-4, Merk,Darmstadt

3.3.4.2.2 Working parameters

Flow rate……………………………………………………………………0,8 ml/min

Detector wavelength…….…………………………………….……………….. 250 nm

Injection volume ……………………………………………….……………….. 20 µl

Temperature……………………………………………………….…………….. ambient

Mobile phase………….. mixture of phosphate buffer (pH 1.4; 0.01M) acetonitrile (60:40)

3.3.4.2.3 Calibration curve

Accurately weighed amounts of doxorubicin were dissolved in 5 ml of the mobile phase. This solution was further diluted with the mobile phase to obtain solutions with known concentrations in the range of 1 – 25 µg/ml. The chromatograms of these solutions were registered and the peak areas were measured.

3.3.4.2.4 Sample preparation

The procedure for the sample preparation was the same as for the samples measured by spectrophotometer (3.3.3.2.3).

Peaks area were measured and the amount of doxorubicin in the samples was estimated.

Calculation of relative drug loading by HPLC was described above (3.3.3.2.3). The percent of drug loading was measured for DOX PBCA NP prepared as usual (3.2.2) and for different formulations of DOX NP by spectrophotometer and by HPLC.

3.3.5 Yield (gas chromatography)

3.3.5.1 Equipment

GC system………..……….…………HP5890 Series II, Hewlett Packard, Bad Homburg

Column…………..…………..Fused Silica Capillary Column, Permabon-FFAP-DF-0,1

5 m x 0,25 mm ID, Machery-Nagel, Düren

3.3.5.2 Working parameters

Injector-temperature………..……………… 250°C (split / splitless HP 19251 – 60540)

Detector (FID)…………………………………………………….. temperature: 250°C

Oven temperature……................. (gradient) 45°C (3 min) → 10°C 1/min → 130°C (4 min)

Gas:

- Aux gas: Helium 5.0

- Column flow: 1.0 ml / min

- Split flow: 10.0 ml /min

- Septum flow: 1.1 ml / min

- Column + Aux: 35 ml / min

- Column + Aux + Air : 430 ml / min

- Column + Hydrogen + Aux: 65 ml / min

- Column head pressure : 94 kPa

3.3.5.3 Procedure

The polymerisation yield was measured by means of gas chromatography (GC) as described by Langer et al. (1994, 1997). 0.5 ml of NP suspension were mixed with 0.5 ml of 2 N NaOH and shaken overnight at room temperature to hydrolyse to polymer. 50 µl of this solution were mixed with 50 µl of internal standard (pentanol approx. 0.5 %, accurately weighted) and diluted with 900 µl of Milli-Q water. 500 µl of this dilution were extracted with 1000 µl of methylene chloride. The methylene chloride was dried with water-free sodium sulphate and 1 µl of the sample was injected into the GC system.

3.4 Nanoparticles release studies

3.4.1 Background

The drug release studies present difficulties due to the small size of particles. Therefore it is necessary optimise the system of drug release.

Different methods are necessary to determine the drug release, considering that the contemporary drug release assessment is possible only for determinate drugs. These methods are:

- Filtration through small porosity filters

- Dialyse

- Ultracentrifugation

By all the procedures mentioned exists the problem that during the estimation of the drug released, the process of drug release continues. The exact kinetic of drug release is not possible by fast release process.

Although the extreme difficulty to realize the optimal drug release system, this study was performed.

3.4.2 Materials

Dyalisis Tube………………………….….…Spectra/Por ® *CE, Irradiated DispoDialyzer*

Spectrum Laboratories Inc, Breda, Netherlands

Microtubes…………….………….…….……………… Safe-seal micro tube 2 ml, Nümbrecht

Microcentrifuge Filters…………..…………… Ultrafree -Mc 100 000 NMWL Filter Unit

Millipore Corporation, Bedford, U.S.A.

3.4.3 Methods

The release of DOX from nanoparticles was studied. Different methods were used to evaluate the kinetics of drug release. These are described as follows:

3.4.3.1 Dialysis membrane

1 ml of nanoparticles was diluted with 4 ml of water and the total amount of 5 ml was transferred to a dialysis tube (MWCO 300 000). The content of doxorubicin introduced in the dialysis tube was 0.5 mg/ml. The dialyse occurred against 54 ml of 0.9 % NaCl solution. This volume was chosen to reach a detectable doxorubicin concentration. The maximal concentration that could be detected was 46.3 μg DOX/ml. At various intervals (5 min, 10 min, 15 min , 30 min, 45 min, 1 h, 2 h, 4 h, 8 h) 1 ml of the dialysis solution was sampled. The concentration of drug was measured by HPLC.

The release studies by dialysis membranes were performed for the following preparations: standard preparation of DOX-PBCA NP, DOX-PBCA NP with improved loading, NP polymerised with the monomer iso-BCA, DOX solution.

3.4.3.2 Microtubes

1 ml of doxorubicin nanoparticles was transferred into a glass beaker containing 53 ml of NaCl 0.9 %. The maximal doxorubicin concentration attainable was 46.3 μg DOX/ml. This concentration was required to compare the release results by dialysis membranes and by microtubes. At intervals of 5 min, 10 min, 15 min , 30 min, 45 min, 1 h, 2 h, 4 h, 8 h, 1 ml of solution was taken and introduced into a microtube. The samples were centrifuged for 5 minutes and the surnatants were analysed by HPLC. The results obtained with these methods were not reliable and therefore only the release study of one nanoparticles formulation (standard preparation of DOX-PBCA NP, paragraph 3.2.2) was conducted.

3.4.3.3 Microcentifuge filters

The procedure was similar to microtubes (3.4.2.2). Microcentrifuge filters (MWCO 100000) were filled with 0.3 ml of solution, and the filtrate was analysed after centrifugation by HPLC. Due to the unreliability of this method, the study was performed only for the standard preparation of doxorubicin nanoparticles (3.2.2).

3.5 Study of body distribution after intravenous particles injection in rats

3.5.1 Materials

Butyl-2-cyano[3-^{14}C]acrylate nanoparticles……..Amersham Biosc, Buckinghamshire, UK

1-ml insulin syringe………..Benson & Dickson, Dublin

Irland Glue.............................Turbo 2000 Kleber Universal, Boldt & Co, Wermelskirchen

Pentobarbital……………..…………………………………………….Merial , Helbergmoos

Polysorbate 80 (Tween$^{®}$ 80)………………..……………………………..…. Fluka, Buchs

Physiological solution…….…………..…………....……. Ampuva$^{®}$, Fresenius, Bad Homburg

Standard rat diet... Harlan-Winkelmann, Borchen

Stereotactic device……………………………………….… Leitz, Wetzlar Tuberculin

Syringe……...…………….................................………………………B.   Braun, Melsungen

Ultrasonicator...Brasonic   12   Europa   B.V,   Soest, Netherlands

3.5.2 Animals

The animals used are Wistar-Rats. They were provided from Harlam Winkelmann GmgH, Borchen, Germany. The animal experiments were performed in accordance to the Russian Guidelines for Animal Experiments and authorized by the Russian Ministry of Health (1045-73 and 52-F3-24.04.95) or the German Tierschutzgesetz and the Allgemeine Verwaltungsvorschrift zur Durchführung des Tierschutzgesetzes and were authorized by the Regierungspräsident Darmstadt (II 25.3 – 19 c 20/15 – F 31/10).

3.5.3 Animals keeping

The rats were kept at 24 ± 2 °C and at 55 ± 10 % of humidity. They were acclimatized for 1 week and caged in groups of five. They were fed *ad libitum* with standard laboratory food and water.

3.5.4 Choose of animals

Four male rats with body weight between 180 - 220 were used for the injection of each preparation at each time point.

3.5.5 Tumour model system

The employed 101/8 tumour-cell-line came from the laboratory of A.S. Khalansky, Institute of Human Morphology, Moskow, Russia. The tumour cells were initially produced by local injection of an α-di-methylbenzanthracene (DMBA) pellet into a rat cerebellum and maintained by continuous passages by intracerebral implantation. For long-term storage the tumour tissue was kept at $-196°$.

3.5.6 Tumour inoculation

For tumour implantation, animals were deeply anesthetized by intraperitoneal injections of pentobarbital (50 mg/kg) and then placed in a stereotactic device. Through a midline sagittal incision, a burr hole of 1.5 mm in diameter was made with a dental drill at a point 2 mm posterior to the right coronal suture and 2 mm lateral to the sagittal midline. Tumour material (approx. 10^6 cells) from the frozen stock was introduced into a tuberculin syringe linked to a 21-gauge needle. The tip was placed 4 mm below the bone surface and the tumour tissue was injected into the bottom of the right lateral ventricle. The scalp incision was sewn or closed with glue. After development of pronounced clinical signs of the disease (usually day 14) the animals were sacrificed by carbon dioxide asphyxiation, then decapitated. The brain was immediately removed. The tumour was excised and chopped with a scalpel; a tumour implant (5 mg) was inoculated into the brain of new experimental animals, as described above. The appropriate coordinates were confirmed and the technique refined by repeated pilot experiments.

3.5.7 Preparation of the injection formulations

3.5.7.1 Suspension of empty butyl-2-cyano[3-^{14}C]acrylate (^{14}C-PBCA) nanoparticles

40 mg lyophilized particles were reconstituted in 4 ml of physiological solution and ultrasonicated for about 30 min at 50 kHz in a bath type ultrasonicator. In order to obtain loaded doxorubicin nanoparticles by adsorption, the labeled nanoparticles were dispersed in a doxorubicin solution (0. 45 mg/ml) and stirred over night.

3.5.7.2 Preparation of polysorbate 80-coated ^{14}C-PBCA nanoparticles

The lyophilized particles (40 mg) were resuspended in 3.6 ml of physiological solution. After ultasonicating particles for 30 min, 400 μl of 10 % (v/v) polysorbate 80 solution was added and the mixture was incubated for 30 min.

3.5.7.3 Preparation of doxorubicin-loaded ^{14}C-PBCA nanoparticles

In order to obtain loaded doxorubicin nanoparticles by adsorption, the labelled nanoparticles were dispersed in a doxorubicin solution (0.45 mg/ml) and stirred over night. Then polysorbate 80 was added to give a final solution of 1 % (v/v) and the mixture was stirred for 30 min.

3.5.8 Particles characterization

3.5.8.1 Zeta potential

In order to study the influence of plasma, ^{14}C-PBCA nanoparticles, polysorbate 80-coated nanoparticles, and DOX-loaded nanoparticles, were incubated in undiluted Wistar rat plasma at 37 °C. The concentration of doxorubicin was 0.3 mg (corresponding to 6.7 mg of PBCA nanoparticles) /10 ml of serum, simulating a single injection of 1.5 mg/kg doxorubicin to a rat. After 30 min, the incubation medium was ultracentrifuged (145 000 × g, 1 h, 4 °C) and the nanoparticles pellet was redispersed in water. The size and surface

charge (zeta potential) were then determined and compared with the values obtained before incubation.

3.5.8.2 Charge

The mean particles diameter was determined by photon correlation spectroscopy (PCS).

3.5.8.3 Loading

To determine the doxorubicin entrapment efficiency, lyophilized DOX nanoparticles were resuspended in water, and the particles were separated from the solvent by centrifugation. Concentration of free DOX dissolved in supernatant was determined by HPLC. Relative drug loading (% of total amount) was calculated by subtraction of free drug in the supernatant from the total amount in the vials.

The assessment of drug loading was described in detail in paragraph 3.3.3.2.

3.5.9 Injection of nanoparticle suspensions in rats

The injections were performed with a 1-ml insulin syringe. The nanoparticle preparation was injected i.v. to group of four rats. The nanoparticle preparations - uncoated particles, coated and doxorubicin loaded particles - were injected into the lateral vein (3.33 ml/kg body weight) at the rate of 1.5 ml/min using a sterile canula lock No. 18. The dose was 1000 MBq/Kg body weight.

3.5.10 Sacrifice of rats

3.5.10.1 Healthy rats

Animals were placed in CO_2 chamber 10 min, 1 h, 6 h, 24 h, 3 days, 1 week, 4 weeks after injection until narcosis. Finally they were sacrificed by decapitation.

3.5.10.2 Tumour bearing rats

The injections were performed on day 5th, 8th, 10th post tumour implantation. The animals were killed by CO_2 chamber and decapitated 10 min, 1 h, 6 h, 24 h, after injection.

3.5.11 Preparation of organs

After decapitation, blood was collected, the abdomen and chest were opened and liver, lungs, heart, kidneys, spleen, gonads, brain were removed. Two samples were taken from each organ and weighed. The weight range of the samples was of 80 - 130 mg per vial.

The tail was also assayed for residual radioactivity in order to allow the quantification of the injected i.v. dose. The whole tail was dissected into 6 parts that were assayed using the same conditions as for the other organ samples.

3.5.12. Assessment of organs radioactivity

3.5.12.1 Chemicals

Tissue solubilizer...*BTS-450, Beckman, München*

Ready organic scintillation cocktail……………….……………..………. *Beckman, München*

Acetic acid ………………………………………………….*August Hedinger, Stuttgart*

Hydrogen peroxide 30 %……...…………………………………. *August Hedinger, Stuttgart*

3.5.12.2 Instrument

Liquid scintillation counter……………………*Wallac 1409 DSA, PerkinElmer, Jügesheim*

3.5.12.3 Determination of the activity of the injection suspensions

100 µl of each injection preparation were taken and the radioactivity was determined by scintillation counter.

3.5.12.4 Preparation of samples and measurement of radioactivity

1 ml tissue solubilizer was added and the vials were stored at 50 °C until all tissue was solubilized. For tail samples 3 ml of tissue solubilizer were added. 30 % H_2O_2 was added until the colour disappeared. The addition of glacial acetic acid (70 µl) was necessary to reduce the pH and minimize the possibility of chemo luminescence. After the addition of 10 ml scintillation cocktail, the samples were stored for about one week in darkness. The radioactivity was counted in a scintillation counter. The total radioactivity in the tail was subtracted from the total dose in order to calculate the radioactivity of the organs.

3.6 Chemotherapy studies

3.6.1 Chemicals

Polysorbate 80 (Tween® 80)………..……………………….………..… *Fluka, Buchs*

Poloxamer 188 (Pluronic® F 68)……………………….………….….*BASF, Ludwigshafen*

Poloxamine 908 (Symperonic® T908)……………..…………….……..*BASF, Ludwigshafen*

3.6.1.1 Polysorbate 80 (Tween® 80)

Polysorbate 80 is a relative homogenous viscous liquid (270-430 centistokes). The base chemical name of the major component of Tween® 80 is polyoxyethylene-20-sorbitan monooleate (Fig 3.1) which is structurally similar to the polyethyleneglycols.
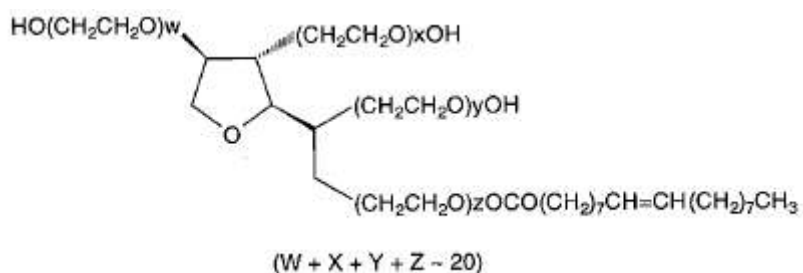
Figure 3.1. Chemical structure of polysorbate 80.

Like most non-ionic surfactants, Tween® 80 is capable of forming micelles in aqueous solution with critical micellar concentration of 0.01% (weight/volume) in protein-free aqueus solution (Tije et al. 2003). The chemical-physical properties of Tween® 80 are summarized in Tab 3.I.

Phisical-chemical characteristics	
Form	viscous liquid
Color	jellow pale
Density	Ca. 1.08 g/cm^3 25 °C
Viscosity	425 mPa.s 25 °C
Boiling point	>100 °C
Solubility in water	soluble

Solubility in other solvent	Soluble in ethanol and iso-propanol
Acute Toxicity	LD50 (rats) > 38g/Kg

Tab 3.I

3.6.1.2 Poloxamer 188 (Pluronic® F 68, Pluronic® PE 6800)

Poloxamers consist of a central polyoxypropylene molecule, which is flanked on both sides by two hydrophilic chains of polyoxyethylene (Fig 3.2). Poloxamer 188 has an average molecular weight of 8400 (Tab 3.II).
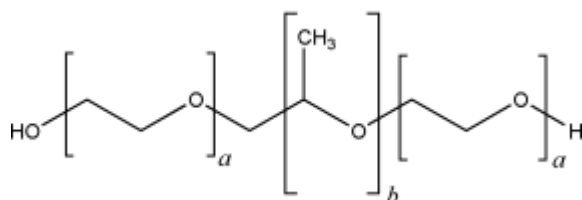
Figure 3.2. Chemical structure of poloxamer 188.

This molecule possesses haemorheological activities, has antithrombotic properties, is capable to stimulate the phagocytosis and the production of superoxide anion. Moreover, it provokes neutrophil degranulation and cell membrane sealing (Moghimi and Hunter 2000).

Phisical-chemical characteristics	
Form	Cast Solid / Prill / Pastille
Average molecular weight	8400
Viscosity, cps at 77 °C	1000
Melting point	52 °C
Cloud point (1% aqueus)	>100 °C
Solubility in water	>10 % at 25 °C
pH (2,5% aqueus)	5.0-7.5

Tab 3.II

3.6 .1.3 Poloxamine 908 (Symperonic® T908)

Poloxamines are tetrafunctional block copolymers with four polyoxypropylene–polyoxyethylene blocks joined together by a central ethylene diamine bridge (Fig 3.3). Poloxamines adsorb strongly onto the surface of hydrophobic nanospheres [e.g. polystyrene, poly(lactide-co-glycolide), poly(phosphazene), poly(methyl methacrylate) and poly(butyl 2-cyanoacrylate) nanospheres] via their hydrophobic polyoxypropylene centre block (Storm et al. 1995).

$H(OC_2H_4)y(OC_3H_6)x$ $\qquad$ $(C_3H_6O)x(C_2H_6O)yH$

NCH_2CH_2N

$H(OC_2H_4)y(OC_3H_6)x$ $\qquad$ $(C_3H_6O)x(C_2H_6O)yH$
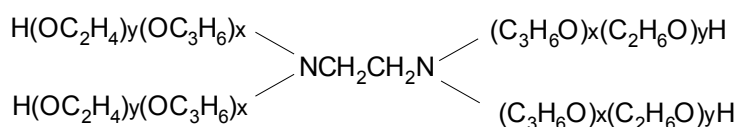
Figure 3.3. Chemical structure of poloxamine 908.

Poloxamine 908 characteristics are summarized in the Table 3.III.

Phisical-chemical characteristics	
Form	scurfs
Color	white
Density	1,14 g/cm³ 77 °C
Melting point	57 °C
Point of combustion	>150 °C
Solubility in water	>100 g/l 20 °C
pH	8-10 at 20 °C

Table 3.III

3.6.2 Drug treatment

Antitumoural drug-loaded nanoparticles were evaluated for the chemotherapeutic treatment of glioblastomas. The choose of animals, the tumour model system, and the procedure of tumour implantation were described in the chapter: "Study of body distribution after *i.v.* particles injection" (3.5).

Tumour bearing rats were used in two different sets of experiments.

One set received doxorubicin nanoparticles coated with different surfactants (polysorbate 80, poloxamer 188, poloxamine 908) or a solution of doxorubicin.

The animals of the other set were treated with different formulations of nanoparticles, and each formulation was coated only with the surfactant polysorbate 80. A doxorubicin

solution was used as well.

These preparations were injected i.v. into the tail vein in the dose regimen of 3 x 1.5 mg/kg on days 2, 5, and 8 post tumour implantation. The concentration of doxorubicin in the injection solutions was 0.25 %.

 The period of observation was 180 days post tumour implantation. Then the surviving animals were sacrificed and necropsied. The experiments were run in duplicate.

3.6.2.1 Set 1

3.6.2.1.1 Doxorubicin solution

A solution of 0.45 mg/ml of doxorubicin hydrochloride was prepared. The amount of doxorubicin injected to rats was 1.5 mg/kg, and the volume of solution administrated was 3.33 ml/kg body weight.

3.6.2.1.2 n-PBCA doxorubicin loaded nanoparticles coated with polysorbate 80

Particles were prepared as described previously (3.2.2). Lyophilized particles were resuspended in physiological solution and ultrasonicated for about 5 min. A determined amount of polysorbate 80 10 % (w/v) solution was added to obtain a concentration of 1 %. The mixture was stirred for 30 min to ensure the coating of the particles and the preparation was injected in the amount of 1.5 mg/Kg of doxorubicin per injection.

3.6.2.1.3 iso-PBCA doxorubicin loaded nanoparticles coated with polysorbate 80

The polymerisation was carried out using 1 % of iso-butyl(cyano acrylate) instead of 1 % n-butyl(cyano acrylate). The preparation of the injection solutions is described above (3.6.2.1.2).

3.6.2.1.4 PBCA nanoparticles with improved doxorubicin loading (new formulation) coated with polysorbate 80

The usual procedure of preparing doxorubicin nanoparticles (3.2.2) was modified in order to obtain particles with higher content of doxorubicin. The "new formulation" was prepared as follows: 0.75 % (w/v) of n-butyl(cyano acrylate) was added to 2 % (w/v) solution of dextran 70 000 in 0.01 N HCl (pH 2) under constant stirring. DOX was added immediately after the beginning of polymerisation in the concentration of 0.25 % (w/v).

After 4 h the mixture was neutralized with 0.1 NaOH, filtered, filled in vials (2ml/vial), and freeze-dried with addition of 3 % (w/v) mannitol as cryoprotector. The preparation of the injection solution was performed as described in paragraph 3.6.2.1.2.

3.6.2.2 Set 2

3.6.2.2.1 Doxorubicin solution

A solution of doxorubicin hydrochloride was prepared as described in the paragraph 3.6.2.1.1. Then doxorubicin solution was injected.

3.6.2.2.2 PBCA doxorubicin nanoparticles coated with polysorbate 80

PBCA doxorubicin nanoparticles were resuspended in physiological solution, ultrasonicated, and a solution of 10 % (w/v) polysorbate 80 was added to the suspension to reach the final concentration of 1 %. The particles were stirred for 30 min, and the formulation was injected.

3.6.2.2.3 PBCA doxorubicin nanoparticles coated with Poloxamine 908

The injection solution was prepared as described above (3.6.2.2.2) using a poloxamine 908 solution instead of polysorbate 80.

3.6.2.2.4 PBCA doxorubicin nanoparticles coated with poloxamer 188

A solution of poloxamer 188 was used to coat PBCA doxorubicin nanoparticles as described above (3.6.2.2.2).

3.7 Whole-body autoradiography (WBA) studies

3.7.1 Principle

Autoradiography is a process by which radioactive materials are located by exposure to a photographic emulsion forming a pattern on the film corresponding to the location of the radioactive compounds within the cell.

Studies of WBA were carried out to evaluate the distribution of [14-^{14}C] doxorubicin bound to nanoparticles tissues and organs at certain time points. Moreover the WBA permitted the determination of sites of accumulation and retention of [14-^{14}C] DOX PBCA NP and the assessment of penetration across the BBB.

3.7.2 Materials and Methods

The autoradiography studies were performed by Sanofi-Aventis, Frankfurt am Main, who provided devices and chemicals.

[14-^{14}C] doxorubicin was purchased from Amersham Biosciences, Buckinghamshire, UK.

3.7.2.1 [14-^{14}C] - Doxorubicin hydrochloride
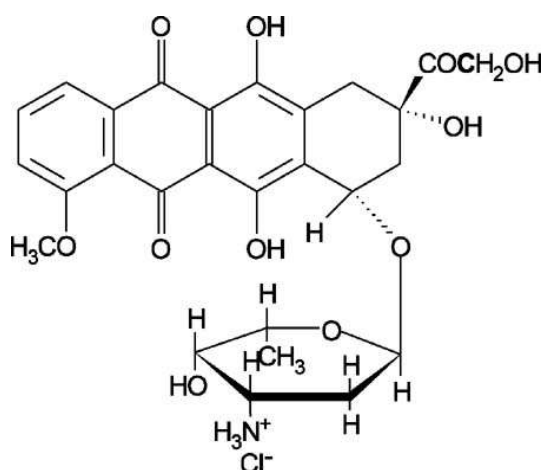
The molecular weight of the radiolabelled [14-^{14}C] - doxorubicin hydrochloride is 582 and the specific radioactivity is 94.5 μCi/mg.

3.7.3 Preparation of the injection formulations

4 rats of 200 g weight were utilized to perform the WBA studies. 1 ml of the [14-^{14}C] - DOX preparation was injected intravenously in each rat. The preparations administrated are described as follows:

3.7.3.1 [14-^{14}C] Doxorubicin solution + polysorbate 80

Cold DOX and [14-^{14}C] - DOX were blended and dissolved in a solution of 1 % polysorbate 80 in order to obtain 1 ml of solution containing 0.3 mg/ml DOX and 22.5 µCi.

3.7.3.2 [14-^{14}C] Doxorubicin poly(butyl cyanoacrylate) nanoparticles coated with polysorbate 80

The procedure to prepare DOX PBCA NP was described in the paragraph 2.3.3.
The amount of each reagent was accurately weighted in order to obtain the limited NP volume of 3 ml. Briefly, 25 µL of BCA were added to 2.5 ml of 1 % dextran solution at pH 2. After 30 min, 90 µl of [14-^{14}C] – DOX + DOX solution were added. The polymerization process was carried out for 2.30 h and it was stopped by addition of 244 µL NaOH 0.1 N.
For the NP coating, 300 µL of polysorbate 80 10 % (w/v) were added to give a final solution of 1 % (v/v), and the mixture was stirred for 30 min.

3.7.4 Administration of [14-^{14}C] - DOX preparations

[14-^{14}C] - DOX PBCA NP coated with PS 80 were injected i.v. in three rats which were sacrificed at 1 h, 2 h, 4 h post injection.
[14-^{14}C] - DOX + PS 80 was injected in only one rat and it was sacrificed at 2 h post injection. Each rat received the radioactive dose of 22.5 µCi.

3.7.5 Section preparation and radioluminograms development

After scarification of rats, each carcass was snap-frozen and set individually in carboxymethyl cellulose. The blocks were sectioned on a cryomicrotome at approximately –25 °C, and each section was placed on an adhesive tape. The sections were placed on phosphor imaging plates for a few hours. Scanning each plate with a laser beam allowed to prepare radioluminograms of high resolution.

By addition of blood samples fortified with radiolabelled drug in the frozen block, the amount of radioactivity in each tissue could be quantified by linear calibration. The phosphor imaging plates were scanned with a state-of-the-art phosphor imaging system equipped with quantification software.

4 Results

4.1 Nanoparticles characterization

Doxorubicin loaded to polysorbate 80-coated nanoparticles demonstrated a high antitumour effect against the rat glioblastoma 101/8 (Steiniger et al. 2004). For this reason the aims of the present study was to investigate the optimization of this formulation by modification of the reaction parameters. Drug loading, size, and polymerization yield were determined for each nanoparticles formulation.

4.1.1 Drug loading

Table 4.I summarizes the experimental results with respect to the joint effect of dextrans and n-BCA concentration, pH values, the polymerization time, and the type of the monomer on doxorubicin loading in nanoparticles. It can be seen that the modification of the parameters used for the standard formulation 0 could not improve the drug loading to a major extent. A relevant reduction of drug loading occurred at lower (pH 1, formulation No 4) and higher pH values (pH 3, formulation No 6, and pH 4, formulation No 7) than pH 2. A slight increase in the drug loading of the particles was obtained by reducing the concentration of n-BCA from 1% w/v to 0.75 % w/v whereas a further decrease in monomer concentration to 0.5 % w/v decreased the drug loading to 65.40 %. The influence of dextran concentration was not considerable: at the concentration of 0.5 %, the loading was slightly decreased to 61.5 % (formulation No 4), whereas the increase of concentration to 2 % produced no significant effect (formulation No 3). In the standard formulation, doxorubicin was added to the reaction medium 30 min after the start of polymerization. However, nanoparticles with similar properties also could be formed at a n-BCA concentration of 0.75 % combined with a simultaneous increase in stabilizer (dextran) content to 2 % when the drug was added before the monomer (formulation No 9). Another butyl cyanoacrylate isomer, iso-butyl(cyanoacrylate), was used instead of n-butyl (cyanoacrylate) for the synthesis of formulation No 10. This monomer was chosen based on the data of its lower toxicity, as compared to n-BCA (Kante et al. 1982).

Formulation	Dextran [% w/v]	pH	Monomer concentration [% w/v]	Reaction time [h]	Particle size (SD) [nm]	NP capacity [mg DOX/mg PBCA]	Drug loading measured by HPLC [%] (SD) *	Drug loading measured by spectroph. [%] (SD)*
0	1	2	1	2.30	210 (10.01)	0.33	71.10 (2.59)	53.21 (3.63)
1	1	2	0.75	2.30	208 (12.17)	0.33	72.50 (1.61)	55.34 (2.53)
2	1	2	0.5	2.30	235 (6.24)	0.30	65.40 (4.65)	50.87 (4.68)
3	2	2	1	2.30	205 (17.04)	0.33	73.50 (4.18)	61.5 (4.48)
4	0.5	2	1	2.30	250 (17.21)	0.28	61.10 (2.55)	51.1 (4.12)
5	1	1	1	2,30	251 (26.25)	0.24	58,21 (3,51)	40.21 (3.21)
6	1	3	1	2.30	248 (16.09)	0.24	52.47 (4.43)	42.45 (5.56)
7	1	4	1	2.30	253 (27.87)	0.22	49.23 (4.00)	39.29 (5.56)
8	1	2	1	4.00	218 (20.66)	0.33	72.40 (2.62)	65.21 (2.45)
9**	2	2	0.75	4.00	198 (6.43)	0.35	76.34 (1.78)	69.25 (4.20)
10***	1	2	1	2.30	215 (10.02)	0.34	73.38 (1.62)	64.25 (2.98)
11#	1	2	1	2.30	190 (4.1)	0.10	30.20 (2.13)	20.21 (1.58)

* [mg DOX adsorbed/mg tot DOX in the colloidal suspension] x 100
** doxorubicin was added into the medium before the monomer
*** polymerization was carried out utilizing iso-BCA
# Pluronic F68 was used instead of Dextran

Table 4.I

Doxorubicin loaded in n-poly(butyl cyanoacrylate) and iso-poly(butyl cyanoacrylate) nanoparticles: influence of the reaction variables on the formulation parameters (n = 4).

Finally the application of 1 % of pluronic F 68 instead of 1 % of dextran led to a dramatic reduction of drug loading (Formulation 11).

Noteworthy is the significant difference of the drug loading values assessed by spectrophotometer and HPLC. The loading measured by HPLC was 10 - 20 % more than the value assessed by spectrophotometer for all the formulations.

The measurements performed by HPLC were supposed to be more reliable. HPLC reduces the effect of light scattering and is not influenced by turbidity of the samples that can falsified the measure of concentration. Moreover the reliability of the HPLC measurements was confirmed by the reduced values of standard deviation (SD) in comparison to the SD calculated from the spectrophotometer estimations (Tab 4.I).

4.1.2 Particles size

No considerable size differences were shown between the nanoparticles formulations (Tab 4.I). A smaller NP size was observed for the standard formulation No 0 and for the formulation No 1, in which the monomer concentration was reduced to 0.75 % (208-210 nm). However a further reduction of the n-BCA concentration to 0.5 % caused the increase in NP size (235 nm). A size increase of nanoparticles was observed at pH-values of 3, 4, 1 whereas the smallest particles were obtained at pH 2.

4.1.3 Nanoparticle loading capacity

The determination of nanoparticle loading capacity (mg DOX/mg PBCA) was possible after assessment of the polymerization yield (paragraph 3.3.4). The results are shown in Table 4.1.

The capacity was reduced at pH values deviating from pH 2. For all the remaining formulations no significant differences in drug capacity were observed.

4.2 Release Studies

Drug release studies were performed with the formulations which showed an increased loading (Tab 4.I). The formulations selected were: 1) standard formulation (formulation No 0); 2) formulation No 9 (0.75 % n-BCA, 2 % dextran, 4 h polymerization); 3) formulation No 10 (application of iso-BCA). The characterization of these preparations is shown in Tab 4.I.

4.2.1 Dialysis membrane

The drug release curves of the different preparations are shown in Figure 4.1. As shown by the release curve of doxorubicin solution, more than 30 % of doxorubicin was absorbed on the dialysis membrane. The release of doxorubicin for all the formulations was characteristically biphasic with an initial fast release phase followed by a second much slower first-order release phase.

The release of doxorubicin from the standard formulation No 0 and formulation No 10 was comparable.

Formulation No 9 showed a slower drug release in comparison to formulation No 0 and No 10.
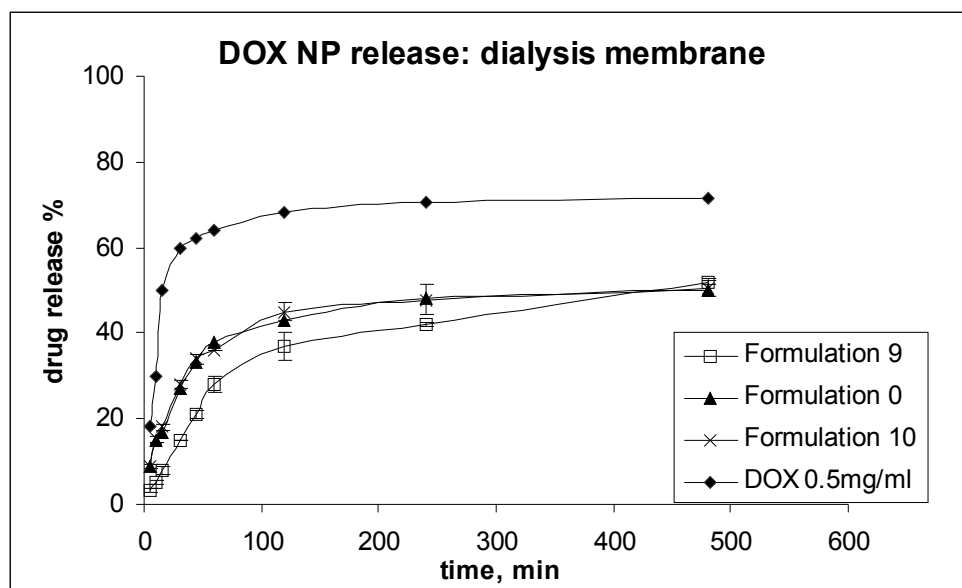
Figure 4.1. Release curves of DOX solution and of formulations 0, 9, and 10 with dialysis membrane.

4.2.2 Microtubes

The release of doxorubicin from nanoparticles determined using microtubes was extremely fast, probably due to the high g-force. The results obtained with this method were not useful for the present study.
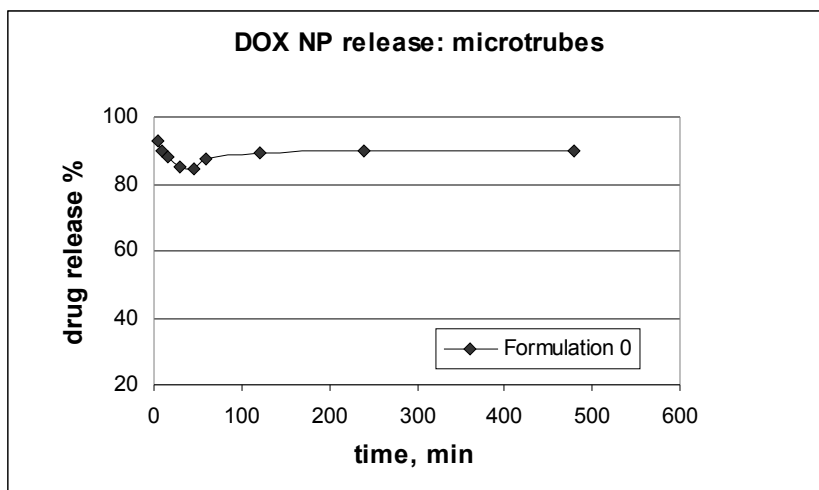
Figure 4.2. Release curve of standard formulation 0 with microtube devices.

4.2.3 Microcentrifuge filters

The results with microcentrifuges filters were similar to those obtained with microtubes. Additionally adsorption of about 30 % doxorubicin on the filters occurred.
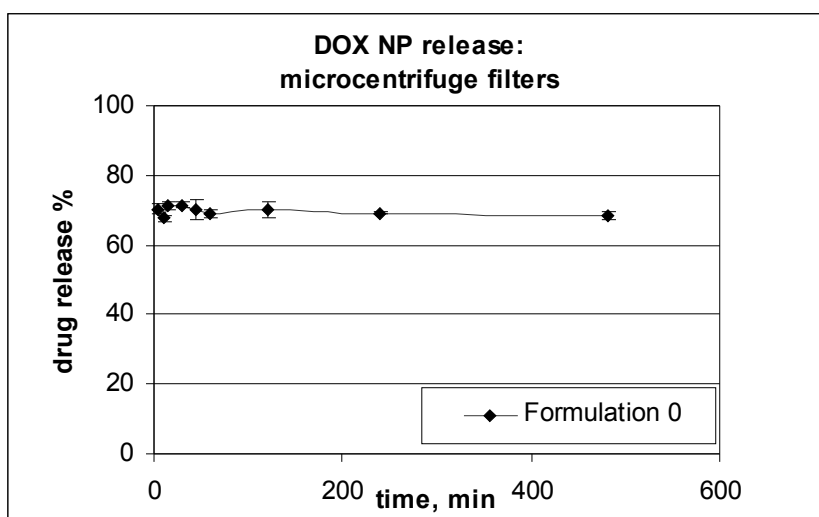
Figure 4.3. Release curve of standard formulation 0 with microcentrifuge filter devices.

4.3 Chemotherapy studies

4.3.1 Treatment of rats bearing intracranial transplanted glioblastoma 101/8 using different nanoparticle formulations of doxorubicin coated with polysorbate 80

Formulations No 9 and No 10 were chosen to evaluate their anti-tumour efficacy in glioblastoma-bearing rats and compared with the standard formulation No 0. The rationale of choosing these formulations for chemotherapeutical studies was their improved loading. It was reasoned that an higher amount of doxorubicin bound to the particles increased the quantity of the drug that can be transported into the brain. Moreover, since it was previously shown that the coating of PBCA nanoparticles with polysorbate 80 (PS 80) enabled the transport of bound drugs across the blood-brain barrier (BBB) after i.v. injection (Kreuter 2002), these formulations were coated with PS 80.

As shown in Table 4.I, formulations No 0, 9, and 10 had similar physico-chemical characteristics, which allowed an adequate comparison of their biological effects at equal doses. The treatment regimen and the tumour model were chosen based on the results of previous studies, where the standard formulation No 0 coated with polysorbate 80 demonstrated high anti-tumour effects (Steiniger et al. 2004).

Fig. 4.4 shows the Kaplan-Meier survival curves of the rats exposed to treatment with various DOX formulations in the present study. It can be seen that the standard formulation No 0 was the most effective formulation: 35 % (7/20) of the animals treated with formulation No 0 (Figs. 4.4 and 4.5) survived for 180 days after tumour implantation. These animals were sacrificed, and no signs of tumour growth were observed after necropsy. In the groups treated with formulations No 9 and No 10, the percentage of long-term survivors was 15 % (3/20) and 10 % (2/20), respectively. Free DOX in solution was less effective: 10 % of the animals (2/20) survived for 65 days. All control animals died between day 18 and day 24.
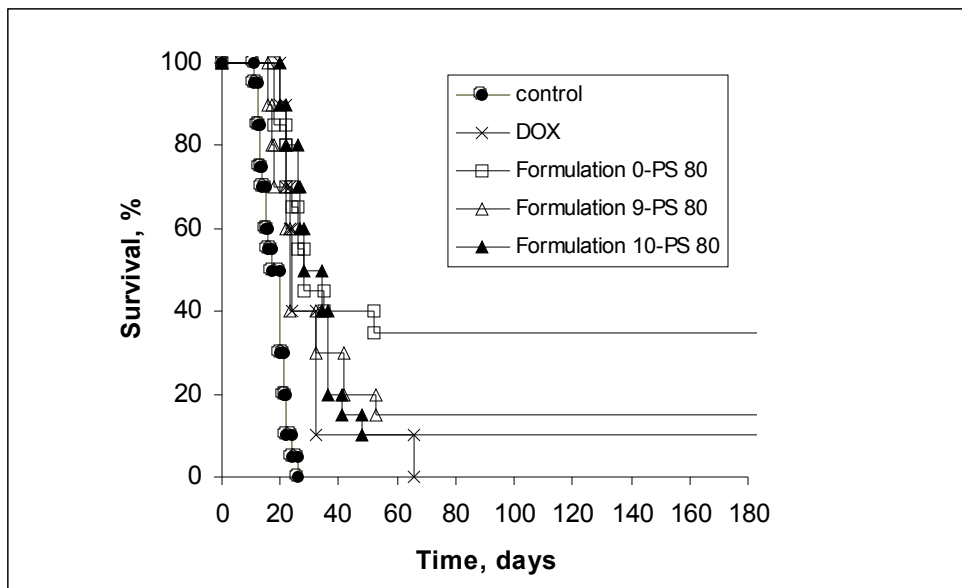
Fig. 4.4. Influence of nanoparticle polymer and formulation on the survival (Kaplan-Meier plot) of rats bearing intracranially transplanted glioblastoma 101/8 after i.v. injection of the following doxorubicin formulations: free doxorubicin in saline (DOX), formulation 0, 9, and 10 in 1 % polysorbate 80 solution. Treatment regimen: 3 x 1.5 mg/kg on days 2, 5 and 8 post tumour implantation (n = 20; summarized data of 2 experiments).

4.3.2 Treatment of rats bearing intracranial transplanted glioblastoma 101/8 with DOX NP PBCA nanoparticles coated with different surfactants

In the second set of experiments, the influence of surfactants on the survival time of glioblastoma 101/8-bearing rats was investigated. The efficacy of DOX PBCA NP coated with poloxamer 188 and poloxamine 908 in the treatment of glioblastoma was evaluated and compared with polysorbate 80. As shown in Fig. 4.5, the standard reference formulation – DOX-PBCA nanoparticles coated with polysorbate 80 – again was the most effective. The percentage of long-term survivors treated DOX loaded in the nanoparticles coated with poloxamer 188 or poloxamine 908 was 20 % (4/20).
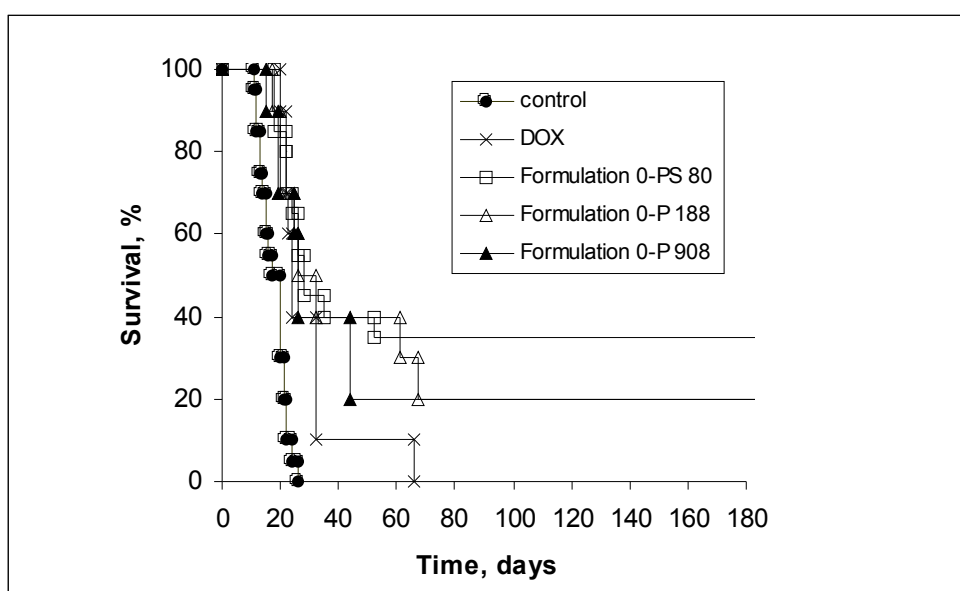
Fig. 4.5. Influence of surfactants on the survival (Kaplan-Meier plot) of rats bearing intracranially transplanted glioblastoma 101/8 after i.v. injection of the following doxorubicin formulations: free doxorubicin in saline (DOX), formulation 0 in 1 % solution of polysorbate 80 (PS 80), poloxamer 188 (P 188), or poloxamine 908 (P 908). Treatment regimen: 3 x 1.5 mg/kg on days 2, 5 and 8 post tumour implantation (n = 20; summarized data of 2 experiments).

4.4 Body distribution studies

4.4.1 Objective of the study

The objective of the present study was to evaluate the body distribution of uncoated, coated, and doxorubicin-loaded ^{14}C-poly(butyl cyanoacrylate) nanoparticles, utilizing polysorbate 80 as surfactant in healthy and tumour bearing rats. Attention was particularly focused on the biodistribution of nanoparticles into the brain.

4.4.2 Healthy Rats

4.4.2.1 Surface charge

The charge of the particles appears to influence the body distribution. Therefore the zeta potential of nanoparticles was investigated (Brigger et al. 2004). PBCA NP and PS 80-coated PBCA NP showed negative zeta-potentials in distilled water, a general phenomenon of theoretically uncharged polymeric particles (Table 4.II). Adsorption of doxorubicin on the surface modified the charge of nanoparticles towards a positive value, caused by the charge of this drug. However, after contact with serum the zeta-potential of these particles was changed to negative again and was not significantly different from particles without doxorubicin.

	NP	NP+PS 80	NP+DOX	NP+PS 80+DOX
Mean diameter [nm]	185 - 200	220 - 260	230 - 280	210 - 250
Polydispersity index	< 0.2	< 0.2	< 0.2	< 0.2
Entrapment efficiency*[%]	~	~	59 %	30 %
Drug loading** [%]	~	~	5.7	2.9
Surface Charge [mV]	-14	-10.2	8	2

*[mg DOX adsorbed/mg tot DOX in the colloidal suspension]x100
** [mg DOX adsorbed/mg BPCA nanoparticles]x100

Table 4.II. Physicochemical properties of poly(butyl cyanoacrylate) nanoparticles.

4.4.2.2 Body distribution

The body distribution of the butyl-2-cyano[3-^{14}C]acrylate nanoparticles (^{14}C-PBCA nanoparticles) is shown in Table 4.III (percent of dose) and Table 4.IV (µg/g tissue weight) and in Figs 4.6 - 4.7.

Time	Sample	NP		NP+PS 80		NP+PS 80+DOX	
		Percent dose	S.D.	Percent dose	S.D.	Percent dose	S.D.
10 min	Blood	11.39	2.66	17.00	4.02	23.00	5.37
	Heart	0.62	0.09	0.52	0.15	0.48	0.05
	Lungs	12.25	1.50	9.19	1.39	5.70	0.71
	Liver	49.99	8.53	41.64	6.98	43.23	3.08
	Spleen	4.49	1.12	1.94	0.95	3.41	0.65
	Testicles	0.90	0.00	0.90	0.57	0.96	0.19
	Kidneys	4.12	0.69	5.84	1.14	6.83	0.27
	Brain	0.32	0.02	0.34	0.04	0.39	0.04
1 h	Blood	8.17	3.05	9.87	1.80	9.62	2.22
	Heart	0.44	0.23	0.67	0.25	0.40	0.11
	Lungs	3.30	1.02	6.51	1.69	4.07	1.03
	Liver	47.48	9.12	30.59	4.44	48.30	9.10
	Spleen	2.25	1.20	1.13	0.99	2.26	0.23
	Testicles	0.41	0.10	0.82	0.08	0.80	0.42
	Kidneys	3.06	0.46	4.43	0.42	3.06	0.53
	Brain	0.34	0.12	0.61	0.04	0.44	0.12
6 h	Blood	1.84	0.27	3.27	0.53	3.18	1.37
	Heart	0.63	0.17	0.16	0.01	0.22	0.04
	Lungs	2.88	1.18	5.43	0.45	2.00	0.78
	Liver	19.54	5.32	16.2	3.77	22.61	3.31
	Spleen	0.52	0.58	0.98	0.64	1.89	0.48
	Testicles	0.54	0.19	0.37	0.19	0.28	0.05
	Kidneys	0.62	0.08	0.93	0.13	0.89	0.15
	Brain	0.12	0.02	0.15	0.06	0.19	0.08
24 h	Blood	0.96	0.02	1.08	0.03	2.76	0.08
	Heart	0.15	0.02	0.12	0.01	0.14	0.02
	Lungs	0.60	0.02	0.18	0.01	3.72	0.71
	Liver	15.18	0.81	12.76	1.56	21.12	4.57
	Spleen	0.21	0.02	0.08	0.11	2.19	0.23
	Testicles	0.10	0.00	0.24	0.19	0.38	0.14
	Kidneys	0.29	0.03	0.28	0.08	1.25	0.18
	Brain	0.07	0.02	0.36	0.12	0.14	0.06
3 days	Blood	1.45	0.90	1.29	0.21	0.43	0.30

Heart	0.25	0.16	0.12	0.05	0.05	0.11
Lungs	0.05	0.40	0.46	0..37	0.31	0.42
Liver	12.17	1.23	9.71	1.52	4.25	2.41
Spleen	0.88	0.73	0.46	0.38	0.29	0.23
Testicles	0.19	0.06	0.16	0.01	0.07	0.01
Kidneys	0.45	0.25	0.50	0.10	0.20	0.07
Brain	0.07	0.04	0.12	0.03	0.05	0.03
1 week Blood	0.59	0.21	0.67	0.24		
Heart	0.12	0.01	0.06	0.02		
Lungs	0.40	0.20	0.43	0.25		
Liver	9.29	1.98	10.97	2.36		
Spleen	0.90	0.54	0.60	0.53		
Testicles	0.20	0.04	0.12	0.02		
Kidneys	0.53	0.05	0.32	0.12		
Brain	0.08	0.03	0.07	0.02		
4 weeks Blood	0.64	0.55	0.55	0.1		
Heart	0.03	0.02	0.04	0.01		
Lungs	0.50	0.30	0.30	0.14		
Liver	2.23	0.94	7.94	1.78		
Spleen	0.24	0.15	0.53	0.1		
Testicles	0.08	0.03	0.11	0.01		
Kidneys	0.15	0.04	0.26	0.04		
Brain	0.03	0.01	0.05	0.01		

Table 4.III. Body distribution of ^{14}C as percent of the dose after intravenous administration of ^{14}C-PBCA nanoparticles, polysorbate 80-coated ^{14}C-PBCA nanoparticles, and DOX ^{14}C-PBCA loaded nanoparticles in healthy rats.

Time	Sample	NP		NP+PS 80		NP+PS 80+DOX	
		µg NP/g	S.D.	µg NP/g	S.D.	µg NP/g	S.D.
10 min	Blood	51.66	12.06	77.11	13.71	104.32	18.30
	Heart	37.49	5.44	31.45	6.82	29.03	2.27
	Lungs	444.49	54.43	333.45	37.93	206.82	17.21
	Liver	247.35	42.21	206.03	25.97	213.90	11.45
	Spleen	488.76	121.92	211.18	77.77	371.20	53.17
	Testicles	19.59	0.00	19.59	9.26	20.95	3.04
	Kidneys	117.95	19.76	167.18	24.55	195.58	5.90
	Brain	10.25	0.32	10.89	0.48	12.49	0.48
1 h	Blood	37.07	13.83	44.76	8.16	43.64	10.65
	Heart	26.57	13.91	40.28	15.12	24.18	6.65
	Lungs	119.63	36.95	236.18	40.93	147.58	37.37
	Liver	234.94	45.13	151.35	21.97	238.96	45.03
	Spleen	245.04	90.21	123.35	51.21	314.92	89.35
	Testicles	8.93	2.18	17.85	1.74	17.42	215
	Kidneys	87.78	13.18	126.96	12.03	87.60	15.18
	Brain	10.89	2.14	19.53	2.60	14.09	2.82
6 h	Blood	8.35	1.23	14.83	2.26	14.42	5.72
	Heart	38.37	10.36	9.68	0.57	13.30	2.23
	Lungs	104.32	43.08	197.15	15.38	72.57	26.14
	Liver	96.68	26.51	80.16	17.53	111.87	15.07
	Spleen	56.60	23.59	106.68	25.47	205.74	48.07
	Testicles	11.65	4.19	7.95	3.91	5.99	0.99
	Kidneys	17.69	2.37	26.71	3.46	25.42	4.06
	Brain	3.84	0.32	4.80	0.90	6.08	1.18
24 h	Blood	4.35	0.96	4.90	0.52	12.52	2.11
	Heart	9.25	2.21	7.08	1.50	8.71	2.10
	Lungs	21.77	3.09	6.53	2.44	134.98	30.94
	Liver	75.11	10.53	63.14	18.25	104.50	40.23
	Spleen	22.86	1.11	8.71	3.18	238.39	24.82
	Testicles	2.18	0.00	5.12	9.72	8.27	2.70
	Kidneys	8.31	1.79	8.16	4.50	35.92	5.82
	Brain	2.18	0.83	11.53	4.49	4.48	0.84
3 days	Blood	6.58	3.41	5.85	0.92	1.95	1.10
	Heart	15.12	8.09	7.26	2.92	3.02	2.93
	Lungs	17.69	11.51	16.81	16.33	11.37	32.42
	Liver	60.22	5.09	48.04	7.26	21.03	28.60
	Spleen	95.79	66.42	50.07	39.95	31.57	18.25
	Testicles	4.14	1.03	3.48	0.30	1.52	0.00
	Kidneys	12.96	6.09	14.25	2.79	5.73	3.02
	Brain	2.24	1.23	3.84	0.94	1.60	1.01

1 week	Blood	2.68	0.90	3.04	1.32
	Heart	7.26	0.57	3.63	1.46
	Lungs	15.06	6.05	15.60	11.14
	Liver	45.97	9.28	54.28	14.13
	Spleen	97.97	55.67	65.31	42.83
	Testicles	4.35	0.87	2.50	0.56
	Kidneys	15.11	1.35	9.20	4.16
	Brain	2.56	0.39	2.24	0.30
4 weeks	Blood	2.90	3.13	2.49	0.52
	Heart	1.81	1.52	2.42	0.70
	Lungs	16.87	6.32	10.70	4.73
	Liver	11.03	5.83	39.29	10.16
	Spleen	26.13	7.47	57.69	6.56
	Testicles	1.74	0.77	2.39	0.36
	Kidneys	4.20	1.50	7.38	1.39
	Brain	0.96	0.01	1.60	0.02

Table 4.IV. Body distribution (in μg nanoparticles per g tissue weight) after intravenous administration of ^{14}C-PBCA nanoparticles, polysorbate 80-coated ^{14}C-PBCA nanoparticles, and DOX ^{14}C-PBCA loaded nanoparticles in healthy rats.

The brain is the most relevant organ for the polysorbate 80-coated nanoparticles since these particles enabled an enhanced drug transport into this organ after intravenous injection targeting (Kreuter 1983a, Alyautin et al. 1995, Kreuter et al. 1995, Schröder and Sabel 1996, Alyautin et al. 1997, 1998, Gulayev et al. 1999). Therefore, most emphasis was put on this organ in the present study. In brain, ^{14}C-PBCA nanoparticles, PS 80-coated ^{14}C-PBCA nanoparticles, and DOX ^{14}C-PBCA nanoparticles showed similar concentrations 10 minutes after injection (Fig 4.6).

Precisely, the brain concentration of the mentioned formulations reached 0.2 % dose/gr tissue. Enhanced brain concentrations of polysorbate 80-coated ^{14}C-PBCA nanoparticles appeared after 1 hour and continued for the rest of the study. After 1 h the percentage of the dose/gr tissue was increased by 0.80 % with the polysorbate 80-coated particles and by 0.30 % with the DOX ^{14}C-PBCA nanoparticles.

The amount in the blood was increased slightly (statistically not significant) after coating with polysorbate 80 and at 10 min post injection even statistically significant after coating with doxorubicin plus polysorbate 80. These differences diminished after longer time periods (Tables 4.III and 4.IV).
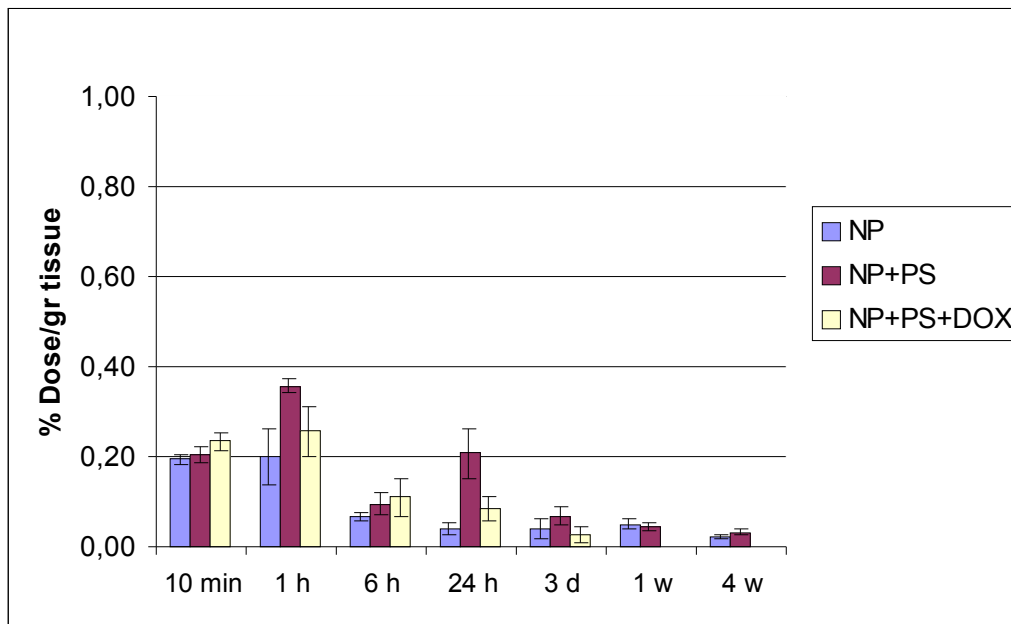
Figure 4.6. Biodistribution of nanoparticles (NP), nanoparticles + polysorbate 80 (PS), and doxorubicin-loaded and polysorbate-80 coated nanoparticles (NP+PS+DOX) in rat brain of healthy rats after intravenous administration of 20 mg/kg of nanoparticles.

In the organs of the reticulo endothelial system (RES), i.e. liver, spleen, lungs, the picture was more complex. In general, polysorbate 80-coating reduced the liver and spleen concentrations by about 40 to 50 %, but in some cases (1 h, 6 h, 3 days) increased the lung concentrations. The addition of doxorubicin to these particles in general compensated the effects of polysorbate 80-coating and resulted in similar RES organ concentrations as the uncoated particles.
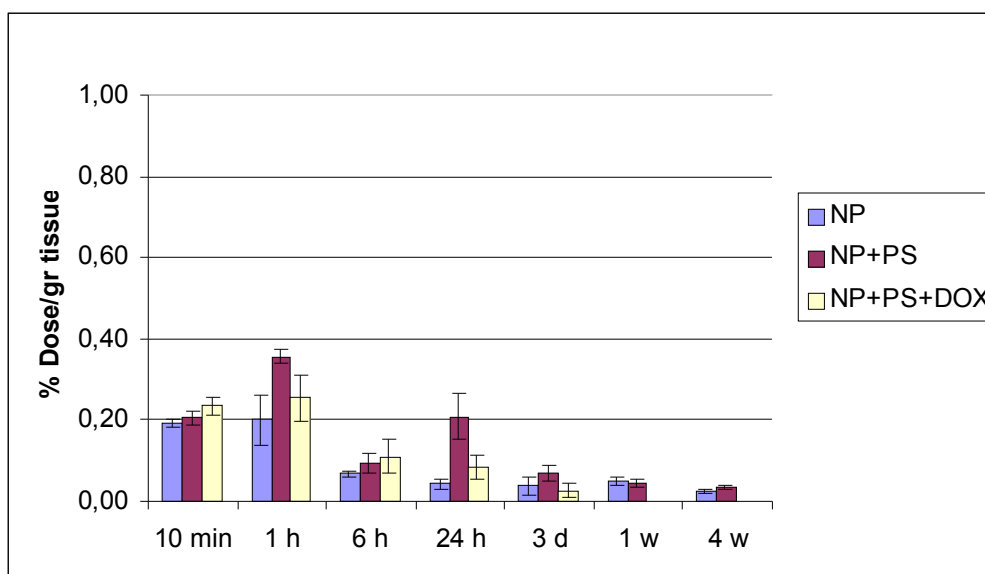
Figure 4.7. Biodistribution of nanoparticles (NP), nanoparticles + polysorbate 80 (PS), and doxorubicin-loaded and polysorbate-80 coated nanoparticles (NP+PS+DOX) in main organs of healthy rats 1 h after

intravenous administration of 20 mg/kg of nanoparticles.
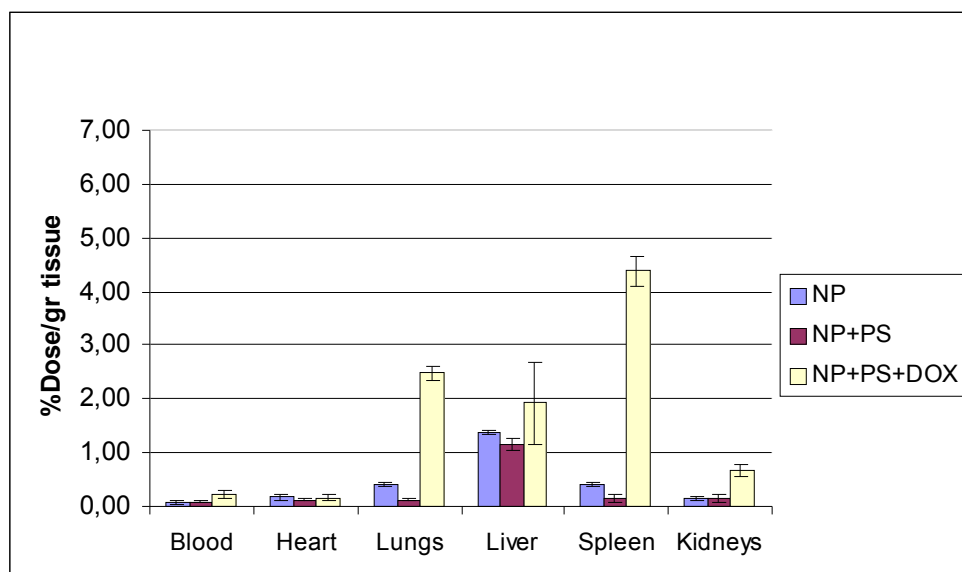
Figure 4.8. Biodistribution of nanoparticles (NP), nanoparticles + polysorbate 80 (PS), and doxorubicin-loaded and polysorbate-80 coated nanoparticles (NP+PS+DOX) in main organs of rats, 24 h after intravenous administration of 20 mg/kg of nanoparticles.

Similar fluctuations in concentrations were observed in the other organs investigated, i.e. heart, kidneys, and testicles, and probably were caused by the biological variations. No important or relevant concentration increases or decreases were caused by any of the three preparations (Figs 4.7 and 4.8).

4.4.3 Tumour-bearing rats

4.4.3.1 Five days glioblastoma bearing rats

4.4.3.1.1 Body Distribution

In rats to which the nanoparticles were injected i.v. 5 days after tumour-implantation, the concentration of nanoparticles in the blood was decreased of 5 % dose after coating with polysorbate 80 and binding with doxorubicin (Tables 4.V and 4.VI) at 10 minutes post injection. After 1 hour and 6 h, DOX ^{14}C-PBCA nanoparticles displayed the lowest blood concentration (7.3 % and 2.5 % of dose respectively).

Regarding the organs of the reticulo endothelial system (RES) i.e. liver, spleen, lungs, an accumulation of particles was shown in those organs. The concentrations of the three formulations in those organs were different: the coating with polysorbate 80 reduced the uptake by the organs of the RES. The percent of dose of NP in the liver at 10 min post

injection was 43 % whereas at the same time and in the same organ NP+PS 80 displayed a reduced concentration of 19.5 % of the administered dose. The addition of doxorubicin to the particles led to a concentration of 45 % of the dose. A comparable tendency was as well shown at 1 h, 6 h, post injection.

In general the coating with the surfactant reduced the uptake and the adsorption of doxorubicin neutralized the effect of polysorbate 80 of diminished uptake by the RES.

Concerning the concentrations of nanoparticles in the brain, PS 80-coated ^{14}C-PBCA nanoparticles, and DOX ^{14}C-PBCA nanoparticles showed higher concentrations of ^{14}C-PBCA nanoparticles, 10 minutes after injections (0.30, 0.31, 0.21 % of the dose/g tissue respectively) (Fig 4.9). After 1 hour PS 80-coated ^{14}C-PBCA nanoparticles reached 0.37 % of the dose/g tissue while ^{14}C-PBCA nanoparticles and DOX ^{14}C-PBCA nanoparticles decreased the brain concentrations (0.13 %, 0.22 % dose/g tissue, respectively). However these values were not statistically relevant. The nanoparticles brain concentration of all three formulations diminished at extended times.

Time	Sample	NP		NP+PS 80		NP+PS 80+DOX	
		Percent dose	S.D.	Percent dose	S.D.	Percent dose	S.D.
10 min	Blood	17.82	2.87	12.84	4.31	12.49	2.85
	Heart	1.07	0.42	0.59	0.15	0.78	0.16
	Lungs	11.16	2.99	7.79	4.87	8.18	1.73
	Liver	43.27	1.44	19.50	7.46	44.83	5.95
	Spleen	4.67	1.56	1.46	0.89	2.20	0.51
	Testicles	1.06	0.36	0.54	0.09	0.73	0.11
	Kidneys	7.39	4.43	4.61	1.02	8.36	2.19
	Brain	0.35	0.17	0.50	0.17	0.51	0.11
1 h	Blood	9.84	2.18	9.46	3.19	7.32	1.06
	Heart	0.50	0.18	0.58	0.33	0.36	0.07
	Lungs	2.25	0.73	6.89	1.02	4.66	1.35
	Liver	33.85	9.20	22.20	12.10	28.66	3.97
	Spleen	1.71	0.65	0.96	0.61	2.08	1.13
	Testicles	0.71	0.13	0.72	0.36	0.63	0.05
	Kidneys	3.22	0.58	3.31	1.35	2.65	0.68
	Brain	0.24	0.23	0.64	0.32	0.38	0.04
6 h	Blood	4.41	0.78	4.01	0.84	2.52	1.05
	Heart	0.24	0.04	0.65	0.81	0.18	0.02
	Lungs	1.11	0.28	5.21	0.58	2.11	0.43
	Liver	17.80	3.94	15.33	2.48	27.14	1.48
	Spleen	1.23	0.52	2.91	3.66	1.64	0.59
	Testicles	0.51	0.24	0.22	0.04	0.29	0.04
	Kidneys	1.06	0.24	1.20	0.19	1.20	0.14
	Brain	0.14	0.04	0.13	0.02	0.24	0.03
24 h	Blood	1.69	0.20	1.49	0.48	2.04	0.62
	Heart	0.15	0.07	0.15	0.14	0.15	0.04
	Lungs	0.55	0.27	2.57	0.51	0.96	0.43
	Liver	12.42	4.10	13.09	1.18	21.10	3.16
	Spleen	1.19	0.34	1.02	0.20	1.20	0.35
	Testicles	0.18	0.04	0.15	0.02	0.22	0.05
	Kidneys	0.71	0.29	0.59	0.20	0.85	0.04
	Brain	0.03	0.01	0.05	0.03	0.09	0.02

Table 4.V. Body distribution of ^{14}C as percent of the dose after intravenous administration 5 days after tumour transplantation of ^{14}C-PBCA nanoparticles, polysorbate 80-coated ^{14}C-PBCA nanoparticles, and DOX ^{14}C-PBCA loaded nanoparticles.

Time	Sample	NP		NP+PS 80		NP+PS 80+DOX	
		µg NP/g	S.D.	µg NP/g	S.D.	µg NP/g	S.D.
10 min	Blood	80.84	13.03	58.26	19.53	57.46	8.88
	Heart	50.21	25.42	35.71	8.91	40.23	1.46
	Lungs	405.05	108.34	317.53	157.91	350.08	103.57
	Liver	214.11	7.13	101.3	36.91	233.87	45.81
	Spleen	358.90	70.16	159.20	96.51	220.93	88.62
	Testicles	22.99	7.76	11.79	2.02	18.05	1.44
	Kidneys	211.75	126.98	132.13	29.22	262.96	14.71
	Brain	17.49	5.36	19.08	5.53	23.40	3.41
1 h	Blood	44.63	9.90	42.93	14.48	33.20	4.80
	Heart	30.53	10.76	35.00	20.03	22.00	4.02
	Lungs	81.61	26.51	250.12	37.01	168.95	49.10
	Liver	167.48	45.52	109.82	59.85	141.83	19.64
	Spleen	185.96	70.90	104.00	66.50	226.55	122.85
	Kidneys	92.18	16.53	94.81	38.71	75.81	19.59
	Brain	13.35	7.27	40.44	10.18	25.15	1.41
6 h	Blood	20.01	3.56	18.21	3.79	11.43	4.76
	Heart	14.22	2.19	39.37	48.95	11.18	0.91
	Lungs	40.17	10.01	188.96	21.02	80.56	15.68
	Liver	88.05	19.48	75.87	12.27	134.27	7.32
	Spleen	101.39	56.67	200.95	19.77	139.70	64.68
	Testicles	4.21	5.22	1.82	0.95	1.92	0.91
	Kidneys	30.30	6.93	34.47	5.55	34.48	3.89
	Brain	8.74	1.33	7.09	0.77	10.61	1.00
24 h	Blood	7.67	0.92	6.76	2.18	9.24	2.79
	Heart	9.04	4.48	8.92	8.22	9.15	2.43
	Lungs	19.94	9.68	93.30	18.39	34.83	15.74
	Liver	61.47	20.30	64.78	5.85	104.40	15.65
	Spleen	129.08	36.64	111.44	22.22	130.35	37.79
	Testicles	3.91	0.87	3.27	0.52	4.79	0.99
	Kidneys	16.30	8.18	20.76	5.70	24.46	1.04
	Brain	3.20	0.29	3.96	0.80	4.64	0.77

Table 4.VI. Body distribution (in µg nanoparticles per g tissue weight) after intravenous administration 5 days after tumour transplantation of ^{14}C-PBCA nanoparticles, polysorbate 80-coated ^{14}C-PBCA nanoparticles, and DOX ^{14}C-PBCA loaded nanoparticles.
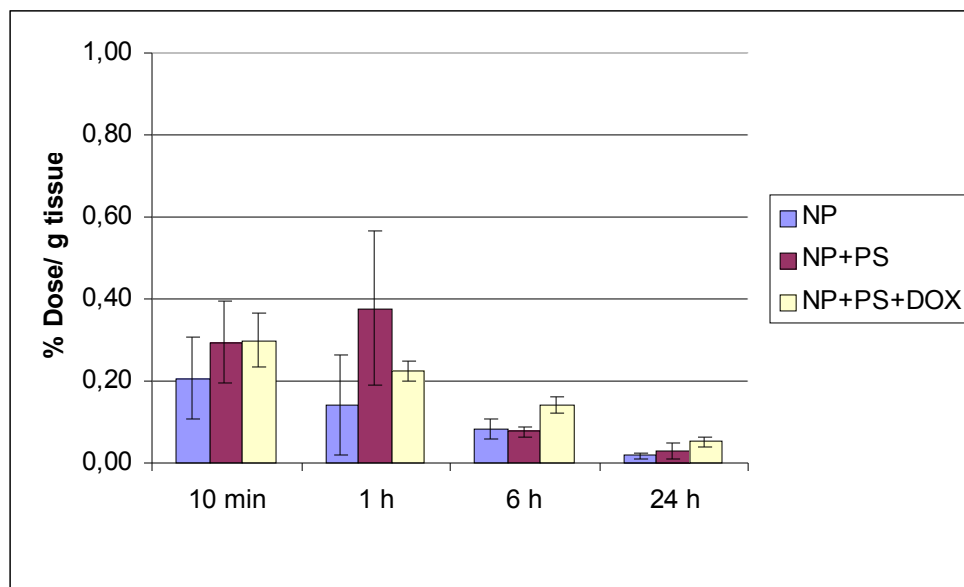
Figure 4.9 Brain distribution after intravenous administration of 20 mg/kg ^{14}C-PBCA nanoparticles, polysorbate 80-coated ^{14}C-PBCA nanoparticles, and DOX ^{14}C-PBCA loaded nanoparticles 5 days after tumour transplantation.

4.4.3.1.2 Nanoparticle concentrations in glioblastoma

Fig. 4.10 shows the concentration of nanoparticles in glioblastoma 101/8, the principal target of the nanoparticles of the present study.

The most prominent results was the relative high concentration reached by DOX ^{14}C-PBCA nanoparticles after 1 h and 6 h (0.68 % and 0.51 % dose/g tissue). However the small tumoural mass 5 days after the tumour implantation limited the reliability of the data presented.
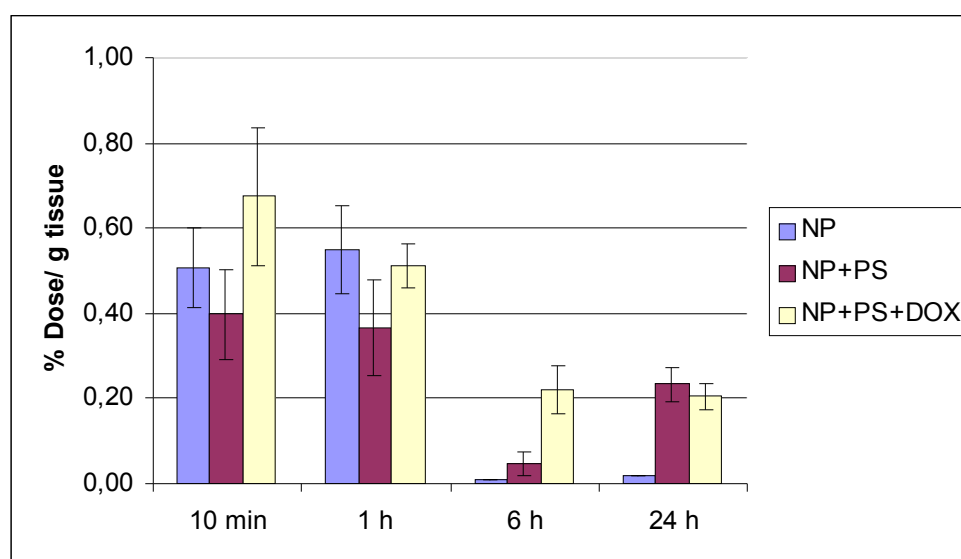
Figure 4.10. Concentration of nanoparticles (NP), nanoparticles + polysorbate 80 (PS), and doxorubicin-loaded and polysorbate-80 coated nanoparticles (NP+PS+DOX) in glioblastoma after i.v. injection of 20 mg/

kg nanoparticles 5 days after tumour transplantation.

4.4.3.2 Eight days glioblastoma bearing rats

4.4.3.2.1 Body distribution

In the rats that obtained the nanoparticle formulations 8 days after tumour transplantation, the coating of nanoparticles with PS 80 led to a significant increase of NP concentration in the blood 10 min after nanoparticle injection. As Tables 4.VIII and 4.IX show, the blood NP+PS 80 concentration was of 22 % of the injected dose and 29 % of the dose for NP+PS 80+DOX. The blood concentration of uncoated and unloaded NP after 10 min was only 5.4 % of the dose/ g. After 1 h the differences in blood concentration for all three formulations were diminished. The particles blood concentration was not significant at 6 h and 24 h post injection.

An important accumulation of particles was shown in the liver (Tables 4.VIII and 4.IX) being the major organ of the RES. At 10 min post injection NP+PS 80 reached the concentration of 34 % of the dose while the uncoated NP concentration was 17 % of the dose. The liver concentration observed after DOX binding was 20 % of the dose.

After 1 h NP+PS 80+DOX achieved a liver concentration of 30 % of the dose whereas NP, and NP+PS 80 achieved in the liver the concentration of 21 % and 26 % of the dose, respectively.

Noteworthy was the liver accumulation of coated nanoparticles (NP+PS 80 and NP+PS 80+DOX) at 6 h post injection.

Regarding the particles concentration in the spleen, no important differences were displayed 10 min after injection between the three formulations. At 1 h the spleen concentration of NP and NP+PS 80+DOX were about two-fold higher than that of NP+PS 80.

Time	Sample	NP		NP+PS 80		NP+PS 80+DOX	
		Percent dose	S.D.	Percent dose	S.D.	Percent dose	S.D.
10 min	Blood	5.36	1.58	21.65	5.78	28.63	10.13
	Heart	0.45	0.49	1.02	0.22	1.51	0.62
	Lungs	2.59	2.05	7.06	4.44	5.28	3.27
	Liver	16.80	9.14	33.73	3.73	20.26	7.86
	Spleen	0.95	0.73	1.15	0.37	0.99	0.29
	Testicles	0.30	0.12	0.96	0.22	1.21	0.49
	Kidneys	1.78	0.80	8.15	2.20	8.58	0.74
	Brain	0.37	0.11	0.55	0.18	0.58	0.26
1 h	Blood	4.34	0.59	9.57	1.06	8.32	1.74
	Heart	0.22	0.03	0.51	0.16	0.49	0.17
	Lungs	11.55	8.76	3.08	0.59	8.73	2.10
	Liver	21.37	3.45	26.34	1.99	30.41	4.28
	Spleen	1.46	0.27	0.76	0.06	1.69	0.61
	Testicles	0.44	0.19	0.63	0.09	0.66	0.14
	Kidneys	1.51	0.52	3.45	0.65	4.52	2.86
	Brain	0.26	0.08	0.57	0.06	0.67	0.37
6 h	Blood	0.21	0.02	0.48	0.15	2.52	1.05
	Heart	0.01	0.00	0.02	0.01	0.18	0.02
	Lungs	0.12	0.02	0.55	0.21	2.11	0.43
	Liver	19.74	0.09	23.75	0.60	27.14	1.48
	Spleen	0.07	0.02	0.11	0.04	1.64	0.59
	Testicles	0.01	0.00	0.03	0.01	0.29	0.04
	Kidneys	0.06	0.02	0.13	0.06	1.20	0.14
	Brain	0.11	0.00	0.12	0.00	0.24	0.03
24 h	Blood	0.46	0.02	1.93	0.31	1.77	0.29
	Heart	0.03	0.01	0.14	0.05	0.17	0.04
	Lungs	0.46	0.34	0.80	0.13	1.80	0.34
	Liver	3.97	1.50	14.00	2.28	19.43	2.85
	Spleen	0.43	0.25	0.56	0.15	1.30	0.44
	Testicles	0.04	0.02	0.19	0.03	0.24	0.04
	Kidneys	0.15	0.05	0.71	0.07	0.86	0.19
	Brain	0.02	0.00	0.11	0.02	0.17	0.05

Table 4.VIII. Body distribution of ^{14}C as percent of the dose after intravenous administration 8 days after tumour transplantation of ^{14}C-PBCA nanoparticles, polysorbate 80-coated ^{14}C-PBCA nanoparticles, and DOX ^{14}C-PBCA loaded nanoparticles.

Time	Sample	NP		NP+PS 80		NP+PS 80+DOX	
		µg NP/g	S.D.	µg NP/g	S.D.	µg NP/g	S.D.
10 min	Blood	24.29	7.15	84.55	8.44	104.86	83.06
	Heart	17.02	6.21	57.65	12.30	73.28	61.62
	Lungs	121.92	63.34	270.75	105.73	210.47	76.74
	Liver	83.14	45.25	160.24	16.19	105.11	38.89
	Spleen	107.80	67.53	132.22	24.81	115.78	50.59
	Testicles	6.42	2.53	18.69	2.30	21.34	17.52
	Kidneys	50.99	22.95	200.54	47.95	217.82	131.35
	Brain	13.76	3.38	22.84	1.84	29.20	12.97
1 h	Blood	19.68	2.65	42.33	5.16	39.25	8.72
	Heart	13.30	1.77	31.35	10.68	29.73	11.48
	Lungs	319.46	45.25	68.95	15.09	251.98	89.66
	Liver	105.72	17.08	128.42	9.98	148.37	24.14
	Spleen	158.39	29.04	79.83	4.55	176.35	76.50
	Testicles	9.50	4.08	13.50	1.82	14.80	3.49
	Kidneys	43.11	14.82	97.02	21.75	151.06	83.59
	Brain	8.20	2.63	18.89	2.23	30.95	13.43
6 h	Blood	0.97	0.08	2.07	0.78	8.63	7.86
	Heart	0.60	0.00	1.21	0.38	7.15	5.55
	Lungs	4.31	0.66	19.23	8.16	49.23	40.97
	Liver	96.99	13.46	117.49	30.31	135.74	55.15
	Spleen	7.62	1.93	9.98	3.80	135.33	117.28
	Testicles	0.24	0.08	0.65	0.19	3.91	3.08
	Kidneys	1.58	0.61	3.53	1.90	21.33	16.53
	Brain	2.32	0.00	2.53	0.17	4.73	3.69
24 h	Blood	2.08	0.08	9.03	1.49	8.10	1.56
	Heart	1.61	0.31	8.57	3.12	10.48	2.47
	Lungs	16.51	12.20	31.14	2.82	66.16	13.75
	Liver	19.66	7.44	74.66	5.28	93.97	15.98
	Spleen	46.63	27.69	66.95	14.58	138.43	55.80
	Testicles	0.83	0.35	4.17	0.73	5.01	0.79
	Kidneys	4.34	1.54	20.53	1.99	24.40	6.39
	Brain	0.24	0.00	3.74	0.69	5.23	4.82

Table 4.IX. Body distribution (in µg nanoparticles per g tissue weight) after intravenous administration 8 days after tumour transplantation of ^{14}C-PBCA nanoparticles, polysorbate 80-coated ^{14}C-PBCA nanoparticles, and DOX ^{14}C-PBCA loaded nanoparticles.
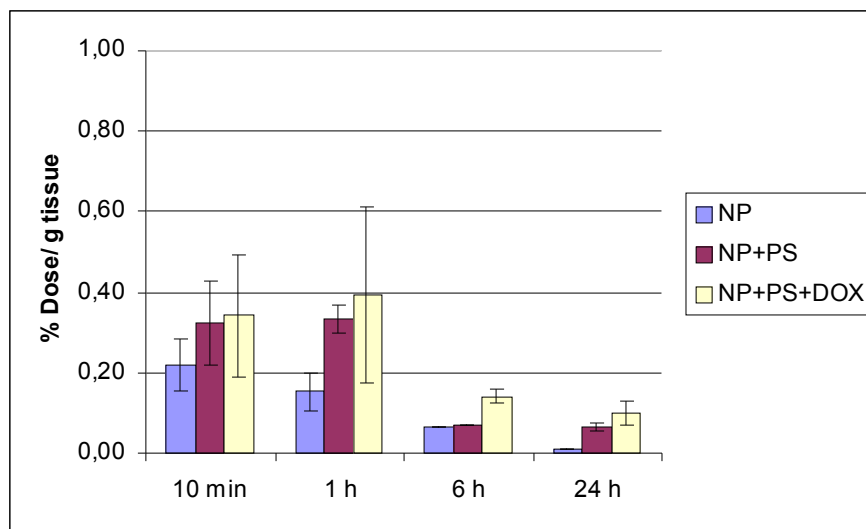
Figure 4.11. Brain distribution after intravenous administration of 20 mg/kg 14C-PBCA nanoparticles, polysorbate 80-coated 14C-PBCA nanoparticles, and DOX 14C-PBCA loaded nanoparticles 8 days after tumour transplantation.

Regarding the brain distribution, nanoparticles without coating showed the lowest brain concentration (Figure 4.11). The coating with polysorbate 80 enhanced the brain up-taking. Finally doxorubicin nanoparticles reached the highest concentration at each time point.

4.4.3.2.2 Nanoparticles concentration in glioblastoma

A concentration of almost 1 % of the dose/g tissue was obtained by DOX ^{14}C-PBCA nanoparticles after 10 min post injection (Fig 4.12).
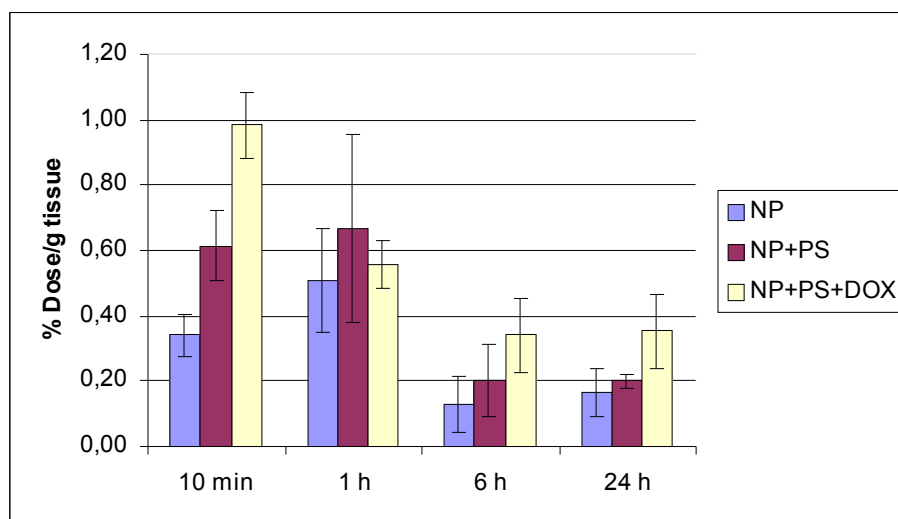
Figure 4.12. Concentration of nanoparticles (NP), nanoparticles + polysorbate 80 (PS), and doxorubicin-loaded and polysorbate-80 coated nanoparticles (NP+PS+DOX) in glioblastoma after i.v. injection of 20 mg/kg nanoparticles 8 days after tumour transplantation.

The concentration of these particles was reduced to 0.58 % after 1 h. The other nanoparticle preparations yielded lower concentrations in the glioblastoma, except the ^{14}C-PBCA PS 80-coated NP, which reached the concentration of 0.62 % of the dose/ g tissue after 1 h. However this value was not statistically significant.

4.4.3.3 Ten days glioblastoma bearing-rats

4.4.3.3.1 Body Distribution

The body distribution of $[^{14}C]$-PBCA NP in tumour bearing rats 10 days post tumour implantation is shown in Table 4.X (percent of dose) and Table 4.XI (µg/g tissue weight). The blood concentrations 10 min and 1 h post injection were comparable for the three formulations. After 10 min, doxorubicin loaded nanoparticles showed a slightly higher concentration in comparison with NP and NP+PS 80 (15 % versus 11 %, and 9 % of the dose, respectively) (Table 4.X). A similar tendency was observed 1 h and 6 h after injection.

In the organs of the reticuloendothelial system (RES), i.e. liver, spleen, and lungs, the biodistribution pattern was more complex. Polysorbate 80-coating reduced the liver and spleen concentrations of the unloaded particles. In fact, 10 min after injection the liver concentration of NP was ~35 %, whereas the concentration of NP+PS 80 was reduced to ~24 %. The same tendency was displayed at 1 h and 6 h after injection. The concentration of coated and uncoated $[^{14}C]$-PBCA NP at 24 h post injection in liver and spleen was comparable.

The behaviour of doxorubicin-loaded $[^{14}C]$-PBCA NP was different. Although those particles were coated with PS 80, the addition of doxorubicin seemed to abolish the effect of the coating, which resulted in similar or even higher RES organ concentrations, as compared to the uncoated particles.
Investigation of other organs, such as heart, kidneys, and testicles did not reveal any important difference between the three preparations.

Time	Sample	NP		NP+PS 80		NP+PS 80+DOX	
		Percent dose	S.D.	Percent dose	S.D.	Percent dose	S.D.
10 min	Blood	11.49*	2.55	9.12*	0.76	15.24*	2.16
	Heart	0.82*	0.17	0.56*	0.13	0.75*	0.08
	Lungs	3.63	0.92	8.11	4.73	11.93	9.56
	Liver	34.76*	3.49	24.32*	8.62	36.82*	3.40
	Spleen	2.81	0.89	1.54	0.82	4.59	0.57
	Testicles	0.88	0.15	0.58	0.26	0.94	0.39
	Kidneys	5.68*	0.15	3.72*	1.59	8.56	2.36
	Brain	0.49*	0.15	0.59*	0.06	0.56*	0.08
1 h	Blood	7.94*	1.48	6.19*	0.56	9.16*	1.72
	Heart	0.31*	0.08	0.31*	0.03	0.52*	0.02
	Lungs	1.54	0.32	5.46	0.78	5.29	0.88
	Liver	24.41	6.29	18.44*	1.06	36.69*	1.82
	Spleen	1.67	0.65	1.24	0.23	1.50	0.17
	Testicles	0.66	0.18	0.44*	0.04	0.71*	0.06
	Kidneys	2.21	0.61	2.25*	0.31	4.10*	0.05
	Brain	0.49*	0.02	0.76*	0.08	0.93*	0.04
6 h	Blood	2.30	0.28	2.56	0.13	4.43	0.73
	Heart	0.11*	0.01	0.16*	0.01	0.27	0.09
	Lungs	0.64	0.09	2.79	0.97	2.73	0.53
	Liver	14.64*	1.49	10.96*	2.36	20.93*	2.11
	Spleen	1.00	0.11	0.89	0.65	0.93	0.13
	Testicles	0.18*	0.03	0.19*	0.05	0.32*	0.08
	Kidneys	0.58	0.08	0.71	0.14	1.29	0.35
	Brain	0.11*	0.03	0.14*	0.04	0.25*	0.05
24 h	Blood	1.07	0.17	1.28	0.27	1.88	0.30
	Heart	0.08	0.02	0.10	0.04	0.14	0.04
	Lungs	0.29	0.06	0.80*	0.08	7.69*	0.54
	Liver	10.52*	1.41	11.60*	1.00	18.96*	2.67
	Spleen	0.85	0.20	0.87	0.19	1.23	0.21
	Testicles	0.10*	0.02	0.12*	0.03	0.17*	0.04
	Kidneys	0.36*	0.05	0.47*	0.04	0.85	0.10
	Brain	0.05*	0.01	0.07*	0.02	0.10*	0.03

* difference in mean values statistical significant ($P < 0,05$)

Table 4.X. Body distribution of ^{14}C as percent of the dose after intravenous administration 10 days after tumour transplantation of ^{14}C-PBCA nanoparticles, polysorbate 80-coated ^{14}C-PBCA nanoparticles, and DOX ^{14}C-PBCA loaded nanoparticles.

Results

Time	Sample	NP		NP+PS 80		NP+PS 80+DOX	
		µg NP/g	S.D.	µg NP/g	S.D.	µg NP/g	S.D.
10 min	Blood	52.10*	11.57	42.12*	3.71	70.98*	10.75
	Heart	49.29*	10.49	36.99*	6.15	46.67*	4.90
	Lungs	131.59	33.23	203.92	35.71	251.28	101.27
	Liver	171.97*	17.25	129.37*	46.34	186.59*	17.28
	Spleen	305.52	96.70	177.62	102.76	620.30	77.97
	Testicles	19.05	3.36	14.26	5.80	21.73	9.51
	Kidneys	162.71	47.52	114.35	50.96	229.27	71.91
	Brain	15.96*	4.84	19.03*	2.39	18.34*	3.11
1 h	Blood	36.03*	6.70	28.09*	2.52	41.52*	7.81
	Heart	18.82*	4.69	18.90*	1.61	31.30*	1.43
	Lungs	55.83	11.44	198.07	28.31	191.77	31.83
	Liver	120.78	31.11	91.25*	5.23	181.53*	8.99
	Spleen	181.93	70.39	134.85	24.62	163.12	18.07
	Testicles	14.37	4.02	9.47*	0.88	15.40*	1.22
	Kidneys	63.16*	17.56	64.49*	9.02	117.52*	1.43
	Brain	16.03*	0.78	24.65*	2.28	30.37*	1.29
6 h	Blood	10.42	1.28	11.60	0.61	20.10	3.31
	Heart	6.73*	0.75	9.45*	0.72	16.33	5.20
	Lungs	23.09	3.09	101.19	35.08	99.12	19.11
	Liver	72.41*	7.37	54.25*	10.41	103.54*	10.46
	Spleen	108.58	12.39	96.63	71.30	100.98	13.89
	Testicles	3.97*	0.67	4.14*	1.00	7.00*	1.64
	Kidneys	16.69	2.30	20.20	3.87	36.86	10.12
	Brain	3.60*	0.83	4.44*	1.27	8.11*	1.56
24 h	Blood	4.87	0.77	5.82	1.21	8.50	1.36
	Heart	4.99	0.96	5.97	2.34	8.32	2.16
	Lungs	10.48	2.14	29.12*	2.73	279.12*	78.92
	Liver	52.03*	6.99	57.42*	4.97	93.82*	13.19
	Spleen	91.98	22.00	94.14	20.24	133.76	23.27
	Testicles	2.26*	0.38	2.64*	0.55	3.67*	0.84
	Kidneys	10.42*	1.43	13.39*	1.26	24.31	2.83
	Brain	1.76*	0.24	2.52*	0.58	3.48*	0.81

* difference in mean values statistical significant ($P < 0,05$)

Table 4.XI. Body distribution (in µg nanoparticles per g tissue weight) after intravenous administration 10 days after tumour transplantation of ^{14}C-PBCA nanoparticles, polysorbate 80-coated ^{14}C-PBCA nanoparticles, and DOX ^{14}C-PBCA loaded nanoparticles.

In brain, ^{14}C-PBCA nanoparticles, PS 80-coated ^{14}C-PBCA nanoparticles, and DOX ^{14}C-PBCA nanoparticles showed similar concentrations 10 minutes after injection (Fig. 4.13). Precisely, the brain concentration of the mentioned formulations reached about 0.3-0.35 % of the dose/ g tissue. Enhanced brain concentrations of polysorbate 80-coated ^{14}C-PBCA nanoparticles appeared after 1 hour. After 1 h the percentage of the dose/ g tissue was increased to 0.45 % with the polysorbate 80-coated particles and to 0.57 % with the DOX ^{14}C-PBCA nanoparticles. After 6 h the brain concentration of all three formulations was significantly decreased. The concentration of DOX ^{14}C-PBCA nanoparticles was still higher than that of the ^{14}C-PBCA nanoparticles and PS 80-coated ^{14}C-PBCA nanoparticles.

Noteworthy is the increase of the NP brain concentration for all formulations from day 5 to day 10, although in most cases this difference was not statistically significant. The highest concentration (statistically significant) was reached using doxorubicin-loaded [^{14}C]-PBCA NP 1 h post injection in 10 days tumour bearing rats (0.93 %, Tab 4.X).
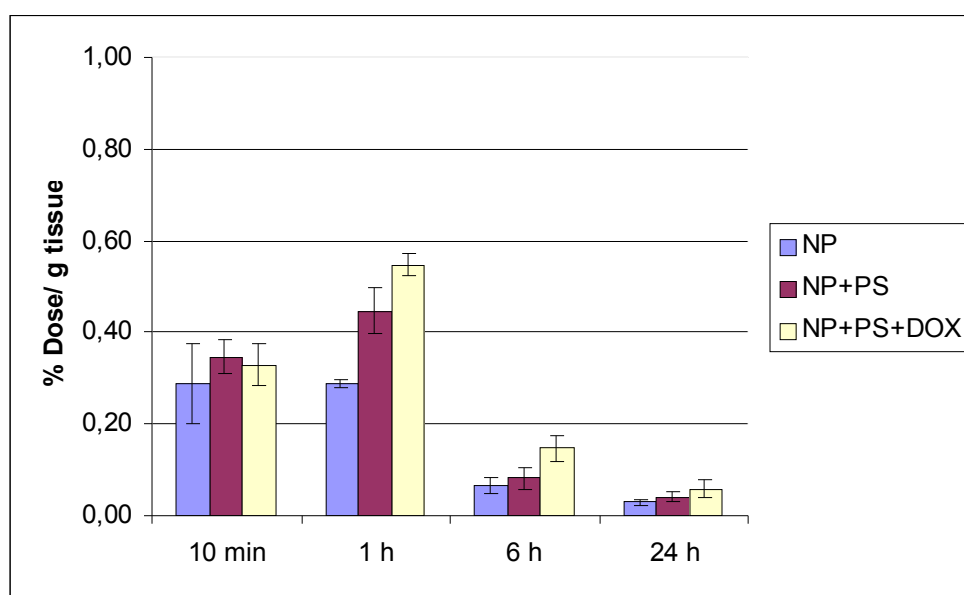

Figure 4.13. Brain distribution after intravenous administration of 20mg/kg of ^{14}C-PBCA nanoparticles, polysorbate 80-coated ^{14}C-PBCA nanoparticles, and DOX ^{14}C-PBCA loaded nanoparticles 10 days after tumour transplantation.

4.4.3.3.2 Nanoparticles concentration in glioblastomas

Ten days post tumour implantation the glioblastomas reached the size range of 2 - 5 mm. The concentration of DOX ^{14}C-PBCA nanoparticles reached a remarkable 2.4 % of the dose/g tissue at 10 min post injection (Figure 4.14). However this value was not statistically significant compared to the other two formulations.
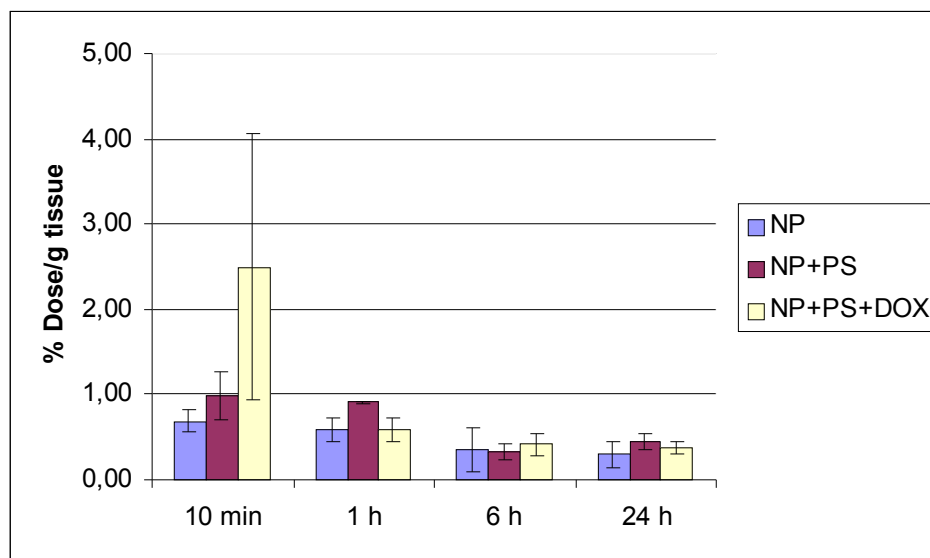

Figure 4.14. Concentration of nanoparticles (NP), nanoparticles + polysorbate 80 (PS), and doxorubicin-loaded and polysorbate-80 coated nanoparticles (NP+PS+DOX) in glioblastoma after i.v. injection of 20 mg/kg nanoparticles 10 days after tumour transplantation.

After 1 h PS 80-coated [^{14}C]-PBCA nanoparticles reached a concentration of 0.9 % dose/g tissue. This value is two-fold of the concentration of ^{14}C-PBCA nanoparticles in the surrounding brain tissue (Figure 4.13). The three formulations maintained a similar concentration (between 0.3 - 0.4 % dose/g tissue) at 6 h and 24 h post injection, and at each time point the nanoparticles tumour concentration is higher than brain concentration. Figure 4.15 shows the percent of the injected dose per g tumour tissue for the three formulations at 1 h post injection in the controlateral hemisphere and in the glioblastoma. The figure is particularly representative for comparing the enhancement of the nanoparticle formulations in the glioblastoma which was more pronounced than in the controlateral hemisphere. Moreover the values were statistically significant ($P < 0.05$).
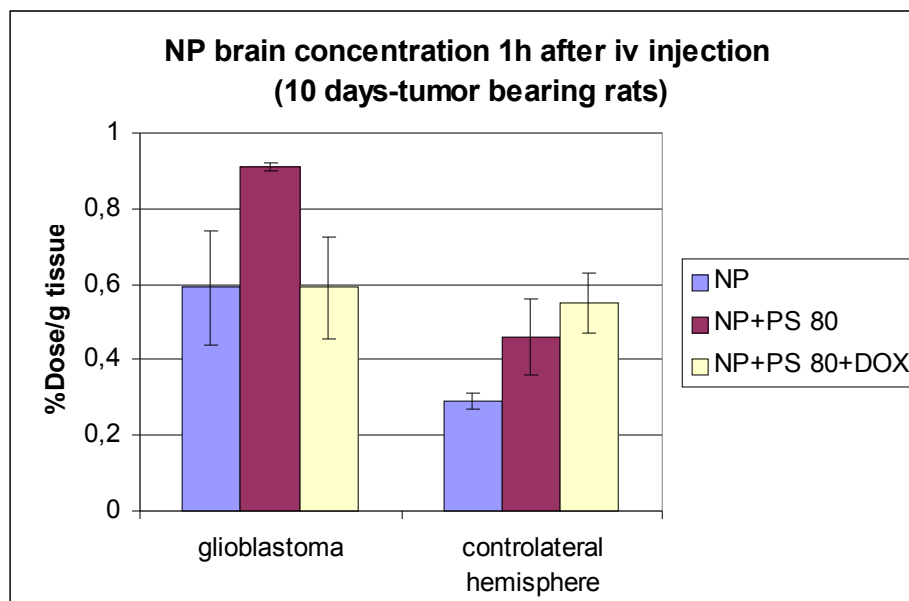
Figure 4.15. Biodistribution of nanoparticles (NP), nanoparticles + polysorbate 80 (PS 80) and doxorubicin-loaded and polysorbate 80 coated nanoparticles (NP+PS 80+DOX), in the brain of tumour-bearing rats, 1 h after intravenous administration of 20 mg/kg of nanoparticles.

Significant extravasation into the glioblastoma was found for unloaded polysorbate 80-coated [14C]-PBCA NP whereas the concentration of other formulations was ~ 0.60 %. For all formulations, [14C]-PBCA NP concentration was slightly higher in the glioblastoma than in the controlateral hemisphere.

4.4.4 Evaluation of the BBB integrity

Evans Blue has been commonly used to demonstrate a defective BBB in transplanted rodent tumours (Ji et al. 1996, Prabhu et al. 2000).

It could be seen that the accumulation of Evans Blue in the tumour remained low for 5 days post tumour implantation (Fig 4.16). BBB disruption became pronounced on day 6 after tumour implantation. Fluorescence in the contralateral hemisphere remained low within the period of observation. The decrease of tumour fluorescence on day 9 may be due to a lower penetration of the dye into the tumour tissue due poor vascularization of the tumour core and necrosis occurring during the later stages of tumour development.
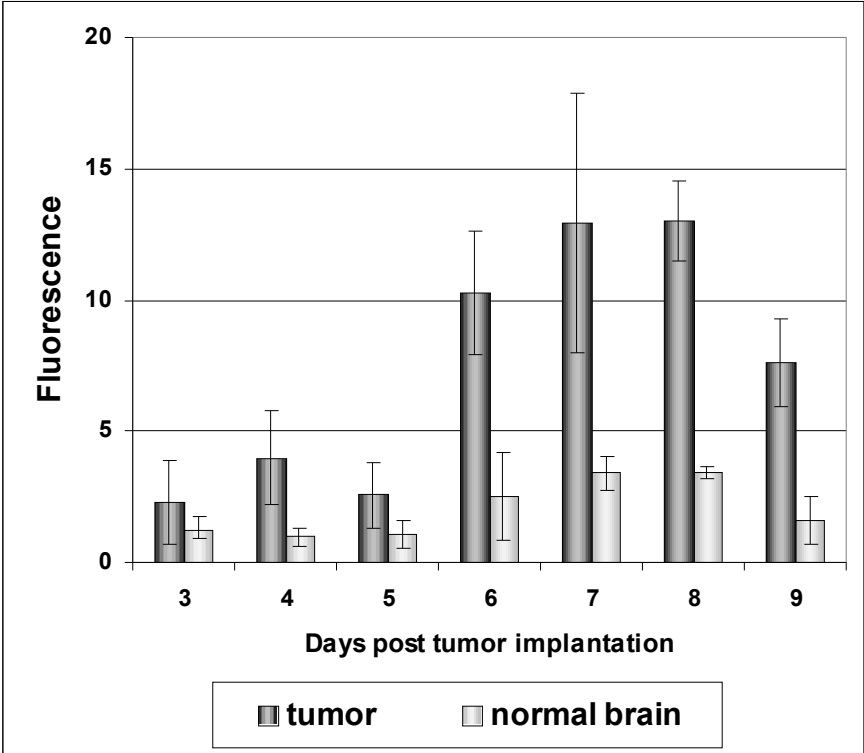
.

Figure 4.16. Fluorescence of Evans Blue in the tumour tissue and normal brain tissue (contralateral hemisphere) at different stages of glioblastoma development (n = 3).

4.5 Whole-body autoradiography (WBA) studies

4.5.1 Body distribution of [14-^{14}C] DOX PBCA NP coated with PS 80 at 1 h, 2 h, 4 h post injection

Figure 4.17 shows the body distribution of the PS 80-[14-^{14}C] DOX PBCA nanoparticles two hours after intravenous injection into the tail vein of a rat. A high activity in the GI-tract occurred due to the faecal elimination of PS 80-[14-^{14}C] DOX PBCA NP (Löbenberg et al. 1998). An accumulation of nanoparticles was also visible in the organ of RES and in the hearth. The results are in accordance with the liquid scintillation study. The body distribution of PS 80-[14-^{14}C] DOX PBCA NP at 1 h and 4 h post injection was comparable (data not shown).
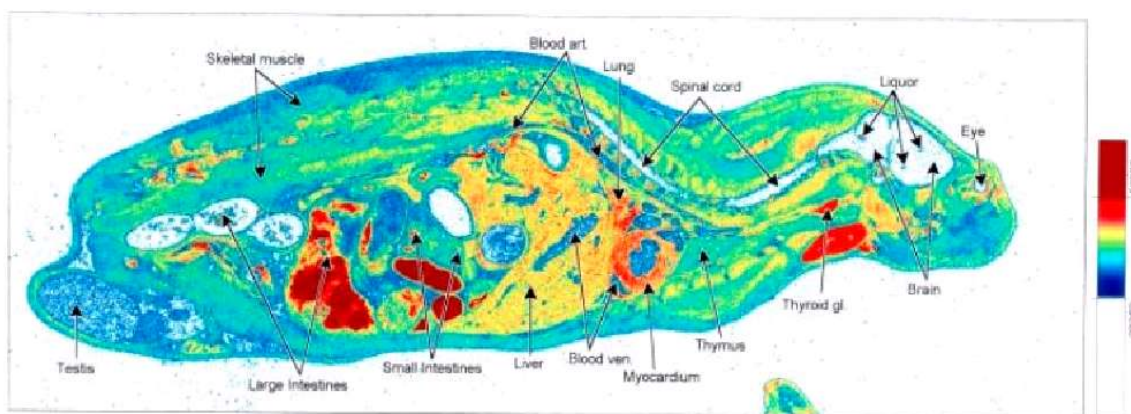
Figure 4.17. Radioluminography of a rat 2 h after i.v. injection of PS 80-[14-^{14}C] DOX PBCA NP.

4.5.2 Body distribution of PS 80-[14-^{14}C] DOX solution at 2 h post injection.

Figure 4.18 shows that PS 80-[14-^{14}C] DOX solution is relative homogeneously distributed in all the cell of most organs.

An important and significant difference between nanoparticles and solution was observed in the liver. The comparison of the autoradiographs (Figs 4.17 and 4.18) after i.v. injection of the two formulations showed a lower concentration of PS 80-[14-^{14}C] DOX PBCA NP in the liver in comparison to the PS 80-[14-^{14}C] DOX solution.
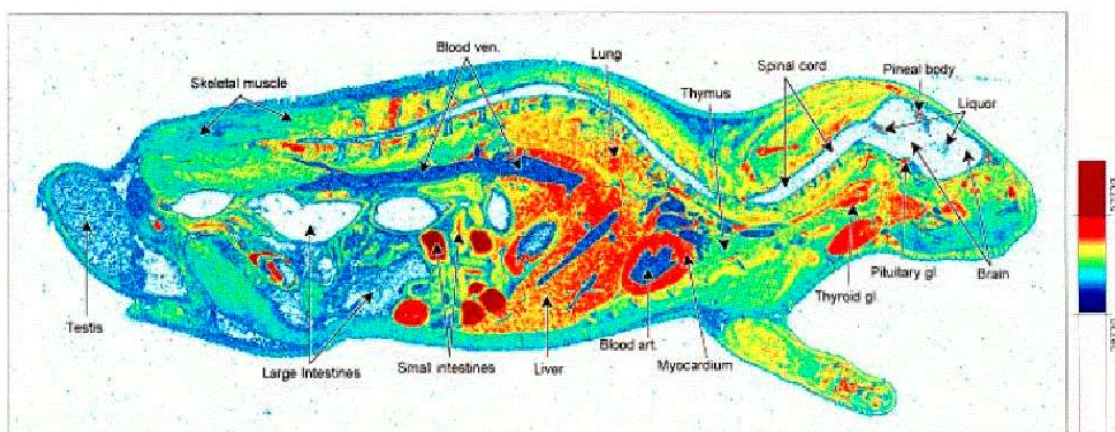
Fig 4.18. Radioluminography of a rat 2 h after i.v. injection of PS 80-[14-^{14}C] DOX control solution.

4.5.3 Brain distribution
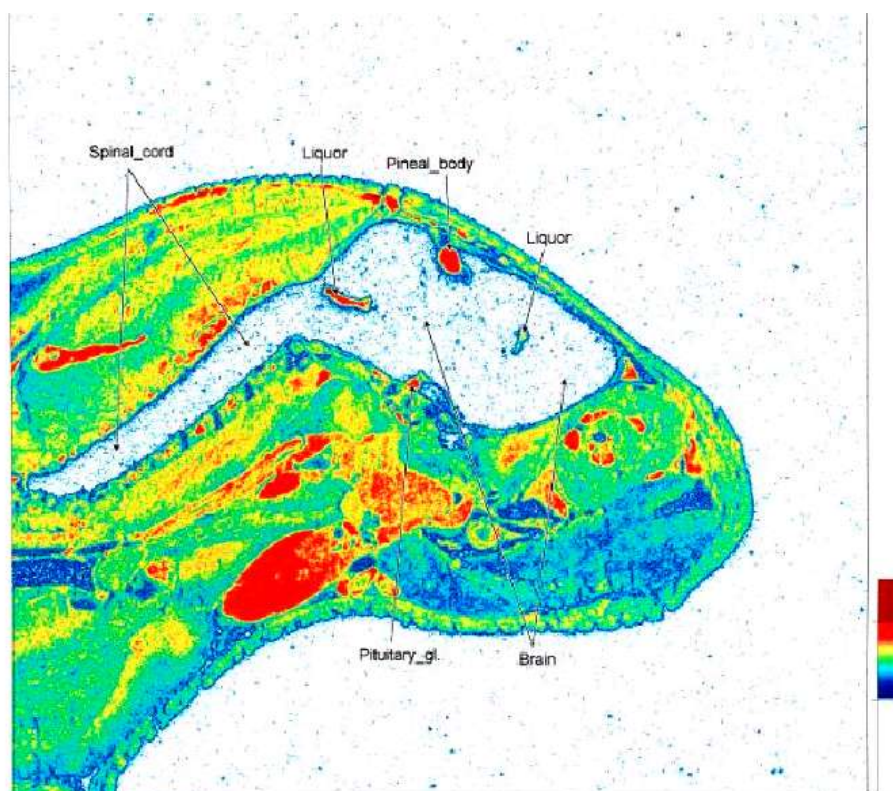

Figure 4.19. Radioluminography of the brain of a rat 2 h after i.v. injection of PS 80-[14-^{14}C] DOX PBCA NP.

The results of the brain distribution were similar for all the four rats. Therefore only the radioluminography of one experiment is illustrated (Fig 4.19). The concentrations in the

liquor and in the pineal body were considerable whereas no activity was observed in the brain.

5 Discussion

5.1 Optimisation of nanoparticles formulation

The first part of the present study was focused on the development of a doxorubicin nanoparticles formulation with an improved drug binding. The study was based on the presumption that particles with higher drug loading could transport a higher quantity of the drug into the brain, thus enhancing the therapeutic drug effect.

5.1.1 Influence of parameters on drug loading

The variations of parameters for nanoparticles preparation influenced the drug loading to a different extent. The parameters investigated in the present study were: 1) concentration and type of steric stabilizer; 2) monomer concentration and type of monomer; 3) pH of the medium; 4) polymerization time. The influence of the latter parameters on nanoparticle features can be described as following:

5.1.1.1 Influence of steric stabilizer

Doxorubicin nanoparticles were prepared at different concentration of dextran 70 000, used as steric stabilizer. Drug loading was increased of ~ 5 % using the concentration of 2 % dextran instead of 1 % (Tab 4.I).

The effect of dextran concentration can be explained according to the theory of particle formation in dispersion polymerization (Douglas et al. 1985, Barret et al. 1975). Nanoparticles formation is believed to occur via a nucleation mechanism. Initiation of polymerization results in the formation of oligomeric chains which grow in solution until they reach a critical molecular weight which depends on the solubility of the oligomer in the medium. The chains then either collapse upon themselves producing particle nuclei or several growing oligomeric chains may associate with each other to form an aggregate which, above a certain critical size, precipitates forming a new stable nucleus. In either case these nuclei can grow by capture of further oligomers from the solution. The stability of the resultant colloidal system is achieved by adsorption of polymeric stabilizer, i.e.,

dextrans.

The initial high number of particle nuclei and their small particle size result in a very large total particle surface area. At low dextran concentration the amount of stabilizer is insufficient to effectively cover the available surface, resulting in a unstable colloidal system. The smaller particles therefore agglomerate until the total particles surface area has decreased to a point such that the amount of dextran available is sufficient to produce a stable suspension.

At increased dextran concentration it is possible to stabilize a larger total particle surface area, resulting in the formation of stable particles of a lower size. If the total particles surface area is larger, a larger surface is available for binding doxorubicin molecules. The consequence is that the total amount of drug bound to the particles is increased as well as the drug loading.

5.1.1.2 Influence of monomer concentration

The concentration of n-BCA was investigated in the range of 0.5 % w/v to 1 % w/v. A decrease in monomer concentration to 0.75 % resulted in a progressive increase of entrapment efficiency. Nevetheless with a further reduction of the monomer concentration the drug loading decreased again. Although the monomer concentration is a factor contributing to the particles size and consequently to the drug loading, the pattern is complex and limited by the importance of a low polydispersity index and a maximum solid content for a free flowing suspension. Indeed at a low monomer concentration below 1 % (v/v) the polydispersity was found to be high, but decreased rapidly with increasing monomer concentration (Douglas et al. 1984).

5.1.1.3 Influence of pH medium

A pH of 2 was optimal for obtaining a significant value of drug loading (Tab 4.I). A deviation from this pH reduced the drug loading substantially.

This result can be explain by reference to the polymerization reaction (Fig 2.6). Polymerization occurs via an anionic mechanism involving initiation by nucleophilic attack on the β-carbon of butyl-2-cyanoacrilate. The resulting carbanion produced reacts with further monomers to form oligomeric chains which nucleate leading to the formation of

nanoparticles. The major initiating nucleophile is OH⁻, the concentration of which varies with pH. At high pH and hence high hydroxyl ion concentration, the polymerization rate is too rapid to allow discrete particle formation and leads to direct polymerization of monomer droplets producing an amorphous polymer mass. As pH decreases the decrease in reaction rate allows nanoparticles formation to occur. However, if the pH is too low the polymerization period is greatly extended and nanoparticles in this system become swollen with monomer. Coagulation of these semi-fluid particles is not reversible and so produces a polydispersed system of larger particles and larger specific surface area on which molecules of drug can bound. Hence a minimum size and higher loading are observed in the pH profile when polymerization is slow enough to give discrete particles but not so slow as to allow excessive particle coagulation (Douglas et al. 1985).

5.1.1.3 Influence of polymerization time

The prolongation of polymerization time up to 4 h led to an increase of 4 % in entrapment efficiency of nanoparticles prepared with 0.75 % monomer and 2 % dextran. This may be attributed to the high monomer to polymer conversion with time, leading to an increase on the amount of the polymer formed, thereby incorporating a larger amount of drug (Reddy and Murthy 2004).

5.1.1.4 Influence of dextran 70 000 and poloxamer 188 (Pluronic® F 68)

The employment of poloxamer 188 as steric stabilizer instead of dextran significantly reduced the quantity of doxorubicin bounded to the particles (~ 30 % of loading less using poloxamer 188), although lower polydispersity and particle sizes are gained by the use of poloxamer 188. To explain this behavior it was necessary investigate the zeta potenzial of nanoparticles stabilized with dextran and poloxamer 188.

It was found out that the zeta potential was −14 mV for dextran nanoparticles and −3.2 mV for poloxamer 188 nanoparticles.

These differences also can be explained on the basis of previous reports. Douglas et al. (1985) reported the presence of residual amounts of dextran in cyanoacrylate nanoparticles in the bulk as well as at the surface. A similar observation was reported by Edman et al. (1980) in the development of polyacryl dextran biodegradable microparticles. High zeta

potential values observed for the nanoparticles prepared using dextran were attributed to the contribution of charge by dextran 70 000 (dextran-O⁻), adsorbed onto the nanoparticle surface. This is not the case for nanoparticles prepared in the presence of the nonionic surfactant poloxamer 188. The nanoparticles stabilized by poloxamer 188 were surfactant stabilized during the polymerization, and hence the possibility of a masking effect on particle charge due to surfactant adsorption cannot be ruled out. Such a decrease in zeta potential after coating with block copolymers also was observed by Hawley et al. (1997) with poly(DL-lactide-co-glycolide) nanospheres. Incorporation of doxorubicin into nanoparticles showed a decrease in zeta potential values in both of the above cases, the decrease being high in dextran nanoparticles (+0.1 mV nanoparticles prepared with poloxamer 188 and +2 mV for particles prepared with dextran). The positive charge due to the doxorubicin on the nanoparticles surface can be attributed to the daunosamine sugar moieties. During the polymerization process, adsorption of doxorubicin onto the nanoparticle surface is possible, contributing to masking the polymer charge. A significant decrease in the zeta potential of doxorubicin nanoparticles prepared with dextran in comparison to those prepared with poloxamer 188, further strengthens the aspect of dextran presence on the particle surface, whose charge is masked by the adsorbed drug, contributing to the overall great decrease of the zeta potential.

The significant change of the zeta-potential in DOX nanoparticles prepared with dextran suggests that strong electrostatic interactions occur between doxorubicin and the negative particle surface, and this phenomenon explains the high entrapment efficacy. Oppositely, the slight variation of zeta potenzial after loading with doxorubicin to particles prepared with poloxamers 188 indicates that the electrostatic interactions are weak, and this aspect affects the drug loading that is significantly decreased.

5.1.1.5 Influence of n-butyl-2- cyanoacrylate and iso-butyl-2-cyanoacrylate

Iso-butyl-2-cyanoacrylate is an isomer of n-butyl-2-cyanoacrylate in which the butyl lateral chain is branched. The doxorubicin loading of iso-PBCA nanoparticles is 5 % higher than n-PBCA. The rationale for the increase of drug entrapment efficacy can be addict to lipophilic interactions between doxorubicin and the polymer. The presence of a branched lateral chain allows extended hydrophobic interaction. The two methyl groups of the iso-BCA enhance the anchorage of doxorubicin by hydrophobic interactions. The lipophilic

anthracycline part is involves in those bounds.

5.2 Release studies

5.2.1 Release with dialysis tube

The release study carried out with dialysis tube exhibited for all the formulations a biphasic pattern (Fig 4.1). The biphasic pattern of doxorubicin solution suggested that this method is not fully revealing the actual release dynamics. The curve relative to DOX solution evidenced that doxorubicin molecules require time to cross the dialysis membrane. Therefore, the curves result from the release of the drug from the particles and plus the time for crossing the membrane. Another limitation of this method was the adsorption of doxorubicin to the dialysis membrane. Almost 30 % of the drug was absorbed 500 min after beginning of the diffusion process.

Despite these limitations, assumptions on the release mechanism of doxorubicin from nanoparticles can be formulated. The release profile of doxorubicin from nanoparticles may be described using a biexponential function:

$$Ct = Ae^{-\alpha t} + Be^{-\beta t}$$

where C_t is the concentration of compound remaining in the nanoparticles at time t, A and B are system-charachteristic constants, and α and β are rate constants that can be obtained from semilogathmic plots (Illum et al 1986b).

The initial release rate was faster. The rapid release was due to the desorption of the drug from the particles surface. This adsorbed drug has little value in drug targeting as it is rapidly removed from the particle surface upon intra-arterial administration (Pramod et al. 1986).

The release of the remaining drug was slow due to the process of diffusion of the drug through the nanoparticles matrix. Thus the release profile suggests that doxorubicin carried by nanoparticles was associated with PBCA nanoparticles either by adsorption onto the particle surface or by inclusion in the nanoparticles matrix.

5.2.2 Release with centrifuge filters and with microtubes

The curves (Figs 4.2 and 4.3) show that almost all the drug was released after nanoparticles centrifugation. The g-force squeezed the nanoparticles and caused the immediate desorption of doxorubicin from the particles.

5.2.3 Interactions between doxorubicin and poly(butyl cyanoacrylate) nanoparticles

The studies of doxorubicin release from the particles present difficulties due to the weakness of the bonds between the drug and the PBCA matrix that led to the immediate release of doxorubicin.

The release of the adsorbed drug depends mainly on the affinity of the drug to the particles surface. The interaction between DOX and the oligomeric poly(alkyl cyanoacrylate) in nanoparticles was studies computationally by Poupaert and Couvreur (2003). The cohesion of drug and particles comes from a blend of dipole-charge interaction, H bonds, and hydrophobic forces. The dipole-charge interaction represents the main stabilizing factor for the complex. Nitrile groups from PBCA were the main actors in this scenario being in close interaction with the ammonium moiety present in the protonated amminosugar moiety of doxorubicin. The protonation of the N(3) amminosugar moiety of the doxorubicin occurs at physiological pH and this positive group has a significant influence on the molecular recognition for doxorubicin binding.

Calculation of the zeta potential reveals that the net positive charge of the ammonium nitrogen irradiates on the neighboring atoms of the amminosugar moiety.

To a lesser extend, ester carbonyls from PBCA interact with hydroxyl groups from the amino sugar.

Another stabilizing factor likely to account for this aggregation property originates from hydrophobic forces that are developed between the naphtoquinone tricyclic system of doxorubicin and the carbon-carbon backbone and the butyl ester side-chain of PBCA.

It can be concluded that oligomeric PBCA's which are highly lipophilic entities scavenge amphiphilic doxorubicin already during the polymerization process by extraction of the protonated species from the aqueous environment to an increasingly lipophilic phase embodied by the growing PBCA's. Noteworthy is the establishment of hydrogen bonds between the ammonium N—H function and the cyano groups.

5.3 Chemotherapy studies

5.3.1 Influence of surfactants on the survival times of glioblastoma-bearing rats

So far, only surface-modified nanoparticles have been shown to mediate a profound brain delivery. In the above mentioned study of Steiniger et al. (2004), the most prominent effect in the brain tumour model was achieved in the group treated with DOX-NP+PS 80. Other DOX formulations, such as drug solutions in saline or in 1% PS 80 and DOX-loaded in the uncoated PBCA nanoparticles, were considerably less effective although they also significantly increased the survival time. The higher efficacy of DOX-NP+PS 80 was explained by the ability of this formulation to deliver DOX across the BBB still intact at an early stage of tumour development due to specific mechanisms activated by the PS 80-coating of the NP (Kreuter et al. 2003). It also was assumed that other formulations could passively diffuse across the leaky endothelium to the tumour. Indeed, as shown by experiments using Evans Blue as a marker, the permeability of the BBB at the tumour site on days 5 and 8 is significantly increased (Ambruosi et al., J. Drug Target., submitted). However, the importance of this passive transport still is not fully elucidated.

It is well known that tumour uptake due to the EPR effect is more pronounced for the long-circulating carriers (Moghimi et al. 2001). The common approach to increase blood half-life of the particles is shielding of their surface and, consequently, a reduction of opsonization that can easily be achieved by coating the nanoparticles with surfactants, such as poloxamers or poloxamines (block copolymers of polyoxyethylene and polyoxypropylene). Indeed, in a number of studies, the enhanced brain delivery of the drug bound to the long-circulating nanoparticles correlated with the increased plasma AUC (Chen et al. 2001, Zara et al. 2002).

In the present study, the role of passive drug transport across the leaky BBB to the brain tumour using PBCA NP coated with two surfactants, poloxamer 188 and poloxamine 908, that have been extensively used for surface modification of the particulate carriers (Moghimi and Hunter 2000) was investigated.

Our results demonstrate that both surfactants considerably increased the anti-tumour effect of DOX-PBCA: long-term remission was achieved in 20 % (4/20) of animals. This result is statistically significant considering that a large number of animals was used in these experiments. The anti-tumoural effect of the surfactant-coated formulations possibly is attributable to the EPR effect. Indeed, poloxamine 908-coated poly(hexadecyl cyanoacrylate) nanoparticles failed to deliver these particles to the healthy brain (Calvo et al 2001). In a parallel manner, the results obtained by Kreuter et al. (1997) demonstrated that loading of the peptide dalargin to PBCA NP coated with poloxamer 188 did not enable a delivery of this drug across the intact BBB, whereas dalargin bound to PS 80-coated NP had a pronounced anti-nociceptive effect in mice, indicating that in the latter case dalargin was transported across the BBB. These observations taken together suggest that both, poloxamer 188 and poloxamine 908 were unlikely to provide transport of the drug-loaded nanoparticles across the BBB as a result of specific mechanisms but their long-circulating properties could facilitate the extravasation of nanoparticles across the BBB at the tumour site.

At the same time, the higher efficacy of the polysorbate 80-coated nanoparticles may be explained by the ability of these carriers to deliver the drug across the intact BBB at an early stage of tumour development due to the receptor-mediated mechanism. In this way, doxorubicin also may reach those parts of the brain, which although affected by the tumour, are still protected by an intact BBB. This result is remarkable since microvascular permeability in gliomas is heterogeneous and in some parts of the tumour the barrier function is retained. The efficacy of DOX-NP+PS 80 most likely cannot be attributed to the permeabilizing action of PS 80, since DOX solution administered with an equal dose of PS 80 was less effective (Steiniger et al 2004).

5.3.2 Influence of formulation variables on the survival times of glioblastoma-bearing rats

The variation of the ratio between monomer and stabilizer concentration had an effect on the particles size but did not influence significantly the drug loading. In particular the mean particle size was influenced by the concentration of dextran but not by the concentration of BCA. This results are in accordance with the study of Alonso et al. (1990). They showed a

decrease of particle size with increasing dextran concentration. This effect is explicable in terms of the particle formation process (Douglas et al.1995) as was previously explained (paragraph 5.1.1.1). Dextran forms a stabilizing layer around the developing nanoparticles. By increasing the concentration of dextran the formation of the layer is completed earlier, i.e. reduces the final particle size.

Relevant was the influence of pH on particle size and on drug loading (paragraph 5.1.1.3). Values of a pH larger than 2 led to a rapid polymerization process and the production of an amorphous polymer mass. However if the pH was too low the polymerization period was greatly extended and nanoparticles in this system become swollen with monomer (Douglas et al. 1985). In both cases, the particles obtained were not applicable in practice.

Nevertheless, the results of the present study showed that the modifications of the variables only led to subtle variation of drug loading. Despite those results, preparations 9 and 10 were selected to evaluate their efficacy in the treatment of glioblastoma.

In the reference preparation 0, the addition of DOX occurred 30 min after the beginning of polymerization to avoid the hydrolytic degradation of doxorubicin in acidic medium (Beijnen et al 1985).

In preparation 10, DOX was added before the start of polymerization process. Despite the prolonged presence of doxorubicin in the acidic medium, the HPLC assay did not reveal the presence of any by-products (data not shown). The addition of doxorubicin before the beginning of polymerization enormously would simplify the process of nanoparticles production. However, the percentage of surviving animals after the treatment with the formulation 10 in the present study was not satisfactory. A possible explanation for the modest efficacy of this preparation may be the increased content in dextran (2 % w/v). The molecules of dextran protrude from the surface of nanoparticles as loops or chains conferring to the particles surface hydrophilic properties (Lemarchand et al. 2004). The excess of dextran molecules on the surface most probably produced an effect very similar to that of the surfactants and, at the same time, interfered with the effective coating of the particles with polysorbate 80. Consequently, the process of endocytosis from the endothelial cells of BBB is diminished as well as the transport of doxorubicin into the

brain.

Regarding the iso-butyl NP, previous study showed that this polymer presented a reduced toxicity in comparison with n-butyl NP. Kante et al. (1982) demonstrated that the cumulative mortality of mice after intravenous administration of NP was significant higher for the latter formulation. Nevertheless, the result of the present study showed that the efficacy of n-PBCA NP in the treatment of glioblastoma was more pronounced than iso-PBCA NP. It may be possible that the two polymers present different behaviors *in vivo* which requires further investigations.

5.4 Body distribution of polysorbate 80 and doxorubicin-loaded [^{14}C]poly (butyl cyanoacrylate) nanoparticles after i.v. administration in healthy rats

The results of our experiments showed that no major alterations in body distribution appeared between the three preparations investigated in the present study, ^{14}C-PBCA nanoparticles, ^{14}C-PBCA nanoparticles overcoated with polysorbate-80, and doxorubicin-loaded ^{14}C-PBCA nanoparticles overcoated with polysorbate-80, 30 min before injection (Figs. 4.7 and 4.8). The highest concentration of all nanoparticles preparations were observed in the organs of the reticulo endothelial system (RES), and they were reduced after polysorbate 80-coating, confirming earlier results with similar particles (Gipps et al. 1986, Gipps et al. 1988, Tröster et al. 1990). Binding of doxorubicin to the nanoparticles, however, counteracted the polysorbate-coating.

In contrast, polysorbate 80 almost doubled the concentrations in the brain after 1 hour, but again this effect was counteracted by the doxorubicin-loading (Fig. 4.6). This pattern also was observable after longer time points. The delay in the increase of the brain concentrations with the two polysorbate-coated nanoparticle preparations is typical for a delivery mediated by polysorbate 80-coating (Alyautin et al. 1995, Kreuter et al. 1995, Alyautin et al. 1997, Gulayev et al. 1999) and may be a reflection of the time-consuming process of endocytosis.

In order to investigate the reason for this counteractive effect of doxorubicin, the zeta-potential of the nanoparticles was measured (Table 4.II). The binding of doxorubicin led to the alteration of the surface charge towards positive values.
Although polysorbate 80-overcoating reduced the zeta-potential, a positive net charge remained. If the zeta-potential values were measured after incubation in serum, the charges became negative, and the charge differences diminished, which is a strong indication of an interaction with serum components (Kreuter 1983d). This interaction in turn has a major influence on the body distribution (Tröster et al. 1990, Borchard and Kreuter 1993).

The positive charge due to the DOX on the nanoparticles surface can be attributed to the daunosamine sugar moieties (Brigger et al. 2004). Brigger et al. observed a similar effect caused by doxorubicin loading on the modification of the surface charge as well as the

body distribution of PEG-coated poly(hexaldecyl cyanoacrylate) nanoparticles. In their paper they attributed the alteration of the body distribution to an increase in effective particle size due to particle aggregation caused by the negatively charged plasma proteins. However, with our particles we did not observe a significant increase in particle size (Table 4.II) and therefore rather assume that the alteration is caused by a change-induced difference in cell interaction. In accordance with the positive-inside rule (von Heijne and Gavel 1988, von Heijne 1992), the surfaces of cell membranes exhibit a negative electrostatic charge. This negative charge is created by a prevalence of negative amino acids on the outside of membrane proteins. Therefore, it can be assumed that the electrostatic interactions between the positive DOX-loaded particles and the negative charged cells and tissues were responsible for the differences in the body distribution of polysorbate 80-overcoated nanoparticles with and without DOX as well as for the increased accumulations of the DOX particles in organs of the RES.

It is surprising that coating of the nanoparticles with polysorbate 80 is not increasing their concentration in the brain to a larger extent and that, moreover, doxorubicin-loading reduced this effect rather importantly, although very significant pharmacological effects (Alyautin et al. 1995, 1997) and higher doxorubicin concentrations (Gulayev et al. 1999) as well as significant anti-tumoural effects (Steiniger et al. 2004) were obtained with these preparations. Alyautdin et al. (2001) already observed that polysorbate 80-coating also only doubled the concentration of ^{3}H-dalargin in the brain while a strong non-nociceptive effect was obtained after this coating and no effect without this coating (Kreuter et al. 1995). In all of these studies that are mentioned above, the total brain concentration was measured. It is possible that although this total brain concentration was only slightly increased by the polysorbate 80-coating, the endocytotic uptake into the brain endothelial cells that account for only 1 % of the brain mass (Pardridge 1991) nevertheless was significantly increased.

5.5 Biodistribution of polysorbate 80-coated doxorubicin-loaded [^{14}C]-poly (butyl cyanoacrylate) nanoparticles after intravenous administration to glioblastoma-bearing rats

The results of the present studies indicate different patterns of biodistribution for the three formulation investigated, [^{14}C]-PBCA NP, [^{14}C]-PBCA NP overcoated with PS 80 , and DOX-loaded [^{14}C]-PBCA NP overcoated with PS 80 in tumour bearing rats (Tables 4.V – 4.XI). The results of the body distribution were in accordance with the experiments performed in healthy rats at all tumour stages. Uncoated nanoparticles accumulated in RES organs, such as lung, liver, and spleen. Coating of nanoparticles with PS 80 moderately reduced their uptake in liver and spleen, whereas lung uptake was increased. The influence of surfactant coating on plasma concentrations was not considerable. These observations are in accordance with the results of Tröster et al. (1990) and Araujo et al. (1999) demonstrating that the alteration of the nanoparticle surface properties due to the surfactant leads to an interaction with different opsonins which in turn facilitates the uptake of the particles by different phagocytosing cells.

In contrast, the uptake of PS 80-coated nanoparticles loaded with DOX was similar to that of uncoated particles. In fact, the presence of doxorubicin even led to a slight increase of RES uptake, thus counteracting the polysorbate coating. Similar results were obtained in the healthy rats (5.4). We observed a comparable counteractive effect of DOX against PS 80 coating. The different patterns of nanoparticles distribution may, therefore, be explained by their different physicochemical parameters. Indeed, the measurement of zeta-potential of nanoparticles resuspended in water and nanoparticles incubated in rat plasma demonstrated that while unloaded nanoparticles were negatively charged (- 14 mV), the charge switched to positive after doxorubicin - binding. After the incubation in serum, the charge of DOX loaded NP became again negative indicating a strong interaction with serum components. Similar observations were made by Brigger et al. (2004). Thus, the surface charge present on the nanoparticles plays an important role in proteins interaction, which, in turn, influences the body distribution (Borchard and Kreuter 1993). The similarity of body distribution of the [^{14}C]-nanoparticles in this study performed in tumour-bearing rats and healthy rats suggests that the pathology associated with the brain tumour does not influence the physiology of the whole body, possibly due to the limited mass of

the rat brain (1 % of body weight).

Noteworthy is the accumulation of nanoparticles in RES organs and, in particular, of DOX-loaded NP in lungs 24 h after injection. This phenomenon is explicable considering the particle redistribution over a period of time.

Figure 4.15 shows the concentration of nanoparticles in the contralatereal hemisphere and glioblastoma in tumour-bearing rats 10 days post tumour implantation. These concentrations were significantly higher in comparison with both, NP brain concentration in healthy rats (Fig 4.6) and with NP brain concentration in 5 and 8 days tumour-bearing rats (Figs 4.9, 4.11, 4.13). In the presence of glioblastoma, the transport of NP into the brain is the consequence of several factors. In addition to the ability of PS 80 nanoparticles to cross the BBB which is still intact at an early stage of tumour development, these carriers can extravasate across the leaky endothelium to the tumour due to the EPR effect (Maeda et al. 1989, Maeda 2001).
Indeed, as shown by extravasation after intravenous injection of Evans Blue, the permeability of the BBB at the tumour site on days 5 and 8 was significantly increased (Fig. 4.16), which provides a basis for the EPR-mediated drug delivery.

These observations are important since microvascular permeability in gliomas is heterogeneous (Neuwelt 2004) and whereas in some parts of the tumour, capillaries are hyper-permeable, in other parts the barrier function may be retained. Thus, in the case of brain tumours, the ability of PS 80-coated nanoparticles to deliver drugs across the intact BBB due to receptor-mediated transcytotic mechanisms is also augmented by their enhanced ability to accumulate in tumours due to the EPR effect.

Interestingly, the concentration of PS 80 [^{14}C]-PBCA NP in glioblastoma was found to be significantly higher in comparison to DOX [^{14}C]-PBCA NP concentration. Brigger et al. (2004) observed a similar effect for DOX PEG–coated poly(hexaldecyl cyanoacrylate) nanospheres. In their study of the body distribution in 9L gliosarcoma-bearing rats, DOX-loaded nanospheres accumulated to a 2.5 fold lesser extent in the tumour as compared to the unloaded nanospheres.
This phenomenon can be explained considering the microenvironment of cerebral intra-

tumoural tissue which is different from that in normal brain tissue (Shaller 2004). Regions within brain tumour are transiently or chronically hypoxic (Zagzag et al. 2003). Consequently, the glycolytic metabolism of glucose in hypoxic conditions generates lactate. Because of the accumulation of lactic acid, a physiological hallmark of hypoxia in tumour is an increased acidosis. The intra-tumoural acidity that may extend to the peri-tumoural tissue may have a consequence for the delivery of the charged nanoparticles into the brain. In particular, the positive charge of the tumour area due to the excess of H^+ may interfere with the penetration of the positive charged DOX ^{14}C-PBCA NP.

Nevertheless, the theoretical amount of doxorubicin bound to nanoparticles and delivered into the brain is significant higher in the glioblastoma than in the contralateral hemisphere of tumour-bearing rats and in the brain of healthy rats (Table 5.1).

	Healthy rats	Tumour-bearing rats	
	Brain	Controlateral hemisphere	Glioblastoma
[DOX]	0.50 µg	1.06 µg	1.14 µg

Table 5.I. Brain concentration of doxorubicin (µg/g tissue) at 1 h after intravenous injection into rats of 20 mg/kg of DOX ^{14}C-PBCA nanoparticles.

The concentration achieved appears to be adequate to obtain a therapeutic effect in the treatment of glioblastomas (Steiniger et al. 2004).

5.6 Radioluminography studies

The results of the radioluminography studies demonstrated (paragraph 4.5) the variation of the pattern of body distribution in rats after i.v. administration of polysorbate 80-coated ^{14}C-DOX NP in accordance with the study of the body distribution using liquid scintillation. Indeed, polysorbate 80 conferred to the particle surface hydrophilic properties which permitted a relative avoidance of the RES uptake.

Regarding the brain distribution, the results showed a significant accumulation of the particles in the liquor and in the pineal body, whereas no detectable activity in the brain was observed. These results are surprising and, moreover, are not in accordance with the studies of body distribution using liquid scintillation in which a significant transport of the labelled particle into the brain was shown. It may be argued that the high drug concentrations in the brain homogenisate observed with the nanoparticles were due to the particles remaining in the brain blood vessel lumen or the surrounding endothelial cells.

Already Gulayev et al. (1999) explained the inconsistence of this argument considering the capillary blood volume which represents only 1 % of the total brain volume, and the endothelial cell volume which is 0.1 %. He found the concentration of 6 µg/g of doxorubicin in brain homogenisate. If the particles containing drug had remained in the blood capillaries, the concentration would have been extremely high (6000 µg/g) considering the exclusive uptake by endothelial cells without release into the residual brain. These concentration are unreasonably high and would have led to immediate severe local toxicity which was not observed. Moreover, these concentrations would have shown up in the autoradiographies. For this reason the total brain concentration of about 1 % of the dose in the homogenates has to be attributed to the high liquor and pineal body concentrations.

6 Conclusions

Chemotherapeutical studies performed on glioblastoma–bearing rats provide another evidence of the considerable anti-tumour effect of doxorubicin loaded in polysorbate 80-coated PBCA NP in brain tumours.

Additionally, the results obtained in this study suggest that the mechanism of drug delivery to the brain tumour depends on the surfactant used for nanoparticle modification. Therefore, both the long-circulation characteristics and the cell/particle interactions must be considered in the design of an adequate carrier capable of delivering a drug across the BBB.

Altogether, these results suggest that the surface-modified poly(butyl cyanoacrylate) nanoparticles offer new opportunities for non-invasive chemotherapy of brain tumours.

The studies of body distribution performed in healthy rats and glioblastoma - bearing rats demonstrated that overcoating of poly(butyl-2-cyano[3-^{14}C]acrylate) nanoparticles with polysorbate 80 decreased their concentration in the organs of the reticuloendothelial system, i.e. liver, spleen, and lungs. The loading with doxorubicin counteracts the effects of polysorbate 80-coating. This counteraction by doxorubicin appears to be caused by its positive charge, which alters the interaction with the plasma components and with other cells in the body.

The similarity of the results for tumour-bearing rats and healthy rats suggests that the pathology associated with the brain tumour does not influence the physiology of the whole body.

The accumulation of poly(butyl-2-cyano[3-^{14}C]acrylate) nanoparticles in the tumour site and in the contralateral hemisphere in glioblastoma beating-rats demonstrates the efficacy of the EPR effect on the nanoparticles delivery into the brain. Although the adsorption of doxorubicin on nanoparticles surface counteracts the ability of polysorbate 80 to enhance the transport of nanoparticles into the brain, the actual concentration of doxorubicin delivered to the tumour site is higher than in the contralateral hemisphere of tumour-bearing rats and than in the brain of healthy rats. Hence, doxorubicin loaded poly(butyl-2-cyano[3-^{14}C]acrylate) nanoparticles have a high potential for the treatment of glioblastoma.

7 Summary

Introduction

Systemically administered chemotherapy is often ineffective in the treatment of CNS diseases. One reason for this low efficacy is insufficient drug delivery to the brain due to the presence of the blood-brain barrier (BBB), which restricts exchange of solutes between the blood and brain extracellular fluid. The BBB is formed by the endothelial cells of brain vessels, which, in contrast to peripheral endothelia, are joined by tight junctions. While this structural barrier hampers penetration of hydrophilic substances into the brain by aqueous paracellular diffusional pathways, accumulation of lipophilic molecules in the brain is often restricted due to the very efficient ABC efflux transporters, such as P-gp or multidrug resistance proteins (MRP).

One of the evolving strategies for non-invasive drug delivery to the brain is the employment of nanoparticle technology. Indeed, as shown by the extensive pharmacological studies, poly(butyl cyanoacrylate) nanoparticles coated with polysorbate 80 (Tween® 80) enabled the brain delivery of a number of drugs that are normally unable to cross the BBB. It was also demonstrated that the effect of the polysorbate-coating was unique and other surfactants including poloxamers 188, 338, and 407, and poloxamine 908 could not enable drug delivery into the brain of healthy animals using poly(butyl cyanoacrylate) nanoparticles. This phenomenon was explained by the selective adsorption of certain plasma proteins (in particular, apolipoproteins E and B) on the surface of nanoparticles coated with polysorbate 80. In this way, the coated polymeric particles mimicked the lipoprotein particles and were transported across the BBB by receptor-mediated endocytosis.

However, in the case of brain tumours, when the BBB may be partially disrupted and its permeability at the tumour site is increased, the nanoparticles might additionally target the tumour by the enhance permeability and retention (EPR) effect. It is known that the EPR effect is especially pronounced for the long-circulating nanoparticles that avoid rapid clearance from the circulation and uptake by the mononuclear phagocyte system (MPS), which enhances their extravasation in non-MPS tissues.

In the first part of the present study, nanoparticle loading was optimized by altering

formulation parameters with the objective to develop a formulation with higher efficacy for the therapy of glioblastoma-bearing rats. Moreover, the potential of doxorubicin bound to poly(butyl cyanoacrylate) nanoparticles (DOX – PBCA NP) coated with stealth agents for the chemotherapy of brain tumours was investigated.

In the second part of this study the brain distribution and the body distribution in healthy rats and in glioblastoma 101/8-bearing rats after i.v. administration of poly(butyl-2-cyano [3-^{14}C]acrylate) nanoparticles coated with polysorbate 80 and loaded with doxorubicin (DOX - ^{14}C PBCA + PS 80) was investigated.

Antitumour effect of doxorubicin loaded in poly(butyl cyanoacrylate) nanoparticles in rat glioma model: influence of formulation parameters

The standard formulation of DOX – PBCA NP used in this study was prepared by anionic polymerization of butyl cyanoacrylate (BCA) in presence of DOX. The measurement of the drug loading was performed by HPLC and by spectrophotometer. The drug loading of the standard formulation measured by HPLC was 71 %. Different formulation of DOX-PBCA NP were made by changing the parameters of the normal procedure. Changed parameters were: pH, concentration and type of monomer, concentration and type of steric stabilizator, polymerization time and addition of the drug at beginning of polymerization process. The employment of iso-BCA instead of n-BCA allowed the attainment of nanoparticles with improved loading (73 % of drug loading by HPLC) compared to the standard formulation. A new formulation with improved loading also was obtained by reduction of n-BCA concentration (0.75 % w/v), combined with an increase of dextran concentration (2 % w/v), prolongation of polymerization time to 4 h, and addition of doxorubicin before the start of the polymerization (76 % of drug loading by HPLC).

The therapeutic potential for the treatment of glioblastoma of the following formulations was tested: 1) doxorubicin in saline (DOX); 2) standard formulation coated with polysorbate 80; 3) standard formulation coated with poloxamine 908; 4) standard formulation coated with poloxamer 188; 5) new formulation coated with polysorbate 80; 6) iso-PBCA nanoparticles coated with polysorbate 80. Untreated animals were used as a control. These preparations were injected i.v. into the tail vein using the dose regimen of 3

x 1.5 mg/kg on days 2, 5, and 8 post tumor implantation. The concentration of doxorubicin in the injection solution was 0.25 %.

The results of the present study showed that the standard formulation coated with polysorbate 80 (PS 80) was the most effective: 35 % of the animals treated with this formulation survived for 180 days after tumour implantation. In the group treated with PS 80-coated iso-PBCA nanoparticles the percentage of long-term survivors was 15 % (3/20) whereas the percentage of survivers in the group treated with the new formulation coated with PS 80 was 10 % (2/20). The percentage of long-term survivors treated with DOX-PBCA NP coated with poloxamer 188 or poloxamine 908 was 20 % (4/20). Free DOX in solution was less effective: 10 % animals (2/20) survived for 65 days. All control animals died between day 18 and day 24.

The higher efficacy of DOX-PBCA NP coated with PS 80 may be explained by the ability of these carriers to deliver the drug across the intact BBB at an early stage of tumour development due to the receptor-mediated mechanism activated by the PS 80-coating of the NP. In this way, doxorubicin also may reach those parts of the brain, which though affected by the tumour, are still protected by an intact BBB.

Our results demonstrate also that poloxamer 188 and poloxamine 908 considerably increased the anti - tumour effect of DOX-PBCA NP although earlier studies showed that the coating with these surfactants failed to deliver drugs to the healthy brain. The anti - tumoural effect of the surfactant-coated formulations possibly is attributable to the EPR effect. It is well known that tumour uptake due to the EPR effect is more pronounced for long-circulating carriers. The common approach to increase blood half-life of the particles is shielding of their surface and, consequently, a reduction of opsonization that can be achieved by coating the nanoparticles with surfactants, such as poloxamers or poloxamines. Although poloxamer 188 and poloxamine 908 were unlikely to provide transport of the drug-loaded nanoparticles across the BBB they could still facilitate their extravasation across the BBB at the tumour site.

The percentage of surviving animals after the treatment with the new formulation with increased loading in the present study was not satisfactory. A possible explanation for the

modest efficacy of this preparation may be the increased content in dextran (2 % w/v). The molecules of dextran protrude from the surface of nanoparticles as loops or chains conferring to the particles surface hydrophilic properties which could interfere with the effective coating by polysorbate 80. Consequently, the process of endocytosis by the endothelial cells of BBB may be diminished as well as the transport of doxorubicin into the brain. Regarding the iso-PBCA NP, it may be possible that the two polymers behave differently *in vivo* which requires further investigations.

Body distribution in healthy rats and in glioblastoma 101/8-bearing rats of DOX - ¹⁴C PBCA nanoparticles

Uncoated nanoparticles, polysorbate 80-coated nanoparticles, or doxorubicin loaded nanoparticles were injected into the tail veins of healthy rats. After different time points (10 min, 1 h, 6 h, 24 h, 1 week, 4 weeks), the animals were sacrificed by placing in carbon dioxide and subsequent decapitation. Blood was collected and liver, spleen, lungs, kidneys, gonads, and the brain were removed. Aliquots of organs were digested in tissue solubilizer and the radioactivity was measured by scintillation counting. The same procedure was employed for tumour-bearing rats. Nanoparticle administration was performed on days 5, 8 and 10 after tumour inoculation, and rats were sacrificed at the following time points: 10 min, 1 h, 6 h, and 24 h. Blood and organs were collected and the radioactivity was determined. The pattern of body distribution of the [¹⁴C]-nanoparticles was similar in both tumour-bearing rats and healthy rats. This result suggests that the pathology associated with the brain tumour does not influence the physiology of the whole body. The three formulation investigated, [¹⁴C]-PBCA NP, [¹⁴C]-PBCA NP coated with PS 80 , and DOX-loaded [¹⁴C]-PBCA NP coated with PS 80 showed different patterns of biodistribution. As expected, uncoated nanoparticles accumulated in RES organs, such as lungs, liver, and spleen. Coating of nanoparticles with PS 80 moderately reduced their uptake in liver and spleen, whereas lung uptake was increased. These observations demonstrate that the alteration of the nanoparticle surface properties due to the surfactant led to an interaction with different opsonins, which in turn facilitated the uptake of the particles by different phagocytosing cells. In contrast, the uptake of PS 80-coated nanoparticles loaded with DOX was similar to that of uncoated particles. In fact, the presence of doxorubicin even led to a slight increase of RES uptake, thus counteracting the polysorbate coating. The

different patterns of nanoparticles distribution may be explained by their different physicochemical parameters. Indeed, the measurement of the zeta-potential of nanoparticles resuspended in water and of nanoparticles incubated in rat plasma showed that unloaded nanoparticles were negatively charged, whereas the charge switched to positive after doxorubicin binding. After the incubation in serum, the charge of DOX-loaded NP became again negative indicating a strong interaction with serum components. Thus, the surface charge present on the nanoparticles plays an important role in protein interaction, which, in turn, influences the body distribution.

Regarding the brain distribution, the concentration of nanoparticles in tumour-bearing rats 10 days post tumour implantation was significantly higher in comparison with NP concentrations in healthy rats and NP concentration in 5 and 8 days tumour-bearing rats. In the presence of glioblastomas, the transport of NP into the brain is a consequence of several factors: in addition to the ability of PS 80 nanoparticles to cross the BBB which is still intact at an early stage of tumour development, these carriers can extravasate across the leaky endothelium to the tumour due to the EPR effect. These observations are important since microvascular permeability in gliomas is heterogeneous, and whereas in some parts of the tumour the capillaries are hyper-permeable, in other parts the barrier function may be retained. Thus, in the case of brain tumours, the ability of PS 80-coated nanoparticles to deliver drugs across the intact BBB due to receptor-mediated transcytotic mechanisms also is augmented by their enhanced ability to accumulate in tumours due to the EPR effect.

Interestingly, the concentration of PS 80 [^{14}C]-PBCA NP in glioblastoma was found to be significantly higher in comparison to DOX [^{14}C]-PBCA NP concentration. This phenomenon can be explained considering the microenvironment of cerebral intra-tumoural tissue which is different from that in normal brain tissue. Regions within brain tumours are transiently or chronically hypoxic. A physiological hallmark of hypoxia in tumours is an increased acidosis. The intra-tumoural acidity that may extend to the peri-tumoural tissue may have consequences for the delivery of the charged nanoparticles into the brain. In particular, the positive charge of the tumour area due to the excess of H^+ may interfere with the penetration of the positive charged DOX ^{14}C-PBCA NP. Nevertheless, the doxorubicin concentrations achieved in the glioblastomas appear to be adequate to

obtain a therapeutic effect in the treatment of glioblastomas.

8 References

Allemann E, Leroux JC, Gurny R, Doelker E. 1993. In vitro extended-release properties of drug-loaded poly(DL-lactic acid) nanoparticles produced by a salting-out procedure. Pharm Res 10: 1732–1737.

Alonso MJ, Sanchez A, Torres D, Seijo B, Vila-Jato JL. 1990. Joint effects of monomer and stabilizer concentrations on physico-chemical characteristics of poly(butyl 2-cyanoacrylate) nanoparticles. J Microencapsul 7:517-26.

Alyautdin RN, Gothier D, Petrov V, Kharkevich D, Kreuter J. 1995. Analgesic activity of the hexapeptide dalargin absorbed on the surface of polysorbate 80-coated poly (butylcyanoacrylate) nanoparticles. Eur J Pharm Biopharm 41:44-48.

Alyautdin RN, Petrov VE, Langer K, Berthold A, Kharkevich DA, Kreuter J. 1997. Delivery of loperamide across the blood-brain barrier with polysorbate 80-coated polybutylcyanoacrylate nanoparticles. Pharm Res 14:325-8.

Alyautdin RN, Tezikov EB, Ramge P, Kharkevich DA, Begley DJ, Kreuter J. 1998. Significant entry of tubocurarine into the brain of rats by adsorption to polysorbate 80-coated polybutylcyanoacrylate nanoparticles: an in situ brain perfusion study. J Microencapsul 15:67-74.

Alyautdin RN, Reichel A, Löbenberg R, Ramge P, Kreuter J, Begley DJ. 2001. Interaction of poly-(butylcyanoacrylate) nanoparticles with the blood-brain barrier in vivo and in vitro. J Drug Target 9:209 – 221.

Alberts B, Johnson A, Lewis J, Raff M, Roberts K, Walter P. 2002. Molecular Biology of the Cell, 4th ed, Taylor & Francis Group, London.

Araujo L, Lobenberg R, Kreuter J. 1999. Influence of the surfactant concentration on the body distribution of nanoparticles. J Drug Target 6:373-85.

Banks WA, Kastin AJ, Huang W, Jaspan JB, Maness LM. 1996. Leptin enters the brain by a saturable system independent of insulin. Peptides 17:305-11.

Barret KEJ, Thomas HR. 1975. Dispersion Polymerization on Organic Media. Barret KEJ, Ed. Wiley, London, p. 115.

Beauchesne P. 2002. Promising survival and concomitant radiation plus temozolomide followed by adjuvant temozolomide. J Clin Oncol 20: 3180– 3181.

Beck P, Kreuter J, Reszka R, Fichtner I. 1993. Influence of polybutylcyanoacrylate nanoparticles and liposomes on the efficacy and toxicity of the anticancer drug mitoxantrone in murine tumour models. J Microencapsul 10:101-14.

Begley D, Brightman MW. 2003. Structural and functional aspects of the blood-brain barrier. In L. Prokai, & K. Prokai-Tatrai Eds, Peptide Transport and Delivery into the Central Nervous System. Progress in Drug Research. vol. 61: pp. 3978.

Beijnen JH, Wiese G, Underberg WJ. 1985. Aspects of the chemical stability of doxorubicin and seven other anthracyclines in acidic solution. Pharm Weekbl Sci 7:109-16.

Betz AL, Goldstein GW. 1978. Polarity of the blood-brain barrier: neutral amino acid transport into isolated brain capillaries. Science 202:225-7.

Betz AL, Goldstein GW. 1980. Transport of hexoses, potassium and neutral amino acids into capillaries isolated from bovine retina. Exp Eye Res 30:593-605.

Birrenbach G, And Speiser PP. 1976. Polymerized micelles and their use as adjuvants in immunology. J Pharm Sci. 65: 1763.

Blunk T, Hochstrasse DF, Rudt S, Müller RH. 1991. Two-dimensional electrophoresis in the concept of differential opsonication-An approach to drug targeting. Arch Pharm 324:706.

Borchard G, Kreuter J. 1993. Interaction of serum components with poly (methyl methacrylate) nanoparticles and the resulting body distribution after intravenous injection in rats. J Drug Target 1:15-9.

Bonstelle CT, Kori SH, Rekate H. 1983. Intracarotid chemotherapy of glioblastoma after induced blood-brain barrier disruption. AJNR Am J Neuroradiol 4:810-2.

Brasseur F, Couvreur P, Kante B, Deckers-Passau L, Roland M, Deckers C, Speiser P. 1980. Actinomycin D absorbed on polymethylcyanoacrylate nanoparticles: increased efficiency against an experimental tumor. Eur J Cancer 16:1441-5.

Brasseur N, Brault D, Couvreur P. 1991. Adsorption of hematoporphyrin onto polyalkylcyanoacrylate nanoparticles: carrier capacity and drug release. Int J Pharm 70 :129-135.

Brigger I, Morizet J, Couvreur P. 2004. Negative preclinical results with stealth nanospheres-encapsulated Doxorubicin in an orthotopic murine brain tumor model. J Control Release 100:29-40.

Brightman MW, Reese TS. 1969. Junctions between intimately apposed cell membranes in

the vertebrate brain. J Cell Biol 40:648-77.

Brownlees J, Williams CH. 1993. Peptidases, peptides, and the mammalian blood-brain barrier. J Neurochem 60:793-803.

Brownson EA, Abbruscato TJ, Gillespie TJ, Hruby VJ, Davis TP. 1994. Effect of peptidases at the blood brain barrier on the permeability of enkephalin. J Pharmacol Exp Ther 270:675-80.

Burton E C,and Prados M D. 2000. Malignant gliomas. Curr Treat Options Oncol 1, 459–468.

Butt AM, Jones HC, Abbott NJ. 1990. Electrical resistance across the blood-brain barrier in anaesthetized rats: a developmental study. J Physiol 429:47-62.

Calvo P, Gouritin B, Chacun H, Desmaele D, D'Angelo J, Noel JP, Georgin D, Fattal E, Andreux JP, Couvreur P. 2001. Long-circulating PEGylated polycyanoacrylate nanoparticles as new drug carrier for brain delivery. Pharm Res 18:1157-66.

Cappel MJ, Kreuter J. 1991. Effect of nanoparticles on transdermal drug delivery. J Microencapsul 8:369-74.

Carstensen H, Müller BW, Müller RH. 1991. Adsorption of ethoxylated surfactants on nanoparticles. I. Characterization by hydrophobic interaction chromatograpy. Int J Pharm 67:29.

Cecchelli R, Fenart L, Descamps L, Torpier G, Dehouck MP. 1997. Receptor-mediated transcytosis of blood-borne molecules through blood–brain barrier endothelial cells: Drug targeting by endogenous transport routes. Proc Intl Symp Control Rel Bioact Mater 24: 221-222.

Chen DB, Yang TZ, Lu WL, Zhang Q. 2001. In vitro and in vivo study of two types of long-circulating solid lipid nanoparticles containing paclitaxel. Chem Pharm Bull, Tokyo, 49:1444-7.

Christie RJ, and Grainger DW. 2003. Design strategies to improve soluble macromolecular delivery constructs. Adv Drug Deliv Rev 55: 421– 437.

Cordon-Cardo C, O'Brien JP, Casals D, Rittman-Grauer L, Biedler JL, Melamed MR, Bertino JR. 1989. Multidrug-resistance gene (P-glycoprotein) is expressed by endothelial cells at blood-brain barrier sites. Proc Natl Acad Sci U S A 86:695-8.

Cordonensi M, D'Atri F, Hammar E, Parry DAD, Kendrick-Jones J, Shore D, Citi S. 1999. Cingulin contains lobular and coiled-coil domains and interacts with ZO-1, ZO-2, ZO-3 and myosin. J Cell Biol 147: 1569–1581.

Couvreur P, Grislain L et al. 1986. Biodegradable polymeric nanoparticles as drug carrier for antitumor agents. Polymeric nanoparticles and microspheres. P. Guiot and P. Couvreur. Boca Rton, FL,CRC, Press.

Couvreur P, Tulkens P, Roland M, Trouet A, Speiser P. 1977. Nanocapsules: a new type of lysosomotropic carrier. FEBS Lett 84:323–326.

Crone C, Christensen O. 1981. Electrical resistance of a capillary endothelium. J Gen Physiol 77:349-71.

Davis SS, Illum L. 1986. Colloidal delivery systems. Opportunities and challenges. In Tomlinson, E and Davis S S Eds. Site –Specific Drug delivery, Wiley, pp 93-110

De Vries HE, Kuiper J, de Boer AG, van Berkel TJ, Breimer DD. 1993. Characterization of the scavenger receptor on bovine cerebral endothelial cells in vitro. J Neurochem 61: 1813-1821.

Dehouck B, Fenart L, Dehouck M-P, Pierce A, Torpier G, Cecchelli R.1997. A new function for the LDL receptor: Transcytosis of LDL across the blood–brain barrier. J Cell Biol. 138: 877-889.

Dehouck B, Dehouck MP, Fruchart JC, Cecchelli R. 1994. Upregulation of the low density lipoprotein receptor at the blood–brain barrier: intercommunications between brain capillary endothelial cells and astrocytes. J Cell Bio 126: 465-473.

Diepold R, Kreuter J, Himber J, Gurny R, Lee VH, Robinson JR, Saettone MF, Schnaudigel OE. 1989. Comparison of different models for the testing of pilocarpine eyedrops using conventional eyedrops and a novel depot formulation (nanoparticles). Graefes Arch Clin Exp Ophthalmol 227:188-93.

Dong Y, Feng SS. 2004. Methoxy poly(ethylene glycol)-poly(lactide) (MPEG-PLA) nanoparticles for controlled delivery of anticancer drugs. Biomaterials 25: 2843–2849.

Douglas SJ, Davis SS, Illum L. 1986. Biodistribution of poly(butyl 2-cyanoacrylate) nanoparticles in rabbit. Int J Phatm. 34:145-152.

Douglas S, Illum L, Davis SS, Kreuter J. 1984. Particle Size and Size Distribution of Poly (butyl 2-cyano acrylate) Nanoparticles. I: influence of physicochemical factors. J of Colloid and Interface Science. 101:149-158.

Douglas S, Illum L, Davis SS. 1985. Particle Size and Size Distribution of Poly(butyl 2-cyano acrylate) Nanoparticles. II: influence of the stabilizer. J of Colloid and Interface Science, 103:154-163.

Duffy KR, Pardridge WM, Rosenfeld RG. 1988. Human blood-brain barrier insulin-like

growth factor receptor. Metabolism 37:136-40.

Duvernoy H, Delon S, Vannson JL. 1983. The vascularization of the human cerebellar cortex. Brain Res Bull 11:419-80.

Edman P, Ekman B, Sjoholm I. 1980. Immobilization of proteins in microspheres of biodegradable polyacryl dextran. J. Pharm. Sci. 69:838–842.

El-Samaligy MS, Rohdewald P, Mahmoud HA. 1986. Polyalkyl cyanoacrylate nanocapsules. J Pharm Pharmacol 38:216-8.

Feng SS, Mu L, Win KY, Huang G. 2004. Nanoparticles of biodegradable polymers for clinical administration of paclitaxel. Curr Med Chem 11: 413–424.

Fishbein I, Chorny M, Rabinovich L, Banai S, Gati I, Golomb G. 2000. Nanoparticulate delivery system of a tyrphostin for the treatment of restenosis. J Control Release 65: 221–229.

Fresta M, Cavallaro G, Giammona G, Wehrli E, Puglisi G. 1996. Preparation and characterization of polyethyl-2-cyanoacrylate nanocapsules containing antiepileptic drugs. Biomaterials 17:751-8.

Gallo JM, Hung CT, Terrier DG. 1984. Analysis of albumin microsphere preparation. Int J Pharm 22: 63.

Giometto B, Bozza F, Faresin F, Alessio L, Mingrino S, Tavolato B. 1996. Immune infiltrates and cytokines in gliomas. Acta Neurochir (Wien) 138:50-6.

Gipps EM, Arshady R, Kreuter J, Groscurth P, Speiser PP. 1986. Distribution of polyhexyl cyanoacrylate nanoparticles in nude mice bearing human osteosarcoma. J Pharm Sci 75:256-8.

Gipps EM, Groscurth P, Kreuter J, Speiser PP. 1988. Distribution of polyhexylcyanoacrylate nanoparticles in nude mice over extended times and after repeated injection. J Pharm Sci 77:208-9.

Goldmann EE. 1913. Vitalfärbung am Zentralnervensystem. Berlin.

Gonatas NK, Stieber A, Hickey WF, Herbert SH, Gonatas JO. 1984. Endosomes and Golgi vesicles in adsorptive and fluid phase endocytosis. J Cell Biol 99:1379-90.

Goodman H, Banker GS. 1970. Molecular-scale drug entrapment as a precise method of controlled drug release. I. Entrapment of cationic drugs by polymeric flocculation. J Pharm Sci 59:1131-7.

Gregoriadis G. 1977. Targeting of drugs. Nature. 265:407-11.

Gulyaev AE, Gelperina SE, Skidan IN, Antropov AS, Kivman GY, Kreuter J. 1999.

Significant transport of doxorubicin into the brain with polysorbate 80-coated nanoparticles. Pharm Res 16:1564-9.

Gupta PK, Hung CT, Perrier DG. 1986. Albumin microspheres. I. Release characteristic of adriamycin. Int J. Pharm. 33:137-146.

Harmia T, Kreuter J, Speiser P, Boye T, Gurny R, Kubi A. 1986. Enhancement of the myotic response of rabbits with pilocarpine-loaded polybutylcyanoacrylate nanoparticles. Int J Pharm 33:187.

Hanahan D, and Folkman J. 1996. Patterns and emerging mechanisms of the angiogenic switch during tumorigenesis, Cell 86. 353–364.

Hawley AE, Illum L, Davis SS. 1997. Lymph node localization of biodegradable nanospheres surface modified with poloxamer and poloxamine block co-polymers, FEBS Lett. 400:319–323.

von Heijne G, Gavel Y. 1988. Topogenic signals in integral membrane proteins. Eur J Biochem 174:671-8.

von Heijne G. 1992. Membrane protein structure prediction. Hydrophobicity anlysis and the positive-inside rule. J Mol Biol 225:487-94.

Hickey W. 1999. Leukocyte traffic in the central nervous system: the participants and their roles. Semin Immunol 11: 125–137.

Hofer S, and Merlo A. 2002. Therapeutische Optionen für maligne Gliome WHO-Grad III und IV. Schweiz Med Forum. 32/33: 748-755.

Horisawa E, Hirota T, Kawazoe S, Yamada J, Yamamoto H, Takeuchi H, Kawashima Y. 2002. Prolonged anti-inflammatory action of DL-lactide/glycolide copolymer nanospheres containing betamethasone sodium phosphate for an intra-articular delivery system in antigen-induced arthritic rabbit. Pharm Res 19: 403–410.

Illum L, Davis SS, Wilson CG, Thomas NW, Frier M, Hardy J G. 1982. Blood clearance and organ deposition of intravenously administered colloidal particles. Effect of particle size, nature and shape. Int J Pharm. 12:135-146.

Illum SL, Davis SS. 1983. Effect of the nonionic surfactant poloxamer 338 on the fate and deposition of polystyrene microspheres following intravenous administration. J Pharm Sci 72:1086-9.

Illum L, Davis SS. 1984. The organ uptake of intravenously administered colloidal particles can be altered using a non-ionic surfactant (Poloxamer 338). FEBS Lett 167:79-82.

Illum L, Hunneyball I H, Davis S S. 1986a. The effect of hydrophilic coating on the uptake of colloidal particles by the liver and peritoneal macrophages. Int J Pharm 53: 65.

Illum L, Khan MA, Mak E, S. S. Davis. 1986b. Evaluation of carrier capacity and release characteristics for poly(butyl 2-cyanoacrylate) nanoparticles. Int J Pharm 30:17.

Illum L, Davis S S, Muller R H, Mak E, West P. 1987a. The organ distribution and circulation time of intravenously injected colloidal carriers sterically stabilized with a block copolymer--poloxamine 908. Life Sci. 40:367-74.

Illum L, Davis SS. 1987b. Targeting of colloidal particles to the bone marrow. Life Sci 40:1553-60.

Ji Y, Powers SK, Brown JT, Miner R. 1996. Characterization of the tumour invasion area in the rat intracerebral glioma. J Neuro-Oncol 30: 189-197.

Kabanov AV, Chekhonin VP, Alakhov V, Batrakova EV, Lebedev AS, Melik-Nubarov NS, Arzhakov SA, Levashov AV, Morozov GV, Severin ES, et al. 1989. The neuroleptic activity of haloperidol increases after its solubilization in surfactant micelles. Micelles as microcontainers for drug targeting. FEBS Lett 258:343-5.

Kalenikova EI, Dmitrieva OF, Korobov NV, Zhukovskii SV, Tishchenko VA. 1988. Pharmacokinetics of dalargin. Vopr Med Khim 34:75-83.

Kamen, Martin D. 1985. Radiant Science, Dark Politics: A Memoir of the Nuclear Age, Forward by Edwin M. McMillan, Berkeley: University of California Press.

Kante B, Couvreur P, Dubois-Krack G, De Meester C, Guiot P, Roland M, Mercier M, Speiser P. 1982. Toxicity of polyalkylcyanoacrylate nanoparticles I: Free nanoparticles. J Pharm Sci 71: 786-90.

Kattan J, Droz JP, Couvreur P, Marino JP, Boutan-Laroze A, Rougier P, Brault P, Vranckx H, Grognet JM, Morge X, et al. 1992. Phase I clinical trial and pharmacokinetic evaluation of doxorubicin carried by polyisohexylcyanoacrylate nanoparticles. Invest New Drugs 10:191-9.

Kaufmann U, Franke F, Lampert F. 1979. Adherence of polymethyl-methacrylate particles for characterization of B-Lymphocytes. Eur J Pediatr 130: 238.

Kim SW, Lee RG, Oster H, Coleman D, Andrade JD, Lentz DJ, Olsen D. 1974. Platelet adhesion to polymer surfaces. Trans Am Soc Artif Intern Organs 20 B:449-55.

Krause H-J, Schwarz A, Rohdewald P. 1986. Interfacial polymerization, a useful method for the preparation of polymethyl-methacrylate nanoparticles. Drug Devel Ind Pharm 12:527.

Kreuter J, Hartmann HR. 1983. Comparative study on the cytostatic effects and the tissue distribution of 5-fluorouracil in a free form and bound to polybutylcyanoacrylate nanoparticles in sarcoma 180-bearing mice. Oncology 40:363-6.

Kreuter J. 1983a. Evaluation of nanoparticles as drug-delivery system I: Preparation methods. Pharm Acta Helv 58:196-209.

Kreuter J. 1983b. Evaluation of nanoparticles as drug-delivery systems II: Comparison of the body distribution of nanoparticles with the body distribution of microspheres (diameter greater than 1 micron), liposomes, and emulsions. Pharm Acta Helv 58:217-26.

Kreuter J. 1983c. Evaluation of nanoparticles as drug-delivery systems. III: materials, stability, toxicity, possibilities of targeting, and use. Pharm Acta Helv 58:242-50.

Kreuter J. 1983d. Physicochemical characterization of polyacrylic nanoparticles. Int J Pharm 14:43-58.

Kreuter J, Mills SN, Davis SS, Wilson CG. 1983d. Polybutylcyanoacrylate nanoparticles for the delivery of (75Se) norcholestenol. Int J Pharm 16:105.

Kreuter J. 1985. Factors influencing the body distribution of polyacrylic nanoparticles. Drug Targ. P. Buri and A . Gumma. Amsterdam, Elvier Science Publishers BV.

Kreuter J. 1992. Nanoparticles-preparation and applications. Microcapsules and Nanoparticles in Medicine and Pharmacy. M. Donbrow, ed. Boca Raton, Fla. CRC Press, p 125.

Kreuter J, Alyautdin RN, Kharkevich DA, Ivanov AA. 1995. Passage of peptides through the blood-brain barrier with colloidal polymer particles (nanoparticles). Brain Res 674:171-4.

Kreuter J, Petrov VE, Kharkevich DA, Alyautdin RN. 1997. Influence of the type of surfactant on the analgesic effects induced by the peptide dalargin after its delivery across the blood–brain barrier using surfactant-coated nanoparticles. J Controlled Rel 49:81-87.

Kreuter J. Transport of Drugs Across the Blood-Brain Barrier by Nanoparticles. 2002. Curr Med Chem - Central Nervous System Agents. 2:241-249.

Kreuter J, Ramge P, Petrov V, Hamm S, Gelperina SE, Engelhardt B, Alyautdin R, von Briesen H, Begley DJ. 2003. Direct evidence that polysorbate-80-coated poly (butylcyanoacrylate) nanoparticles deliver drugs to the CNS via specific mechanisms requiring prior binding of drug to the nanoparticles. Pharm Res 20:409-16.

Kante B, Couvreur P, Dubois-Krack G, De Meester C, Guiot P, Roland M, et al. 1982. Toxicity of polyalkylcyanoacrylate nanoparticles I: free nanoparticles. J Pharm Sci 71:786–790.

Kleinberg L, Grossman SA, Carson K, Lesser G, O'Neill A, Pearlman J, Phillips P, Herman T, and Gerber M. 2002. Survival of patients with newly diagnosed glioblastoma multiforme treated with RSR13 and radiotherapy: results of a phase II new approaches to brain tumor therapy CNS consortium safety and efficacy study. J Clin Oncol 20, 3149– 3155.

Kramer PA. 1974. Letter: Albumin microspheres as vehicles for achieving specificity in drug delivery. J Pharm Sci 63:1646-7.

Kusuhara H, Suzuki H, Sugiyama Y. 1998. The role of P-glycoprotein and canalicular multispecific organic anion transporter in the hepatobiliary excretion of drugs. J Pharm Sci 87:1025-40.

Langer K, Seegmüller E, Zimmer A, Kreuter J. 1994. Characterisation of poly(butyl cyanoarylate) nanoparticles: I. Quantification of PCBA polymer and dextrans . Int J Pharm 110: 21.27.

Langer K, Lambrecht G, Moser U, Mutschler E, Kreuter J. 1997. Quantitative colorimetric and gas chromatographic determination of arecaidine propargyl ester. J Chromatogr B Biomed Sci Appl 692:345-50.

Larson AB, Banker GS. 1976. Attainment of highly uniform solid drug dispersions employing molecular scale drug entrapment in polymeric latices. J Pharm Sci 65:838-43.

Lee J, Cho EC, Cho K. 2004. Incorporation and release behavior of hydrophobic drug in functionalized poly(D,L-lactide)-block-poly(ethylene oxide) micelles. J Control Release 94: 323–335.

Lemarchand C, Gref R, Couvreur P. 2004. Polysaccharide-decorated nanoparticles. Eur J Pharm Biopharm 58:327-41.

Lescure F, Zimmer C, Roy D, Couvreur P. 1992. Optimization of polycyanoacrylate nanoparticle preparation: influence of sulfur dioxide and pH on nanoparticle characteristics. J Colloid Interface Sci 154:77-86.

Leu D, Manthey B, Kreuter J, Speiser P, De Luca PP. 1984. Distribution and elimination of coated polymethyl [2-14C]methacrylate nanoparticles after intravenous injection in rats. J Pharm Sci 73:1433-7.

Lherm C, Müller RH, Puisieux F, Couvreur P. 1992. Alkylcyanoacrylate drug carriers: II. Cytotoxicity of cyanoacrylate nanoparticles with different alkyl chain length. Int J Pharm 84: 13–22.

Lobenberg R, Maas J, Kreuter J. 1998. Improved body distribution of ^{14}C-labelled AZT bound to nanoparticles in rats determined by radioluminography. J Drug Target 5:171-9.

Luo Y, Prestwich GD. 2002. Cancer-targeted polymeric drugs. Curr Cancer Drug Targets 2:209-26.Matsumura Y, Maeda H. 1986. A new concept for macromolecular therapeutics in cancer chemotherapy: mechanism of tumoritropic accumulation of proteins and the antitumor agent smancs. Cancer Res 46:6387-92.

Lucarelli M, Gennarelli M, Cardelli P, Novelli G, Scarpa S, Dallapicolla B, Strom R. 1997. Expression of receptors for native and chemically modified low-density lipoproteins in brain microvessels. FEBS Lett 401: 53-58.

Lück M. 1997. Plasmaproteinadsorption als möglicher Schlüsselfaktor für eine kontrollierte Arzneistoffapplikation mit partikulären Trägern. Ph.D. Thesis, Freie Universität, Berlin. pp. 14–24 and 137–154.

Maeda H, Seymour LW, Miyamoto Y. 1992. Conjugates of anticancer agents and polymers: advantages of macromolecular therapeutics in vivo. Bioconjug Chem 3: 351–362.

Maeda H, Wu J, Sawa T, Matsumura Y, Hori K. 2000. Tumor vascular permeability and the EPR effect in macromolecular therapeutics: a review. J Control. Release. 65: 271–284.

Maeda H. 2001. The enhanced permeability and retention (EPR) effect in tumor vasculature: the key role of tumor-selective macromolecular drug targeting. Adv. Enzyme Regul. 41:189–207.

Maeda H, Sawa T, Konno T. 2001. Mechanism of tumor-targeted delivery of macromolecular drugs, including the EPR effect in solid tumor and clinical overview of the prototype polymeric drug SMANCS. J Control. Release 74: 47– 61.

Maeda H, Fang J, Inutsuka T, Kitamoto Y. 2003. Vascular permeability enhancement in solid tumor: various factors, mechanisms involved and its implications: Int Immunopharmacol. 3: 319–328.

Magenheim B and Benita S. 1991. Nanoparticles charachterization: A comprehensive physicochemical approach. STP, Pharma Sci 1:221.

Malaiya A, Vyas SP. 1988. Preparation and characterization of indomethacin magnetic nanoparticles. J Microencapsul 5:243-53.

Mahaley MS, Jr. 1968. Immunological considerations and the malignant glioma problem. Clin Neurosurg 15:175-89.

Matsumoto J, Nakada Y, Sakurai K, Nakamura T, Takahashi Y. 1999. Preparation of nanoparticles consisted of poly(L-lactide)-poly(ethyleneglycol)-poly(L-lactide) and their evaluation in vitro. Int J Pharm 185: 93–101.

McDonald DM, Baluk P. 2002. Significance of blood vessel leakiness in cancer. Cancer Res 62:5381-5.

Méresse S, Delbart C, Fruchart JG, Cecchelli R. 1989. Low-density lipoprotein receptor on endothelium of brain capillaries. J Neurochem 53: 340-345.

Moghimi SM, Hunter AC. 2000. Poloxamers and poloxamines in nanoparticle engineering and experimental medicine. Trends Biotechnol 18:412-20.

Moghimi SM, Hunter AC, Murray JC. 2001. Long-circulating and target-specific nanoparticles: theory to practice. Pharmacol Rev 53:283-318.

Morgan EH, and Moos T. 2002. Mechanism and developmental changes in iron transport across the blood-brain barrier. Dev Neurosci 24: 1378-1389.

Müller RH, Lherm C, Herbort J, Couvreur P. 1990. In vitro model for the degradation of alkylcyanoacrylate nanoparticles. Biomaterials 11:590–595.

Müller RH, Lherm C, Herbort J, Blunk T, Couvreur P. 1992. Alkylcyanoacrylate drug carriers: I. Physicochemical characterization of nanoparticles with different alkyl chain length. Int J Pharm 84:1–11.

Neuwelt E. 2004. Mechanisms of disease: the blood-brain barrier. Neurosurgery 54: 131-40.

Niwa T, Takeuchi H, Hino T, Kunou N, Kawashima Y. 1994. In vitro drug release behavior of D,L-lactide/glycolide copolymer (PLGA) nanospheres with nafarelin acetate prepared by a novel spontaneous emulsification solvent diffusion method. J Pharm Sci 83: 727–732.

Nomura T, Inamura T, Black KL. 1994. Intracarotid infusion of bradykinin selectively increases blood-tumor permeability in 9L and C6 brain tumors. Brain Res 659:62-6.

Oldendorf WH, Cornford ME, Brown WJ. 1977. The large apparent work capability of the blood-brain barrier: a study of the mitochondrial content of capillary endothelial cells in brain and other tissues of the rat. Ann Neurol 1:409-17.

Oldendorf WH, Brown WJ. 1975. Greater number of capillary endothelial cell mitochondria in brain than in muscle. Proc Soc Exp Biol Med 149:736-8.

Panyam J, Williams D, Dash A, Leslie-Pelecky D, Labhasetwar V. 2004. Solid-state solubility influences encapsulation and release of hydrophobic drugs from PLGA/PLA nanoparticles. J Pharm Sci 93: 1804–1814.

Pardridge WM, Triguero D, Yang J, Cancilla PA. 1990. Comparison of in vitro and in vivo models of drug transcytosis through the blood-brain barrier. J Pharmacol Exp Ther 253:884-91.

Pardridge WM. 1991. Peptide Drug Delivery to the Brain. New York: Raven Press. p 52 – 53. Pardridge WM. 1997. Drug delivery to the brain. J Cereb Blood Flow Metab 17:713-31.

Pardridge WM. 1999. Vector-mediated drug delivery to the brain. Adv Drug Deliv Rev 36:299-321.

Peracchia MT, Gref R, Minamitake Y, Domb A, Lotan N, Langer R. 1997. PEG-coated nanospheres from amphiphilic diblock and multiblock copolymers: investigation of their drug encapsulation and release characteristics. J Control Release 46: 223–231.

Pitas RE, Boyles JK, Lee DH, Foss D, Maley RW. 1987. Astrocytes synthesize apolipoprotein E and metabolize apolipoprotein E-containing lipoproteins. Biochem Biophys Acta 917: 148-161.

Poste GR, Kirsh R. et al. 1984. The challenge of liposome targeting in vivo. Liposome technology Vol III: targeted drug delivery and biological interactions. G Gregoriardis. Boca Rton, FL, CRC Press: 1-28.

Poupaert JH, Couvreur P. 2003. A computationally derived structural model of doxorubicin interacting with oligomeric polyalkylcyanoacrylate in nanoparticles. J Control Release 92:19-26.

Prabhu SS, Broaddus WC, Oveissi C, Berr SS, Gillies GT. 2000. Determination of intracranial tumor volumes in a rodent brain using magnetic resonance imaging, Evans blue, and histology: a comparative study. IEEE Trans Biomed Eng 47:259-65.

Quellec P, Gref R, Dellacherie E, Sommer F, Tran MD, Alonso MJ. 1999. Protein encapsulation within polyethylene glycol-coated nanospheres. II. Controlled release properties. J Biomed Mater Res 47: 388–395.

Reese TS, and Karnovsky MJ. 1967. Fine structural localization of a blood-brain barrier to exogenous peroxidase. J Cell Biol 34: 207-17.

Reddy LH, Murthy RR. 2004. Influence of polymerization technique and experimental variables on the particle properties and release kinetics of methotrexate from poly (butylcyanoacrylate) nanoparticles. Acta Pharm. 54:103-18.

Schaller B. 2004. Usefulness of positron emission tomography in diagnosis and treatment follow-up of brain tumors. Neurobiol Dis 15:437-48.

Schröder U, Sabel BA. 1996. Nanoparticles, a drug carrier system to pass the blood-brain barrier, permit central analgesic effects of i.v. dalargin injections. Brain Res 710:121-4.

Seymour LW, Miyamoto Y, Maeda H, Brereton M,.Strohalm J, Ulbrich K, Duncan R. 1995. Influence of molecular weight on passive tumour accumulation of a soluble macromolecular drug carrier. Eur J Cancer 31 : 766– 770.

Shand N, Weber F, Mariani L, Bernstein M, Gianella-Borradori A, Long Z, Sorensen A G, and Barbier, N. 1999. A phase 1–2 clinical trial of gene therapy for recurrent glioblastoma multiforme by tumor transduction with the herpes simplex thymidine kinase gene followed by ganciclovir. GLI328 European-Canadian Study Group. Hum Gene Ther 10, 2325–2335.

Singer JM, Adlersberg L, Hoenig EM, Ende E, Tchorsch Y. 1969. Radiolabeled latex particles ithe investigation of phagocytosis in vivo: clearance curves and histological observations. J Reticuloendothel Soc 6:561-89.

Smith QR, Rapoport SI. 1986. Cerebrovascular permeability coefficients to sodium, potassium, and chloride. J Neurochem 46:1732-42.

Soderquist ME, and Walton AG. 1980. Structural changes in proteins adsorbed on polymer surfaces. J Colloid Interf Sci. 75: 386.

Storm G et al. 1995. Surface modification of nanoparticles to oppose uptake by the mononuclear phagocyte system. Adv Drug Deliv Rev 16: 31–48.

Sugibayashi K, Morimoto Y, Nadai T, Kato Y, Hasegawa A, Arita T. 1979. Drug-carrier property of albumin microspheres in chemotherapy. II. Preparation and tissue distribution in mice of microsphere-entrapped 5-fluorouracil. Chem Pharm Bull (Tokyo) 27:204-9.

Takakura Y, and Hashida M. 1995. Macromolecular drug carrier systems in cancer-chemotherapy –macromolecular prodrugs.Crit. Rev Oncol Hematol 18:207–231.

Tamai I, and Tsuji A. 2000. Transport-mediated permeation of drug across the blood-brain barrier. J pharm Sci 89: 1371-1388.

References

Tentori, L, and Graziani G. 2002. Pharmacological strategies to increase the antitumor activity of methylating agents. Curr Med Chem 9: 1285– 1301.

ten Tije AJ, Verweij J, Loos WJ, Sparreboom A. 2003. Pharmacological effects of formulation vehicles : implications for cancer chemotherapy. Clin Pharmacokinet 42:665-85.

Tran CT, Wolz P, Egensperger R, Kosel S, Imai Y, Bise K, Kohsaka S, Mehraein P, Graeber MB. 1998. Differential expression of MHC class II molecules by microglia and neoplastic astroglia: relevance for the escape of astrocytoma cells from immune surveillance. Neuropathol Appl Neurobiol 24:293-301.

Trent S, Kong A, Short SC, Traish D, Ashley S, Dowe A, Hines F, and Brada M. 2002. Temozolomide as second-line chemotherapy for relapsed gliomas. J Neurooncol 57, 247– 251.

Tröster SD and Kreuter J. 1988. Contact angles of surfactants with a potential to alter the body distribution of colloidal drug carriers on poly(methyl methacrylate) surfaces. Int J of Pharm. 45:91-100

Tröster SD, Müller U, Kreuter J. 1990. Modification of the body distribution of poly (methyl methacrylate) nanoparticles in rats by coating with surfactants. Int J Pharm 61:85-100.

Tröster SD, Kreuter J. 1992a. Influence of the surface properties of low contact angle surfactants on the body distribution of 14C-poly(methyl methacrylate) nanoparticles. J Microencapsul 9:19-28.

Tröster SD, Wallis KH, Müller RH, Kreuter J. 1992b. Correlation of the surface hydrophobicity of 14C-poly(methyl methacrylate) nanoparticles to their body distribution. J Contr Rel 20:247.

Tsuji A. 2000. Specific mechanism for transporting drugs into the brain. In: Begley DJ, Bradbury MW, Kreuter J, editors. The Blood-Brain Barrier and the Drug Delivery to the CNS. New York: Marcel Dekker. p 121-144.

Ubrich N, Bouillot P, Pellerin P, Hoffman M, Maincent P. 2004. Preparation and characterization of propranolol hydrochloride nanoparticles: a comparative study. J Control Release 97: 291–300.

Van Oss CJ, Gilmann CF, Newmann AW. 1975. Phagocytic Engulfment and Cell Adhesiveness as Cellular Surface Phenomena. New York, Marcel Dekker.

Van Oss CJ. 1978. Phagocytosis as a surface phenomenon. Ann Rev Microbiol 32:19.

Van Oss CJ, Absolom DR, , Newmann AW. 1984. Interaction of phagocytes with other blood cells and with pathogenic and non-pathogenic microbes. Ann NY Acad Sci 416:322.

Vauthier C, Dubernet C, Fattal E, Pinto-Alphandary H, Couvreur P. 2003. Poly (alkylcyanoacrylates) as biodegradable materials for biomedical applications. Adv Drug Deliv Rev 55:519–548.

de Verdiere AC, Dubernet C, Nemati F, Soma E, Appel M, Ferte J, Bernard S, Puisieux F, Couvreur P. 1997. Reversion of multidrug resistance with polyalkylcyanoacrylate nanoparticles: towards a mechanism of action. Br J Cancer. 76:198-205.

Vorbrodt AW, Lossinsky AS, Dobrogowska DH, Wisniewski HM. 1993. Cellular mechanisms of the blood-brain barrier (BBB) opening to albumin-gold complex. Histol Histopathol 8:51-61.

Watanabe A, Higashitsuji K, Nishizawa K. 1978. Studies of electro-capillary emulsification. J Colloid Interface Sci 64: 278.

Watling CJ, and Cairncross JG. 2002. Acetazolamide therapy for symptomatic plateau waves in patients with brain tumors. Report of three cases. J Neurosurg 97, 224– 226.

Wesemeyer H, Müller BW, Müller RH. 1993. Adsorption of ethoxylated surfactants on nanoparticles. II. Determination of adsorption enthalpy by microcalorimetry. Int J Pharm 89:33.

Widder KJ, Senyei AE, Ranney DF. 1970. Magnetically responsive microspheres and other carriers for the biophysical targeting of antitumor agents. In S Garattini, A Goldin, F Howking, IJ Kopin and RJ Schnitzer (Eds). Adv. Pharmacol. Chemother. Academic Press, New York. 16:213–271.

Wilkis DJ. 1967a. The biological recognition of foreign from native particle as a problem in surface chemistry. J Colloid Interf Sci 25:84.

Wilkis DJ. 1967b. Interaction of charged colloids with RES. The Reticuloendothelial system and Arteriosclerosis. NR Di Luzio and R Paoletti eds. New York, Plenum Press, p 25.

Wood RW, Li VHK, Kreuter J, Robinson JR. 1985. Ocular disposition of poly-hexyl-2-cyano[3-^{14}C]acrylate nanoparticles in the albino rabbit. Int J Pharm 13:175-183.

Zagzag D, Nomura M, Friedlander DR, Blanco CY, Gagner JP, Nomura N, Newcomb EW. 2003. Geldanamycin inhibits migration of glioma cells in vitro: a potential role for hypoxia-inducible factor (HIF-1alpha) in glioma cell invasion. J Cell Physiol 196:394-

402.

Zara GP, Cavalli R, Bargoni A, Fundaro A, Vighetto D, Gasco MR. 2002. Intravenous administration to rabbits of non-stealth and stealth doxorubicin-loaded solid lipid nanoparticles at increasing concentrations of stealth agent: pharmacokinetics and distribution of doxorubicin in brain and other tissues. J Drug Target 10:327-35.

Curriculum Vitae

Surname:	Ambruosi
Christian name:	Alessandra
Marital status:	Unmarried
Date of birth:	10th of June 1975
Place of birth:	Bari, Italy
Nationality:	Italian

Education:

1982 - 1987	Elementary school at "Scuola elementare N. Zingarelli", Bari, Italy.
1987 - 1989	Hight school at "Scuola media T. Fiore", Bari, Italy.
1989 - 1994	High school at "Liceo Scientifico E.Fermi", Bari, Italy.
1994 - 2000	Studies of Chemical and Pharmaceutical Technology at the University of Pharmacy, Bari, Italy.
2000 - 2001	Practical training at Prof. G. Trapani's Chemical Laboratory on Peripheral-type Benzodiazepin Receptor lygands.
2002	Degree *"Summa cum Laude"* in Chemical and Pharmaceutical Technology at the University of Bari, Italy.

Postgraduate studies:

01.07.2002 - 31.12.2005	Doctoral experimental work at Wolfgang Goethe University, Institute of Pharmaceutical Technology, Frankfurt am Main, Germany.
	Subject: Influence of Formulation Parameters of Doxorubicin - Poly (butyl Cyanoacrylate) Nanoparticles on the Treatment of Glioblastoma and Evaluation of the Body Distribution of Labelled Nanoparticles in Healthy and Glioblastoma Bearing Rats.

Professional training:

06.2004   Applikations- und Blutentnahmetechniken an Maus und Ratte, Frankfurt am Main, Germany.

04.2005   GMP seminar, Institute of Pharmaceutical Technology, Frankfurt am Main, Germany.

Work experience:

03. – 04.2005   Development of poly(butyl cyanoacrylate) nanoparticles bound to labelled doxorubicin and radioluminography studies by Sanofi – Aventis, Frankfurt am Main, Germany.

04.2005   GMP practice, Institute of Pharmaceutical Technology, Frankfurt am Main, Germany.

Publications:

A. Ambruosi, H. Yamamoto, J. Kreuter. 2005. Body Distribution of Polysorbate-80 and Doxorubicin-Loaded [^{14}C]Poly(buty Cyanoacrylate) Nanoparticles after i.v. Administration in Rats. J Drug Targeting. *In press.*

A. Ambruosi, A. Khalansky, H. Yamamoto, S. Gelperina, D. Begley, J. Kreuter. Biodistribution of Polysorbate 80-coated Doxorubicin-Loaded [^{14}C]-Poly(butyl Cyanoacrylate) Nanoparticles after Intravenous Administration to Glioblastoma-Bearing Rats. J Drug Targeting. *In press.*

A. Ambruosi, S. Gelperina, A. Khalansky, S. Tanski, A. Theisen, J. Kreuter. Antitumor effect of doxorubicin loaded in poly(butyl cyanoacrylate) nanoparticles in rat glioma model: influence of formulation parameters. *In preparation*.

Posters:

A. Ambruosi, J. Kreuter. Improvement of the loading of doxorucin poly(butyl cyanoacrylate) nanoparticles. International Meeting of Prarmaceutics, Biopharmaceutics and Pharmaceutical Thecnology, Nuremberg, 2004.

A. Ambruosi, J. Kreuter. Characterization of formulations of doxorubicin poly(butyl cyanoacrylate) nanoparticles with improved loading. Controlled Release Society German Chapter Annual Meeting, Frankfurt, 2004.

Oral presentation:

Body distribution of ^{14}C-poly(butyl cyanoacrylate) nanoparticles after i.v. injection to glioblastoma bearing rats. Controlled Release Society 32nd Annual Meeting & Exposition, Miami Beach, Florida, U.S.A. 2005.

Acknowledgements

I wish to express my sincere thanks to my supervisor Professor Dr. Jörg Kreuter who has encouraged me to develop and independent and self-sufficient approach to my work. His openness and willingness to help truly exemplify the spirit of science.

I also would like to sincerely thank Professor Dr. Jennifer B. Dressman, for involving me in the department activities and for being willing to offer her support in several occasions.

I would like to thank Dr. Svetlana Gelperina for her support, for her innumerable and helpful ideas, for her genuine passion for science.

Particularly thanks to Mrs. Elisabeth Herbert, for her precious support during experiments with radioactive material and animals assistance and for her kindness, disponibility, and patience as well.

I would like to express my sincere gratitude to Dr. Alexander Khalansky and to Dr. Hiromitzu Yamamoto for their incommensurable help during the animal experiments.

The financial support of the German Bundesministerium für Bildung und Forschung (Project Nr. 0312010A) is gratefully acknowledged.

The author is also grateful the Sicor Company, Rho, Italy for the generous gift of doxorubicin.

To Sanofi-Aventis, Frankfurt a.M, the author gives her thanks for supporting the radioluminography studies.

I would like to express my sincere thanks to all the member of the institute of pharmaceutical technology, and in particular to my colleagues Berta Sanchez de Juan, Telli Hekmatara, Alexander Bootz who helped me for the accomplishment of this work.

Most of all I would like to thank my family for the support they provided me through my

entire life.

A very special thanks goes out to my friends, Emanuela, Domingo, Niels, Jürgen, Daniel and in particular to my boyfriend, Gianenrico, without whose encouragement and editing assistance, I would not have finished this thesis.